AMRL-TDR-62-87

HUMAN ENGINEERING CRITERIA FOR MANNED SPACE FLIGHT: MINIMUM MANUAL SYSTEMS

TECHNICAL DOCUMENTARY REPORT NO. AMRL-TDR-62-87

August 1962

Behavioral Sciences Laboratory
6570th Aerospace Medical Research Laboratories
Aerospace Medical Division
Air Force Systems Command
Wright-Patterson Air Force Base, Ohio

Contract Monitor: C. E. Waggoner, Capt, USAF
Project No. 7184, Task No. 718405

[Prepared under Contract No. AF33(616)-8168
by
Donald K. Bauerschmidt
and
Robert O. Besco
Hughes Aircraft Company, Culver City, California]

NOTICES

When US Government drawings, specifications, or other data are used for any purpose other than a definitely related government procurement operation, the government thereby incurs no responsibility nor any obligation whatsoever; and the fact that the government may have formulated, furnished, or in any way supplied the said drawings, specifications, or other data is not to be regarded by implication or otherwise, as in any manner licensing the holder or any other person or corporation, or conveying any rights or permission to manufacture, use, or sell any patented invention that may in any way be related thereto.

Qualified requesters may obtain copies from ASTIA. Orders will be expedited if placed through the librarian or other person designated to request documents from ASTIA.

Do not return this copy. Retain or destroy.

Stock quantities available at Office of Technical Services, Department of Commerce, $3.50.

7-169, 1,000, 10-15-62

Aerospace Medical Division, 6570th Aerospace Medical Research Laboratories, Wright-Patterson AFB, Ohio Rpt. No. AMRL-TDR-62-87. HUMAN ENGINEERING CRITERIA FOR MANNED SPACE FLIGHT: MINIMUM MANUAL SYSTEMS. Final report, Aug 62, viii + 227 pp. incl. illus., tables, 42 refs. Unclassified report

Analytical and experimental investigations were made of simple or minimum manual guidance and control systems. A complete three-degree of freedom static simulator was used to study the manual attitude control of space vehicles. Major controller, display and vehicle configuration parameters were compared experimentally. The system kinematics,

(over)

UNCLASSIFIED

1. Control Systems
2. Guidance
3. Control Simulators
4. Space Navigation
- I. AFSC Project 7184, Task 718405
- II. Behavioral Sciences Laboratory
- III. Contract AF 33(616) - 8168
- IV. Hughes Aircraft Co., Culver City, Calif.
- V. Bauerschmidt, D.K., Besco, R.O.

UNCLASSIFIED

manual control and visual factors of space rendezvous and docking maneuvers were analyzed. Procedures for manual participation in space navigation and guidance were studied and a preliminary design of a simple computational aid was developed. The conclusions of all the studies are presented and recommendations are made for the design of manual guidance and control systems.

UNCLASSIFIED

- VI. In ASTIA collection
- VII. Aval fr OTS: $3.50

UNCLASSIFIED

Aerospace Medical Division, 6570th Aerospace Medical Research Laboratories, Wright-Patterson AFB, Ohio Rpt. No. AMRL-TDR-62-87. HUMAN ENGINEERING CRITERIA FOR MANNED SPACE FLIGHT: MINIMUM MANUAL SYSTEMS. Final report, Aug 62, viii + 227 pp. incl. illus., tables, 42 refs. Unclassified report

Analytical and experimental investigations were made of simple or minimum manual guidance and control systems. A complete three-degree of freedom static simulator was used to study the manual attitude control of space vehicles. Major controller, display and vehicle configuration parameters were compared experimentally. The system kinematics,

(over)

UNCLASSIFIED

1. Control Systems
2. Guidance
3. Control Simulators
4. Space Navigation
- I. AFSC Project 7184, Task 718405
- II. Behavioral Sciences Laboratory
- III. Contract AF 33(616) - 8168
- IV. Hughes Aircraft Co., Culver City, Calif.
- V. Bauerschmidt, D.K., Besco, R.O.

UNCLASSIFIED

manual control and visual factors of space rendezvous and docking maneuvers were analyzed. Procedures for manual participation in space navigation and guidance were studied and a preliminary design of a simple computational aid was developed. The conclusions of all the studies are presented and recommendations are made for the design of manual guidance and control systems.

UNCLASSIFIED

- VI. In ASTIA collection
- VII. Aval fr OTS: $3.50

UNCLASSIFIED

Aerospace Medical Division, 6570th Aerospace Medical Research Laboratories, Wright-Patterson AFB, Ohio Rpt. No. AMRL-TDR-62-87. HUMAN ENGINEERING CRITERIA FOR MANNED SPACE FLIGHT: MINIMUM MANUAL SYSTEMS. Final report, Aug 62, viii + 227 pp. incl. illus., tables, 42 refs. Unclassified report

Analytical and experimental investigations were made of simple or minimum manual guidance and control systems. A complete three-degree of freedom static simulator was used to study the manual attitude control of space vehicles. Major controller, display and vehicle configuration parameters were compared experimentally. The system kinematics,

(over)

UNCLASSIFIED

1. Control Systems
2. Guidance
3. Control Simulators
4. Space Navigation
- I. AFSC Project 7184, Task 718405
- II. Behavioral Sciences Laboratory
- III. Contract AF 33(616) - 8168
- IV. Hughes Aircraft Co., Culver City, Calif.
- V. Bauerschmidt, D.K., Besco, R.O.

UNCLASSIFIED

manual control and visual factors of space rendezvous and docking maneuvers were analyzed. Procedures for manual participation in space navigation and guidance were studied and a preliminary design of a simple computational aid was developed. The conclusions of all the studies are presented and recommendations are made for the design of manual guidance and control systems.

UNCLASSIFIED

- VI. In ASTIA collection
- VII. Aval fr OTS: $3.50

UNCLASSIFIED

Aerospace Medical Division, 6570th Aerospace Medical Research Laboratories, Wright-Patterson AFB, Ohio Rpt. No. AMRL-TDR-62-87. HUMAN ENGINEERING CRITERIA FOR MANNED SPACE FLIGHT: MINIMUM MANUAL SYSTEMS. Final report, Aug 62, viii + 227 pp. incl. illus., tables, 42 refs. Unclassified report

Analytical and experimental investigations were made of simple or minimum manual guidance and control systems. A complete three-degree of freedom static simulator was used to study the manual attitude control of space vehicles. Major controller, display and vehicle configuration parameters were compared experimentally. The system kinematics,

(over)

UNCLASSIFIED

1. Control Systems
2. Guidance
3. Control Simulators
4. Space Navigation
- I. AFSC Project 7184, Task 718405
- II. Behavioral Sciences Laboratory
- III. Contract AF 33(616) - 8168
- IV. Hughes Aircraft Co., Culver City, Calif.
- V. Bauerschmidt, D.K., Besco, R.O.

UNCLASSIFIED

manual control and visual factors of space rendezvous and docking maneuvers were analyzed. Procedures for manual participation in space navigation and guidance were studied and a preliminary design of a simple computational aid was developed. The conclusions of all the studies are presented and recommendations are made for the design of manual guidance and control systems.

UNCLASSIFIED

- VI. In ASTIA collection
- VII. Aval fr OTS: $3.50

UNCLASSIFIED

FOREWORD

This study was initiated by the Behavioral Sciences Laboratory of the 6570th Aerospace Medical Research Laboratories, Aerospace Medical Division, Wright-Patterson Air Force Base, Ohio, The research was conducted by the Research and Development Division, Hughes Aircraft Company, Culver City, California, under Contract No. AF 33(616)-8168. Dr. A.C. Williams, Jr., Manager of the Display Department, Hughes Aircraft Company was the Project Manager. Dr. S.N. Roscoe, Senior Scientist, Hughes Aircraft Company was the Project Engineer. Captain C.E. Waggoner was the contract monitor for the 6570th Aerospace Medical Research Laboratories. The research sponsored by the contract was performed in support of Project No. 7184, "Human Performance in Advanced Systems," and Task No. 718405, "Design Criteria for Crew Stations in Advanced Systems." It was started in April 1961 and was completed in April 1962.

The following authors from Hughes Aircraft contributed major portions of this report: N.A. Boehmer, Dr. W.B. Knowles, Jr., Carolyn S. McElwain, I. Terris, and P.V. Vermont. The respective authors of the sections are cited in the body of the report.

The authors wish to acknowledge the assistance of R.E. Norris, H.M. Meyers, J.J. Leeson, and D.J. Eggert of the R and D Division of Hughes Aircraft Company in mechanizing the analog computer and simulation equipment. J.B. Setto accomplished the detail design of the proportional hand controllers.

Special appreciation is extended to the test pilots from the Aerospace Research Pilot School at Edwards Air Force Base, These men participated in preliminary studies and made constructive suggestions regarding the design of control and display equipment. The following pilots participated: Major Robert S. Buchanan, Captain James A. McDivitt, Major Thomas U. McElmurry, and Major Arthur Torosian.

The pilot-engineers who participated in the experimental simulation program were P.E. Boron, R.A. Boucher, R.J. Boucher, W. Elkins, and D.W. Schuyler of Hughes Aircraft Company.

ABSTRACT

Analytical and experimental investigations were made of simple or minimum manual guidance and control systems. A complete three-degree of freedom static simulator was used to study the manual attitude control of space vehicles. Major controller, display and vehicle configuration parameters were compared experimentally. The system kinematics, manual control and visual factors of space rendezvous and docking maneuvers were analyzed. Procedures for manual participation in space navigation and guidance were studied and a preliminary design of a simple computational aid was developed. The conclusions of all the studies are presented and recommendations are made for the design of manual guidance and control systems.

PUBLICATION REVIEW

This technical documentary report has been reviewed and is approved.

Walter F. Grether

WALTER F. GRETHER
Technical Director
Behavioral Sciences Laboratory

TABLE OF CONTENTS

LIST OF ILLUSTRATIONS

LIST OF TABLES

INTRODUCTION

PURPOSE

Manned space flight is now a reality but man's potential in space is far from being realized. In fact, to a large extent, the potential and nature of man's contribution to space missions are unknown. To supply information of this type large efforts are under way in support of manned vehicle programs such as MERCURY, DYNASOAR, GEMINI and APOLLO. In addition, numerous studies with perhaps more general applicability are being sponsored by various Air Force and NASA organizations.

These study efforts approach the problem of determining man's potential contributions to space operations at literally all levels of investigation. They encompass an extremely wide variety of orbital operations ranging from electronic equipment maintenance to performance of terminal rendezvous guidance. It is not possible to categorize these studies completely, nor would it be appropriate for the purposes of this report. However, a number of studies which relate to the areas of work under this contract are given in the Bibliography.

This study deals with a number of orbital operations with the purpose being to determine the system equipment requirements for the performance of so-called minimum manual modes of control and guidance. The purpose of this effort is to provide results in the form of design criteria and design trade-offs which can be used by system designers to define the characteristics of orbital vehicles and manual orientation and translation control systems as well as control and display equipments.

The study is directed toward minimum manual as opposed to automatic modes of control. There has been a tendency in non-project directed study efforts to deal with the requirements imposed upon equipment development and design to support more complex manually directed operations in space. There is justification for such an approach since characteristically equipment to support these operations requires relatively long design, development, and shakedown time. However, since studies of this type deal with a rather long future time, the tendency has been to consider the man as a system manager, or decision element, rather than a controller or sensor. Unfortunately, with this approach there has typically been little attention

given to the techniques and equipments to allow the man to assume the role of manager or to serve as a backup controller in the event of prime equipment malfunction. Nor does it provide the trade-off criteria necessary for efficient system design which maximizes overall probability of success. It is the purpose of this study to supply just such information.

SCOPE

This study was directed toward determining the system equipment requirements and performance capabilities of the minimum manual modes of three systems: (1) the vehicle attitude control system, (2) the vehicle translation control system, and (3) the orbital navigation system.

The scope and depth of work was different in each of these areas with the majority of the effort being expended in the vehicle attitude control area. The work in this area has encompassed a number of tasks including the following: (1) determination of system requirements and constraints, (2) analytic study of the kinematic relationships, (3) design and implementation of basic analog simulation setups, (4) preliminary simulator study of an exploratory nature, and (5) comparative simulator studies of alternate system configurations. Study of alternate attitude system configurations using the analog computer representation of the attitude control situation received the major emphasis throughout this program. Simulator studies included comparisons of manual performance for alternate control tasks, system torque-to-inertia values, vehicle axes moment-of-inertia ratios, manual controllers, and alternate display configurations. Alternate displays of vehicle attitude and rate information were designed to determine the effect on system performance of the availability of certain classes (attitude, body rate, etc.) of attitude information.

The work in the vehicle translation control area parallels, to a certain point, that in the attitude control area except for additional effort being placed in the definition of information sources. Since in general the application of the results of study in this area would be applied to orbital rendezvous and docking system design, particular emphasis was given to the visually sensed information available to the astronaut during this mission. The work in the translation control area includes a survey of the literature pertinent to this area, categorization of the visual cues present during docking operations, analysis and simulation of the kinematic relationship and visual cues

present in docking as well as performance of preliminary simulator studies. The intent of this portion of the program was to indicate the magnitude of the problem and, by analytical and simulator studies of a preliminary nature, to indicate fruitful lines for further investigation.

Work in the manual orbital navigation area includes analysis of several methods of trajectory determination and guidance computation for high apogee earth-orbital missions as well as a brief survey of state-of-the-art sensing equipments appropriate to this task. Also included in this work is a study of the basic requirements for and the preliminary design of equipment necessary for the efficient performance of manual navigation.

ORGANIZATION OF THE REPORT

The body of the report is organized into three major sections dealing with manual vehicle orientation, manual vehicle translation control, and manual orbital navigation.

The section dealing with the study of manual orientation control is presented first. It contains brief discussions of the vehicle control requirements, definitions of attitude control system configurations and characteristics, and descriptions of the manual controllers and information displays studied. A description of the analog simulation is also included in this section. The detailed analyses and derivations of the applicable kinematic relationships supporting these simulations are included as Appendices I, II, and III. The body of this section is a description of four major experimental studies. These are concerned with the effects on performance of vehicle torque-to-inertia ratios, alternate information displays and c ler configurations, gyroscopic cross-coupling, and viewpoint configu n. Appendix IV contains a discussion of operator loading measures and the secondary task used in the experimental studies.

The second major section of the report deals with orbital vehicle translation control. It presents a survey of the translation control problem and, using the requirements of a docking mission, presents the results of preliminary simulator investigations.

A survey of sensors and computational methods and techniques for manual orbital navigation is presented in the third major section. The discussion of computational techniques in the body of this section is based upon the more detailed mathematical treatments discussed in Appendix V.

Appendix VI supplies a derivation of matrix elements used in the Navigation Section and Appendix VII is a brief review of the matrix operations used in the body of the report and in the Appendices.

Conclusions and recommended future work in the three areas are presented in the final two sections of the report.

MANUAL VEHICLE ORIENTATION CONTROL

by

D. K. Bauerschmidt, R. O. Besco and Carolyn S. McElwain

VEHICLE CONTROL REQUIREMENTS

Mission requirements are the basis for establishing all vehicle attitude and translation control requirements. The mission requirements are the major goals which must be met to accomplish the planned mission. In the simplest form, these goals may be nothing more than a statement of the primary mission objectives such as the attainment of orbital flight and the undamaged return of the payload package. However, for the mission requirements to be used as a basis for the establishment of control requirements, detailed description of the mission objective is necessary. For example, such quantitative information as the desired orbital attitude and the acceptable landing impact may be required.

However, it is not sufficient to specify only the detailed mission requirements. Determination of vehicle control requirements also requires the specification of other onboard and ground-based system requirements. For example, control requirements for vehicle orientation may well be dependent upon aspects of the communications system design such as the high gain antenna orientation requirements.

Many orbital vehicle system parameters must be specified in order to determine the attitude control system requirements. These include the vehicle orientation accuracy tolerances for each mission phase, the range of controllable vehicle body or space angular rates, the fuel expenditure allowances, reliability goals, etc. The most generally discussed attitude control system requirement deals with the accuracy to which a vehicle may be oriented. Accurate orientation may be required for the performance of powered maneuvers, maintenance of skin temperature within predetermined limits, or performance of manual observations such as those required for navigation sensing or earth reconnaissance. Stringent orientation accuracy requirements result from the necessity for pointing onboard sensing equipment which may be part of the navigation (theodolites), communication (high gain antennas), or electrical power systems (solar cells). The payload itself may determine vehicle orientation accuracy requirements. An

example of this is the relatively high orientation accuracy made necessary for the telescopes of the Orbiting Astronomical Observatory. Orientation accuracy requirements ranging from 0.1 second of arc to 10° have been given for various mission functions.

A requirement for establishing and maintaining a particular rate of rotation of the orbital vehicle may result from the necessity for a vehicle to maintain a constant orientation relative to a set of reference axes not fixed in inertial space. An example of this situation is that of the general requirement for the maintenance of one of the vehicle axes in coincidence with the local earth or moon vertical. The station keeping phase of a rendezvous mission may impose similar requirements. Vehicle rate-of-rotation requirements may also result from thermal control considerations or the requirements for single axis spin stabilization.

Fuel requirements for a vehicle attitude control system are determined by weighing many factors. The minimum fuel requirements may often be specified by an estimate of the attitude maneuver requirements. A change in sensor mounting such as the addition of gimballing may further reduce this minimum. At best, particular fuel requirements are difficult to specify early in the system design process. In general, the fuel required is determined by the type of mission and the estimated vehicle orientation maneuver requirements.

The attitude control system reliability requirements are in part specified by the somewhat nebulous factors of mission safety, system cost, etc. Reliability requirements, in turn, make necessary redundant modes of operation and considerable system complexity.

SYSTEM DEFINITION

System Modes

Orbital vehicle attitude control systems generally include components which may be placed into one of three major functional categories: (1) sensing, (2) control, and (3) actuation. Components in the sensing category provide basic orientation, rate and/or acceleration information for the control system. The information may be specified relative to some absolute reference system or as errors from desired values. Typical sensing components include inertial platforms, integrating gyros, rate gyros,

horizon scanners, etc. Components in the actuation category provide the torques for rotating the vehicle about any or all axes. Torques may originate from various sources, however, the most generally discussed actuator types are the reaction jet and the inertial wheel. These devices will be discussed in a later section of this report. The function of the components in the control category is to act upon the sensing component outputs and supply appropriate inputs to the actuation components. The processing performed by these components may include general computation, co-ordinate resolution, integration, analog-to-digital conversion, etc. The nature of the components performing the control function varies widely. It may include analog and/or digital computation, very simple logic circuitry, or it may include an astronaut with his associated displays and manual controllers as well as additional computation and processing equipment.

Since the primary concern of this study has been with the systems including the astronaut, it is necessary at this point to distinguish between alternate manual control modes and to describe the nature of the astronaut's contribution to these modes. For this purpose several basic manual attitude control system modes will be defined. The manual control modes will be defined in terms of the nature and effect of the astronaut's control input.

Attitude Command Mode

In this mode an astronaut makes a control input that requests the attitude control system, in total, to orient the vehicle and mair particular orientation of the vehicle relative to a chosen referen ystem. He may accomplish this by setting three (pitch, roll, and yaw) dials to indicate the chosen orientation. Or, if he desires, he may select a particular attitude relative to predetermined reference axes of onboard sensing equipment. Basically, the operation of this mode consists of the actuating devices being driven by processed signals proportional to the existing attitude errors about each axis. Generally, proper operation of this mode requires additional control stabilization using rate signals.

Rate Command Mode

In this mode the astronaut makes a control input that requests the attitude control system to establish a particular rate of rotation of the vehicle about a particular axis. Generally, the requested rate is relative to an inertial space reference but in certain instances it may be relative to another predetermined rate bias. A continuous manual control device is normally operated by the astronaut for this purpose. The astronaut's control input signals are subtracted from the output signals of rate sensing devices such as rate gyros and supplied as signals to the actuating devices.

Acceleration Command Mode

In this mode an astronaut makes a control input that directly operates the actuating devices. As long as appropriate actuators are energized the vehicle will accelerate about a particular axis. The astronaut's control input signal may be binary, in which case he operates the actuator in an on-off fashion, or proportional, in which case the subsequent vehicle acceleration is proportional to the amplitude of the control input signal. This mode, which does not require control system sensing and summation to produce an error signal, was the primary mode investigated in this study.

Role of Astronaut

The astronaut may be provided with several of the control modes described above. He will perform somewhat differently when operating in different modes. In general, he always performs three functions: (1) sensing, (2) processing, and (3) controlling.

He will act as a sensor by sensing vehicle orientation, rate and acceleration from his displays and from outside views. Vehicle orientation may be shown to the astronaut in various ways with vehicle rate and acceleration shown indirectly only as components of the dynamic orientation display. Vehicle orientation relative to local vertical may be shown to the astronaut as a remote horizon scanner display or directly from a view of the earth through a periscope. Rate information may also be shown to the astronaut on relatively simple rate indicators which would indirectly show vehicle acceleration as the first derivative of the rate display indications.

The astronaut will act as a processor, since he replaces certain of the functions which would be performed by automatic components if the man were not part of the control system. He may perform coordinate resolution, differentiation of orientation indications, integration, stabilization, etc. It is the complexity of the astronaut's processing task that in a sense determines the manualness of the attitude control system. If, for example, the astronaut need only designate an attitude angle in order to orient the vehicle to this angle, the system performing this task is rather automatic. In contrast, if the astronaut must sense orientation as well as rate and acceleration components through the view-port and directly control the actuating devices (acceleration mode) to attain a particular vehicle orientation, the system performing this task is basically manual. The astronaut will act as controller in one of the modes (orientation, rate or acceleration) described above. Manual control devices appropriate for each of these modes have been discussed briefly above.

System Component Characteristics

The performance of the astronaut as a component of the vehicle attitude control system is dependent upon the characteristics of other components in the system. Their dynamic characteristics and potential influence upon manual control performance will be discussed in this section.

For manual attitude control systems operating in the acceleration mode the major dynamic equipment components are the actuating devices. These devices currently fall into two categories: inertial-wheel and reaction-jet actuators.

Inertial-wheel actuators are of two major types: (1) those driven by hysteresis motors and (2) those driven by induction motors. With either of these the dynamic characteristics of the inertial-wheel devices are negligible. For example, the time delays to be expected are less than 0. 01 second. With the hysteresis motor the torque output is independent of inertial-wheel speed while with an induction motor the torque is roughly inversely proportional to wheel speed. Therefore, the system gain (control input to torque output) is generally a constant for the hysteresis motor drive and dependent upon wheel speed for the induction motor drive. Theoretically, the application of inertial wheels is not limited to small vehicles, but because of the usual requirement for fairly rapid maneuvering of large vehicles, a

practical limit of inertial-wheel size is reached. It is expected that vehicle-to-wheel mass ratios from 100:1 to 1000:1 are quite reasonable. However, when wheels are used in large vehicles, the absolute weight and the power requirement increase accordingly. An example of a typical inertial-wheel application is for the Orbiting Astronomical Observatory in which it was proposed that one-foot diameter wheels with maximum torque outputs of 5.0 in-lbs be used. One proposed system contained a hysteresis motor drive system which weighed 25 pounds and consumed 30 watts of power with a total capacity of 5000 in-lbs-sec.

Both inertial wheels and reaction jets may be used onboard a vehicle. When this is the case the reaction-jet system is generally used to desaturate the inertial-wheel system.

Reaction-jet systems are also divided into two types: cold gas and chemical. The simplest and thus the most reliable is the cold gas system which uses the expansion of gas from a liquid or compressed form through a nozzle to produce torque. The torque of this type of system does not have any apparent lower limit; however, it does reach a practical upper limit at approximately 10 pounds of thrust. A measure of system performance is given by the specific impulse. For example, nitrogen gas which is considered best for a cold gas system has a specific impulse of 70 seconds, but because it takes approximately 1.5 pounds of metal to contain 1.0 pound of gas, and because the valve and nozzle weigh about 0.035 pound per 3 pounds of thrust, the overall system specific impulse is approximately 30 seconds.

Reaction jets using chemical reaction to produce thrust have no maximum thrust limit. The minimum thrust level for practical applications is approximately one pound. The specific impulse of this type of device is approximately 300 seconds for a nitrogen tetroxide-hydrazene system and 150 seconds for a hydrogen peroxide system. The hydrogen peroxide system is used in the Mercury capsule and in various unmanned orbital vehicles. For this type of jet, approximately 0.1 pound of metal is required to store 1.0 pound of fuel. The nozzle weight is 15 percent of thrust for one pound of thrust decreasing to 1.2 percent for 1000 pounds of thrust. A catalyst chamber is required for a peroxide system.

The dynamic characteristics of these systems vary with the type of gas or chemical reaction used. The most familiar hydrogen peroxide system has perhaps the worst time delay because of the necessary catalytic

decomposition. It is generally considered to be about 0. 25 second but recent developments may reduce this value to 0. 05 second at the expense of additional system weight. The particular shape of the delay is a sigmoid curve which can be approximated by a second order lag function. The delay of the bipropellant system varies from approximately 3 milliseconds to about 0. 05 second.

The selection of the optimum type of system is not at all obvious since the reaction-jet systems are heavily mission dependent with each maneuver dictating a particular amount of fuel to be carried. Inertial-wheel systems are less mission dependent because electrical power is used for actuation of the wheel.

An orbital vehicle control system capable of operating in rate and attitude command modes contains many other components processing significant dynamic characteristics. Computing time lags, sampled data, and complex linear dynamic lags are a few of the properties of the components which may be expected in these systems. It is not the purpose of this study to define and investigate these characteristics. It is of interest to note them here in order to emphasize the simplicity of the acceleration mode in terms of the equipment required.

Kinematic Relationships

For further study and simulation purposes, it is necessary to specify the kinematic relationships governing the motion of the vehicle in response to a disturbance. Analytical derivations and discussions of the three-dimensional angle and rate relationships are presented in Appendices I and II. A brief discussion of the applicable gyroscopic cross-coupling effects is given in Appendix III.

SIMULATION

Man-in-Space Simulator (MISS)

The Hughes Man-in-Space Simulator (MISS) was used for the simulation of system dynamic characteristics and applicable kinematic relationships, for the generation of display indications and for the recording and processing of experimental data.

The MISS facility consists of a number of spacecraft display and control simulations for particular mission phases including orbital attitude control, rendezvous and docking. All of these simulations utilize a large general-purpose analog computer for the basic kinematic computations, control system simulations, display signal processing and performance measure readout and processing. The computer consists of over 200 high precision operational amplifiers, over 30 resolving and multiplying units as well as large amounts of function generation, relay and diode equipment.

The facility includes several multichannel electronic display generators which may be patched in a manner similar to the prepatch panel of the analog computer.

Analog Computer Representation

The analog computer was programmed to provide all of the computations necessary for this simulation. The basic components of this simulation include the body rate/cross-coupling computation, the space angle rate computation, the space angle display generation, the periscope geometry computation, the fuel consumption computation and the manual controller signal processing. There were, of course, other computations performed during the course of this study but the major components of the computer program are listed above. These are shown in Figure 1.

The body rate/cross-coupling computations reflect Equations (190), (191), and (192) which are derived in Appendix III. It has been assumed that the three principle axes of inertia are in coincidence with the body rate torquing axes of the vehicle. The output of this computation, vehicle body rates p, q, and r, are used to drive the course and fine body rate indicators. The vehicle body rates are also the input to the space angle rate computations. Equations (137), (138), and (139), in Appendix II, are used to program the analog computer for the computation of the space angle rates $\dot{\Phi}$, $\dot{\theta}$, and $\dot{\Psi}$. The sines and cosines of the space angles Φ, θ, and Ψ are modulated and used to display the angles on individual cathode ray tube displays. This method of display angle generation is used to assure precise display indications which are free of mechanical friction.

The periscope geometry computation performs the geometric transformations to convert the space angle rates into suitable deflection signals for the simulated periscope. The program shown in Figure 1 represents

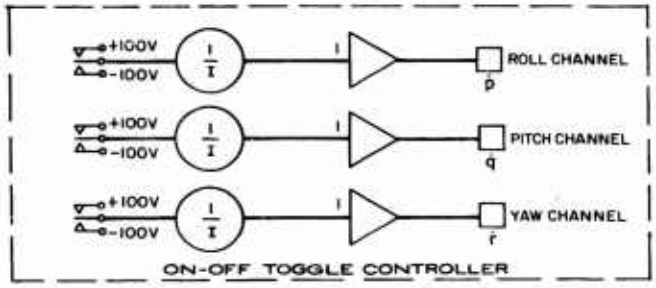
+100V
-100V
ROLL CHANNEL
PITCH CHANNEL
YAW CHANNEL
ON-OFF TOGGLE CONTROLLER

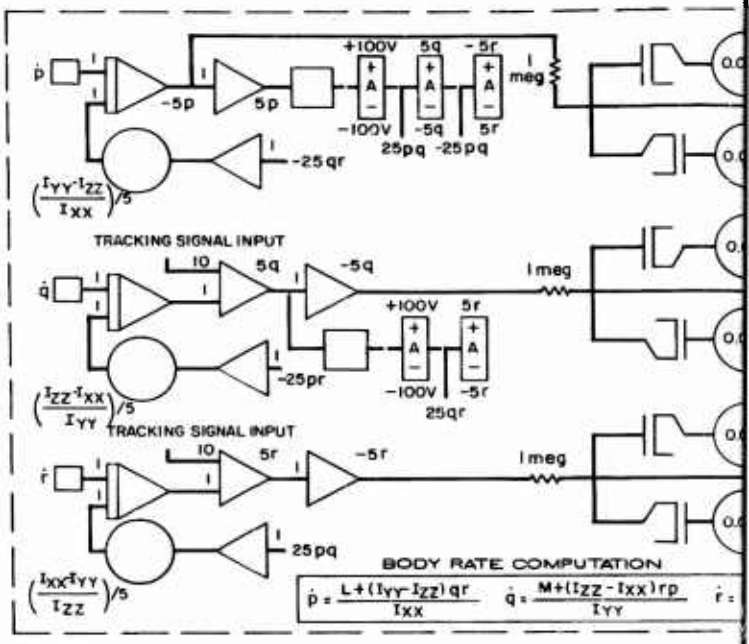
TRACKING SIGNAL INPUT
TRACKING SIGNAL INPUT
BODY RATE COMPUTATION

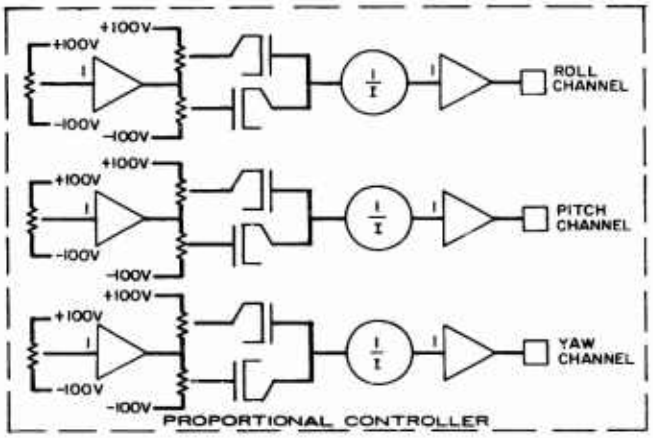
ROLL CHANNEL
PITCH CHANNEL
YAW CHANNEL
PROPORTIONAL CONTROLLER

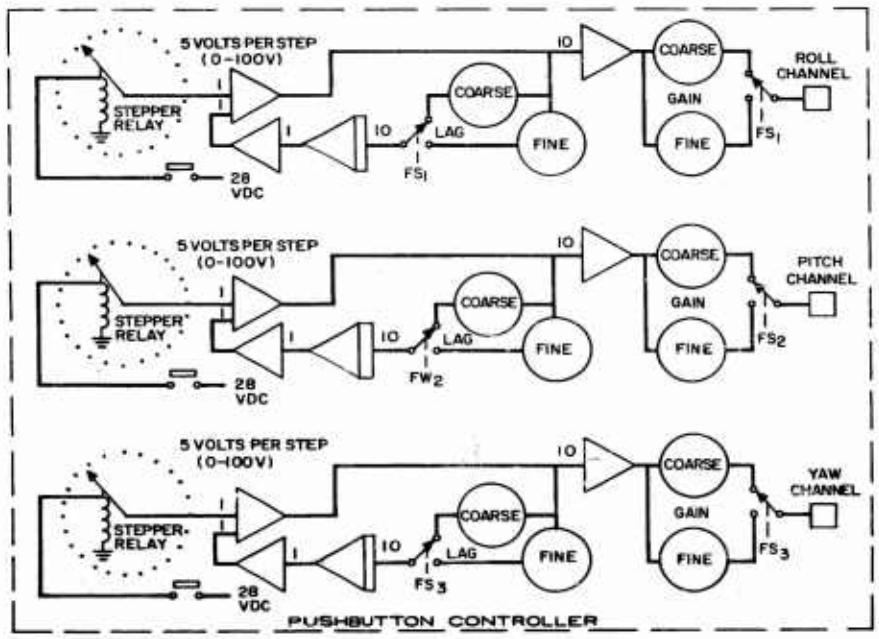
5 VOLTS PER STEP (0-100V)
STEPPER RELAY
28 VDC
COARSE
FINE
LAG
GAIN
ROLL CHANNEL
PITCH CHANNEL
YAW CHANNEL
PUSHBUTTON CONTROLLER

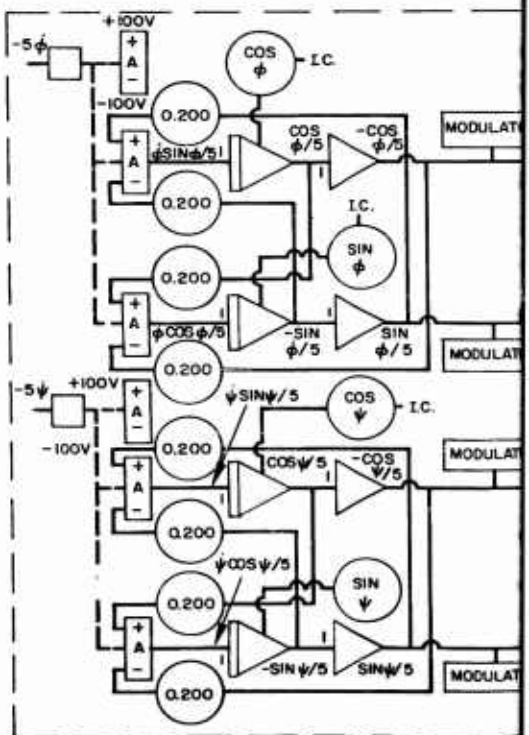
+100V
-100V
COS
SIN
I.C.
0.200
MODULAT

1

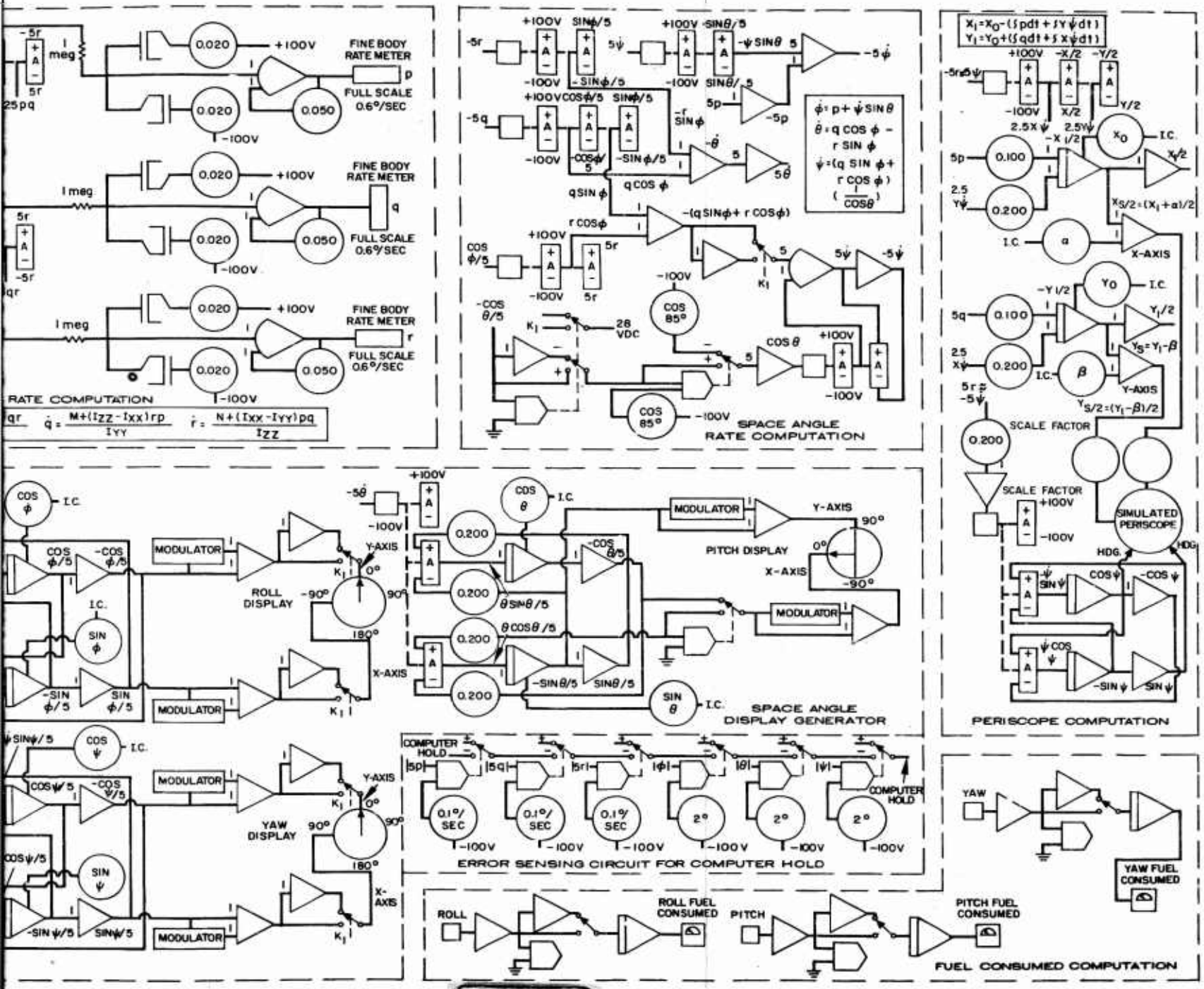

Figure 1. Analog Computer Representation

only the computations for a downward looking periscope. Programs for periscopes oriented in other directions (forward and off-axis) were used during the study but are not shown in Figure 1.

Display Console Design

The display console of the Man-in-Space Simulator is shown in Figure 2. Each display instrument is independently driven from the analog computation and any combination of display devices can be turned off to simulate simpler or degraded system performance.

Accessory Displays

The upper panel of the console contains the accessory displays of elapsed time and individual fuel consumption readouts for each axis of control.

Elapsed Time Readout. The elapsed time readout is the top meter on the upper panel. The three and one-fourth inch arc is scaled to read up to five minutes with major scale divisions at each minute and minor scale divisions for each tenth of a minute.

Fuel Consumption Readouts. The three meters on the lower part of the upper panel display the fuel consumptions in percent for roll, pitch, and yaw respectively from left to right. The one and five-eighths inch scale has divisions at each four percent with major divisions at multiples of twenty percent.

Attitude Displays

Information concerning vehicle attitude angles and the rates of spin about the axes of the vehicle are on the center and lower panels respectively of the display console in Figure 2.

Attitude Angle Displays. The three cathode ray tubes on the center panel are used to display the vehicle attitudes about each axis. The scope faces are three inches in diameter with one degree increments on the dial faces. From left to right, they represent roll, pitch, and yaw angles respectively. These three angles define unambiguously the angular

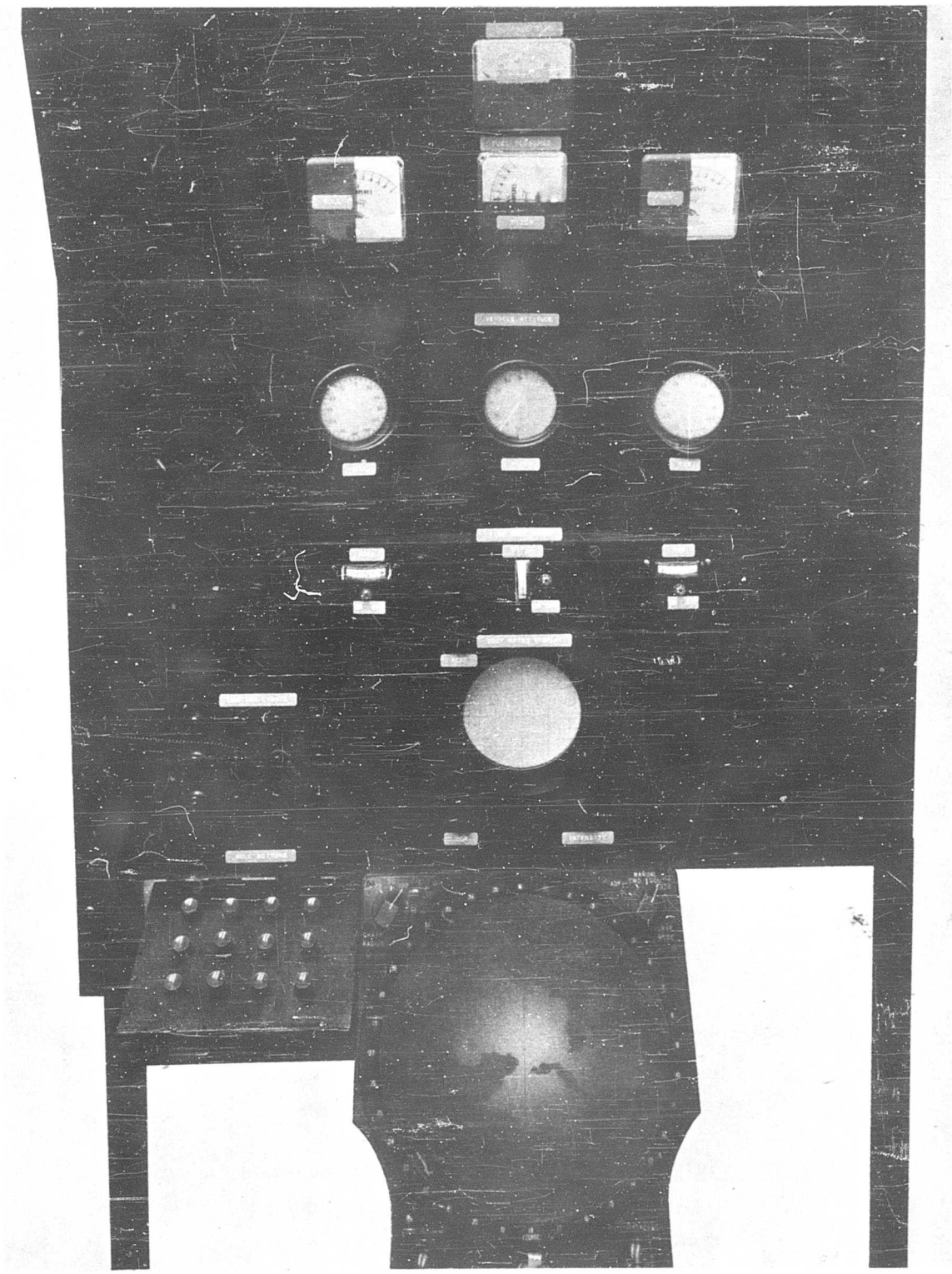

Figure 2. Display Console of the Man-in-Space Simulator

relationships between the set of orthogonal axes fixed in the vehicle (body axes) and the set chosen for display reference (reference axes).

Roll angle is defined as the angle formed by the lateral axis of the vehicle and the horizontal reference plane in a plane normal to the longitudinal axis of the vehicle. Roll angle is defined and displayed from the zero point, at the top of the dial, clockwise and counterclockwise through positive and negative angles, respectively, to a common 180° point.

Pitch angle is defined as the angle formed by the longitudinal axis of the vehicle and the horizontal reference plane measured in a plane normal to the horizontal reference plane. This angle is defined and displayed above and below the horizontal reference plane zero point, located at the nine o'clock position of the dial, from +90° to -90°.

Yaw angle is defined as the angle in the horizontal reference plane formed by the velocity vector and the normal projection of the vehicle longitudinal axis onto the horizontal reference plane. Yaw angle displacements are measured and displayed to the right and left of the velocity vector from the zero point at the top of the dial through positive and negative angles respectively around to the common 180° point.

The basic equations defining these angular relationships may be found in Appendix I.

Fine Body Rates. The fine body-rate meters are located on the lower panel just below the break line between the center and lower panels at approximately eye level for the seated subjects. Roll, pitch, and yaw body rates are arranged in left to right order. These meters present the rate of revolution about the body axes, defined conventionally as p, q, and r. The meters contain very precise rate information about the zero points. They are scaled so that a full scale deflection, from a center zero, 13/16 of one-inch travel, represents a rate of rotation of 0.6° per second. A rate deviation of 0.05° per second is easily readable on the meter.

Combined Body Rates. The five-inch cathode ray tube on the lower panel contains a combined presentation of gross body rates about all three axes. The small inverted "T" symbol, visible in Figure 2, translates along the X and Y axes of the scope face to indicate yaw and pitch rates, respectively. The deflection is scaled linearly so that a one-inch displacement

from the center along either axis represents a three-degree-per-second rate in the indicated direction. The symbol rotates about its own intersection point to display roll rates. This rotation is scaled so that a 45° rotation represents a roll rate of three degrees per second in the corresponding left or right direction.

External Viewing Port. At the bottom center of the console is a modified map display which projects a view of the earth's surface from 100 n. m. above the surface of the earth. The slide and projection are scaled so that the ten-inch diameter viewing surface represents a 180° field of view from a periscope. The projection translates through the X and Y axes to simulate a rotation of approximately 180° in either direction about either or both axes. The projection is also free to rotate continuously about the center.

The earth subtends a visual angle of approximately 154° from 100 n. m. and the earth can be driven completely out of view to simulate attitude angle changes. No attempt is made to simulate the relationships among celestial bodies on the slides used in this study. The visual angle subtended by the earth and the horizon to horizon surface distance are computed and faithfully reproduced on the projection. The view of the earth is centered in the Gulf of Mexico. This location was chosen to maximize the number of distinguishable and familiar land marks.

Secondary Task

To provide a more realistic experimental task and to provide a means for estimating the load on the operator while flying the simulator, a secondary, monitoring task is used. The 3 x 4 arrays of lights and pushbuttons on the lower left corner of the display console in Figure 2 are the stimulus and response boxes used for the secondary task.

This task requires the operator to discriminate a discrete stimulus (one light in the array) and select a discrete response (push the corresponding button to extinguish the light). This task simulates both the monitoring of system status function, via caution lights and out of tolerance gauges, and the performance of taking appropriate remedial actions such as switch throwing and button pushing.

Manual Controller Design

Five hand controllers have been fabricated for use in this program. Two are classified as discrete controllers and three as continuous or proportional controllers. All controllers are mechanized to simulate acceleration inputs to the controlled axes. All controllers can be operated with either hand. In these studies only right hand operation is utilized. A standard straight back chair, modified to have a right hand arm rest, is pictured in Figure 3. The arm rest design permits the hand controllers to be removed and replaced quickly.

Discrete Controllers

The two controllers in the discrete class are a toggle-switch controller and a pushbutton controller.

On-Off Toggle Switches. Figure 4 depicts the controller consisting of three toggle switches mounted vertically on a control box. The insert photo in Figure 4 illustrates the mounting of the on-off toggle controller box on the arm rest. Accelerations about the roll and yaw axes are controlled by the outboard switches on the left and right respectively. The center switch controls the accelerations about the pitch axis. The roll and yaw switches are thrown laterally for left and right acceleration inputs. The pitch toggle is thrown fore and aft as a conventional aircraft joystick. All three switches are spring loaded center-off toggles capable of being held in either on position. Momentary contact in either on position can also be accomplished by flicking the switches. Seven ounces of force are required to actuate the toggles.

Pushbuttons. The pushbutton controller is depicted in Figure 5. The controller has six buttons, one for each direction of each axis. The two buttons on the left control left and right roll. The two center buttons, arranged fore and aft, control pitch up and down respectively. The buttons on the right control left and right yaw. The small toggles directly above each axis grouping select a ten to one gain change.

One depression of a button simulates the release of a metered impulse of energy establishing a specific increment of angular velocity. The rate increment can be cancelled by depressing the button for the opposite direction

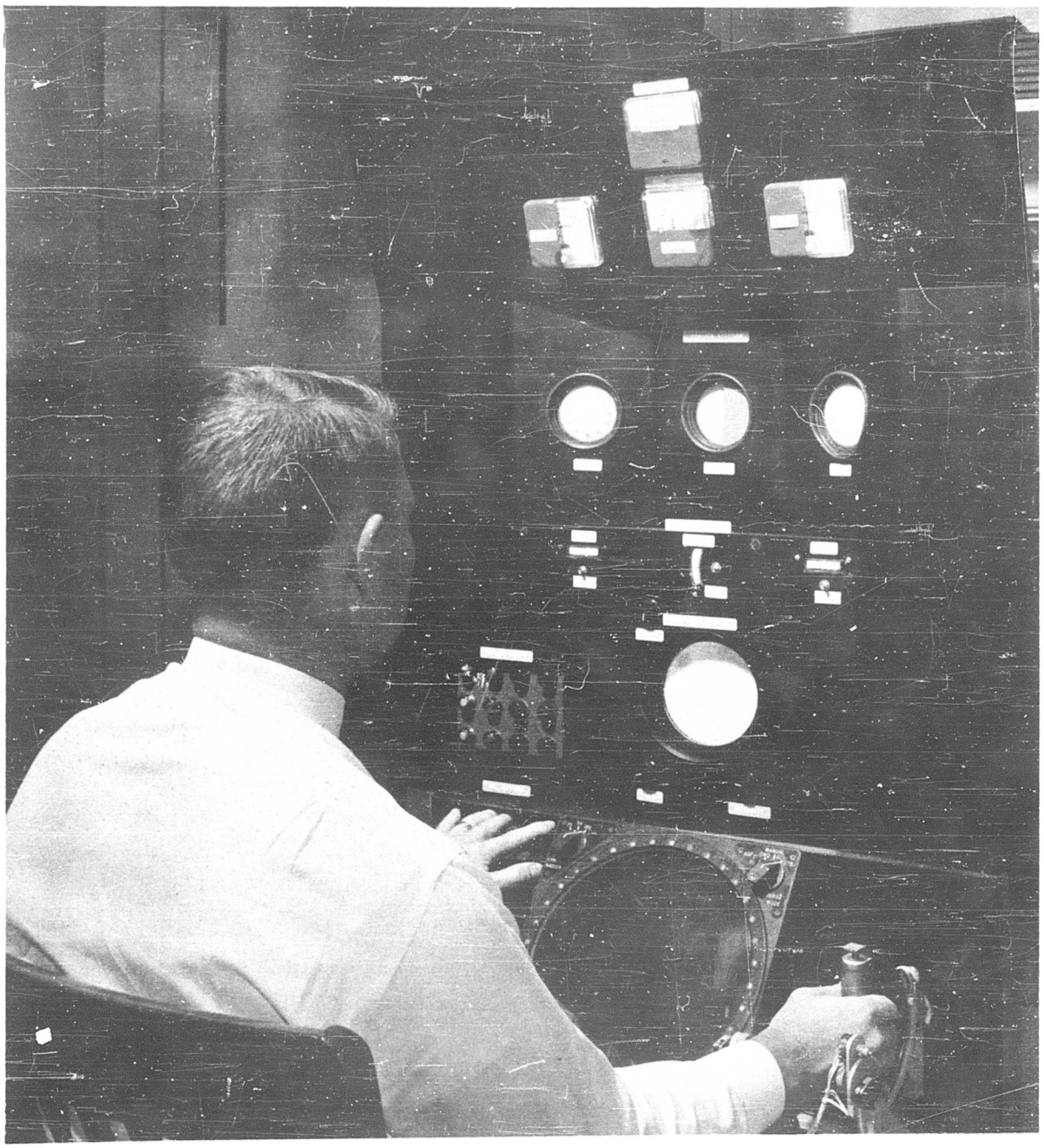

Figure 3. Pilot-Subject Seated in Front of the Display Console

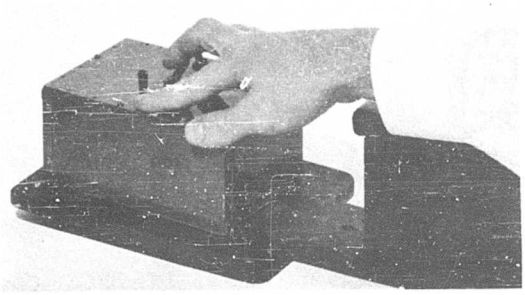

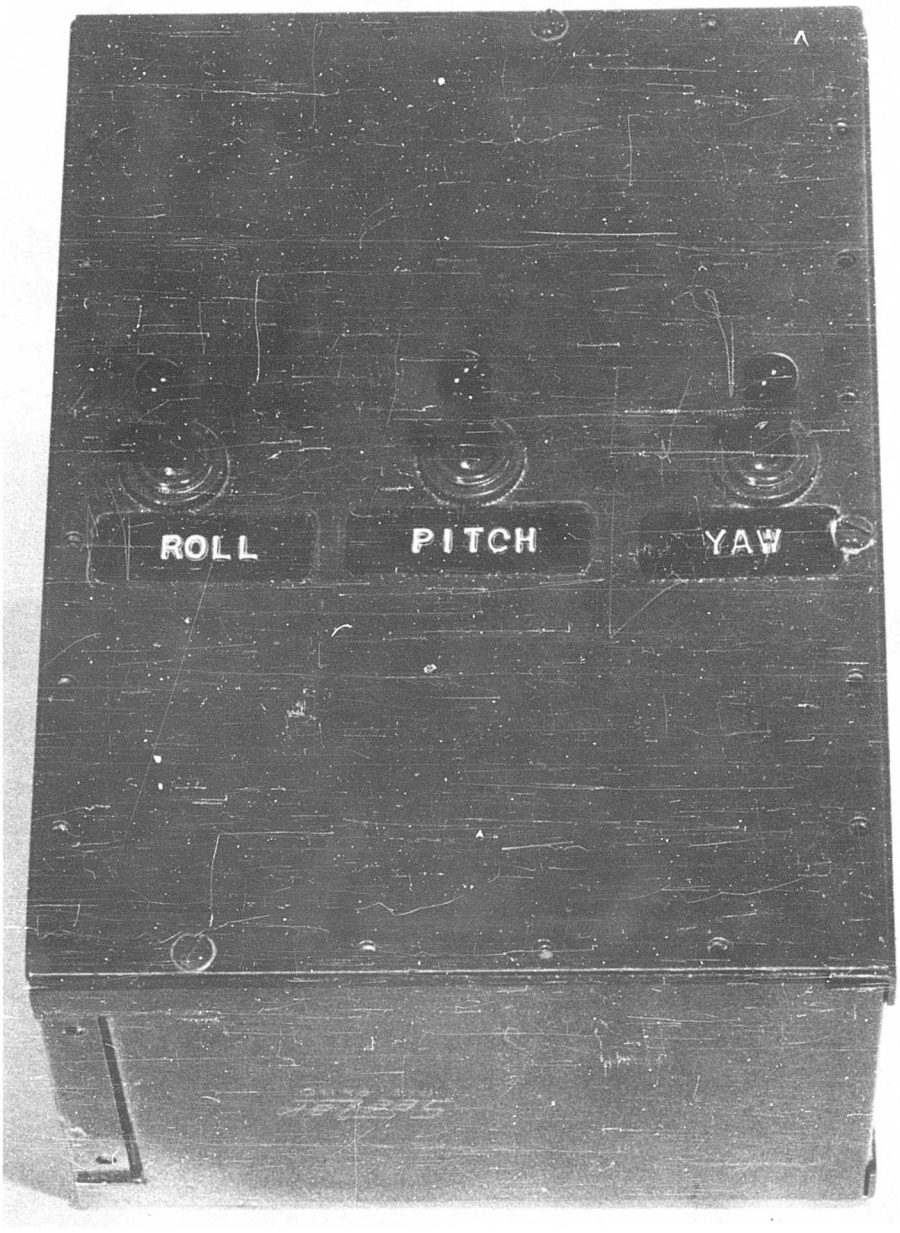

Figure 4. On-Off Toggle Controller

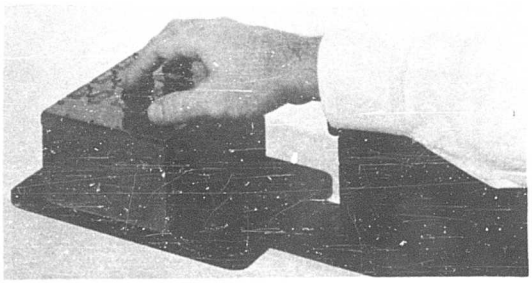

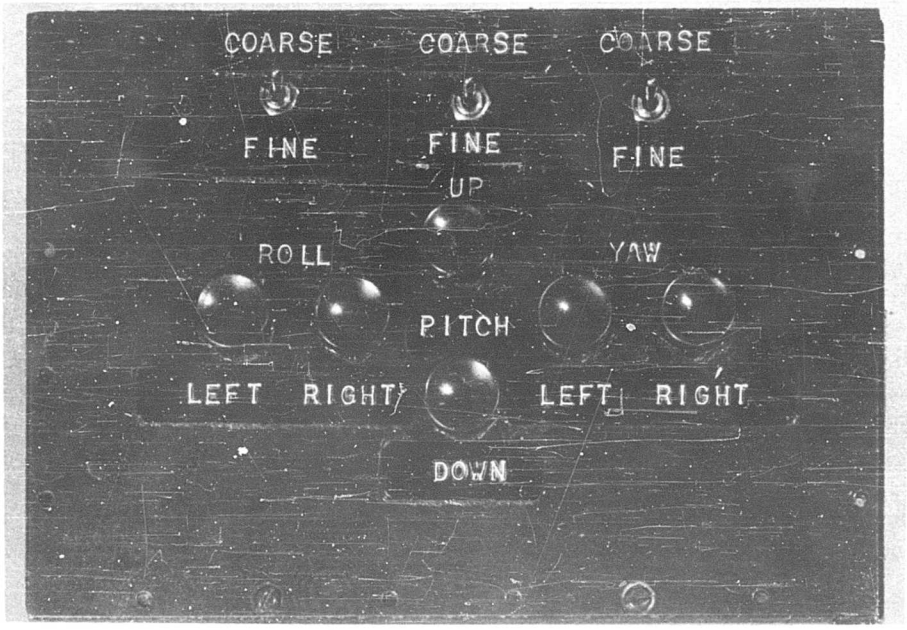

Figure 5. Pushbutton Controller

of the same axis. Twenty-three discrete steps are available in each direction for each axis. The controller can be mechanized so that each depression or beep will result in any desired preset rate increment with a gain change of ten to one available from the coarse mode to the fine mode. The pushbuttons have a breakout force of four ounces. Forty-four ounces of force are required to depress the buttons 1/16 of an inch to the activate point.

Continuous Controllers

Three continuous or proportional controllers were utilized in the program. They are: (1) a combined three-axis hand controller, (2) three single-axis, finger-operated wheels, and (3) three single-axis sticks. All of the control devices have a well-defined, spring-loaded, center-off detent.

Combined Three-Axis. The combined three-axis hand controller is pictured in Figure 6. The controller is rotated about the wrist pivot point for all axes. Rotation in the vertical, longitudinal plane causes angular acceleration about the pitch axis. Rotation in the vertical, lateral plane controls roll acceleration and rotations in the horizontal plane controls acceleration about the yaw axis. The forearm can be secured against acceleration forces without impairing control movements. A plunger on top of the grip locks the roll axis when depressed and can be easily released by pulling the plunger head back out of a detent. The controller has linear force gradients of 0.33 ounce per degree after a breakout force of 7 ounces in the roll axis, 0.10 ounce per degree after a breakout force of 18 ounces in the pitch axis, and 0.36 ounce per degree after a breakout force of 16 ounces in the yaw axis.

Single-Axis Wheels. The controller utilizing an individual finger-operated wheel for each axis appears in Figure 7. The wheels are four inches in diameter. The roll-axis wheel is located on the lower center of the control box, mounted vertically and perpendicular to the longitudinal axis of the vehicle. It is normally operated by the thumb of the right hand. The pitch wheel is on the right center of the control box, mounted vertically and parallel to the longitudinal axis of the vehicle. It is normally operated by the little finger of the right hand. The yaw wheel is mounted on the upper center of the box in a horizontal position. It is normally operated by the index finger of the right hand.

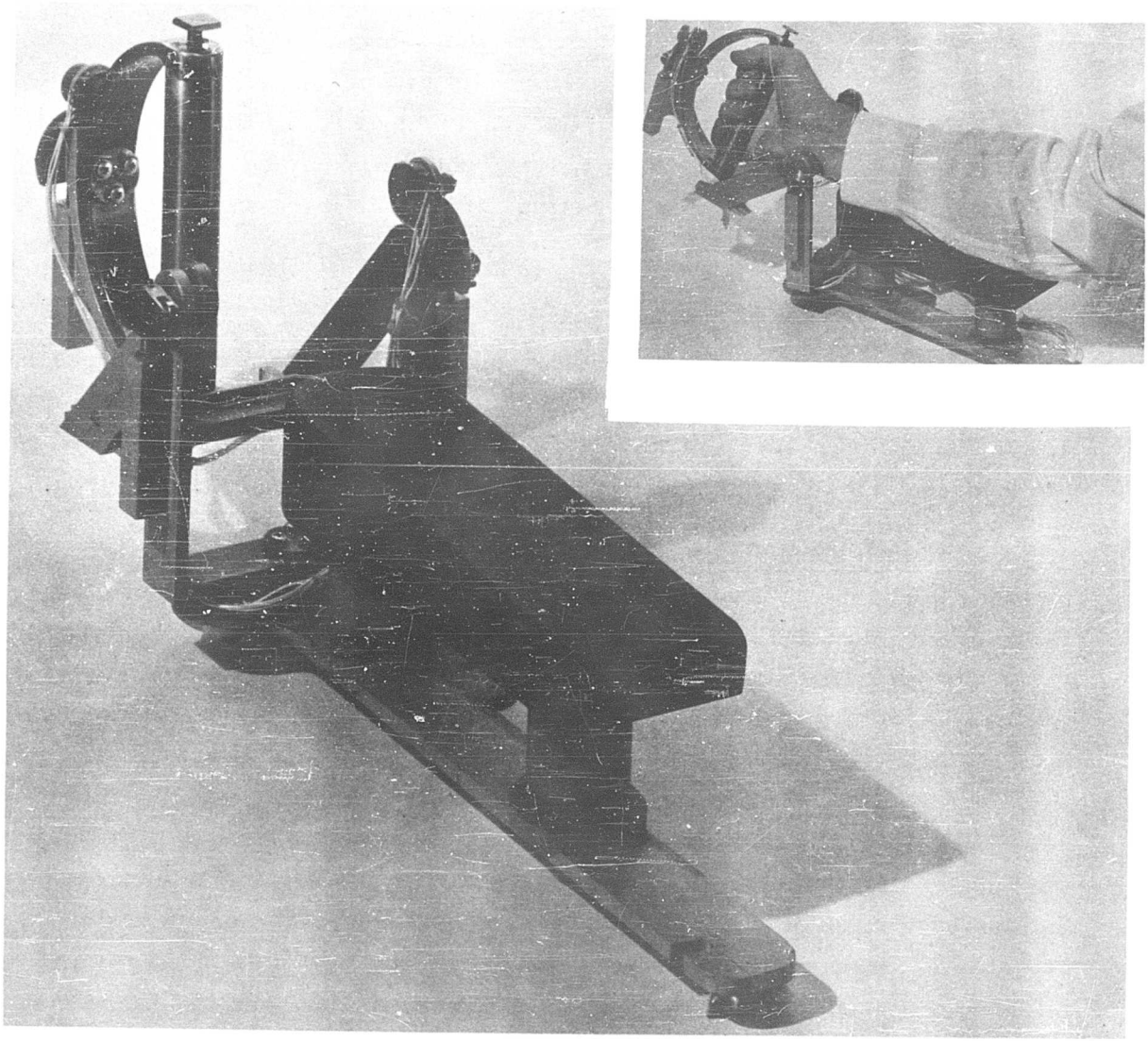

Figure 6. Combined Three-Axis Hand Controller

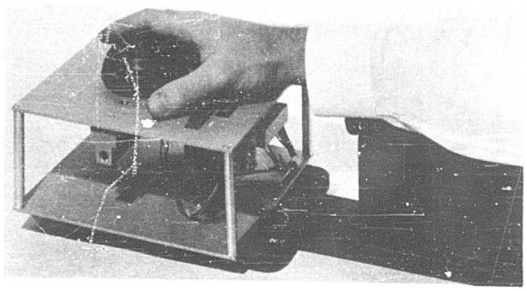

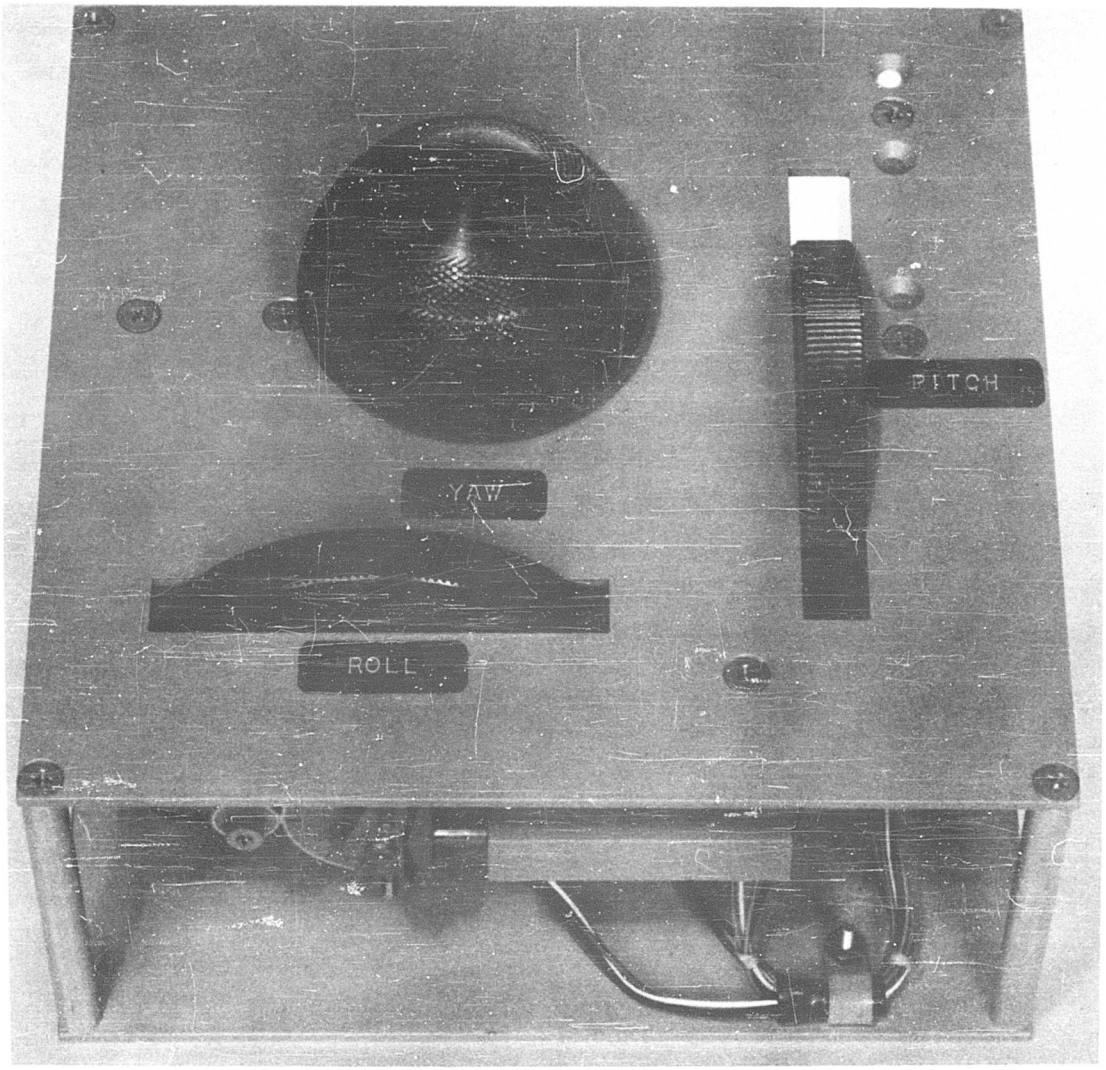

Figure 7. Single-Axis Wheels

The wheels have a force gradient of 0.13 ounce per degree of rotation with a breakout force of 3.3 ounces.

Single-Axis Sticks. The controller, consisting of three hand-operated sticks, is shown in Figure 8. The stick on the left controls the roll axis and is thrown left and right of vertical. The center stick, slightly forward, moves fore and aft to control pitch. The stick on the right is thrown left and right to control yaw. The sticks are 3/4 inch in diameter and four inches long. They are mounted vertically at the corners of an equilateral triangle with five inches on a side. The sticks have a force gradient identical to that of the single axis wheels when the force is measured two inches from the axis of rotation, i.e., two inches.

PRELIMINARY STUDIES

Pilot studies were conducted early in the program to determine the variance of manual performance due to major system configuration changes and to determine the general regions of optimum performance on such variables as torque-to-inertia ratios, scaling of displayed information, actuator delays and hand controller design.

Torque-to-Inertia Ratios

The first preliminary study was concerned with the effect of torque-to-inertia ratio on system performance. Torque-to-inertia ratio refers to the ratio of the torque resulting from the maximum actuator output to the vehicle moment of inertia about a given axis. This ratio provides a convenient parameter of a general design nature since the actuator torque rating and actuator lever arm need not be individually specified. It is analogous to system gain since it determines the speed of response of vehicle body rates to manual acceleration control inputs.

The task consisted of zeroing initial body rates of three degrees per second about each of the three axes. The integral of applied torque about each axis was automatically normalized for vehicle inertia. This measure is proportional to fuel used for a particular vehicle's inertia values, actuator lever arms and actuator efficiency. Equal torque-to-inertia ratios about each axis were utilized.

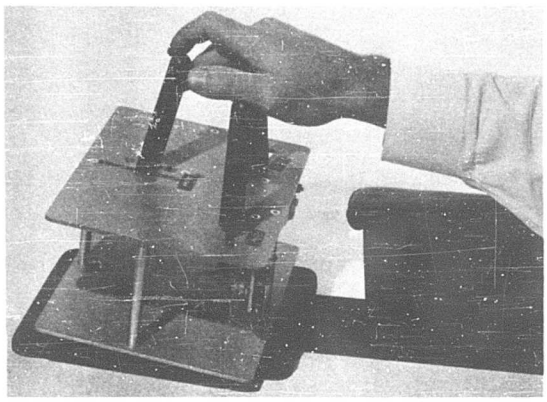

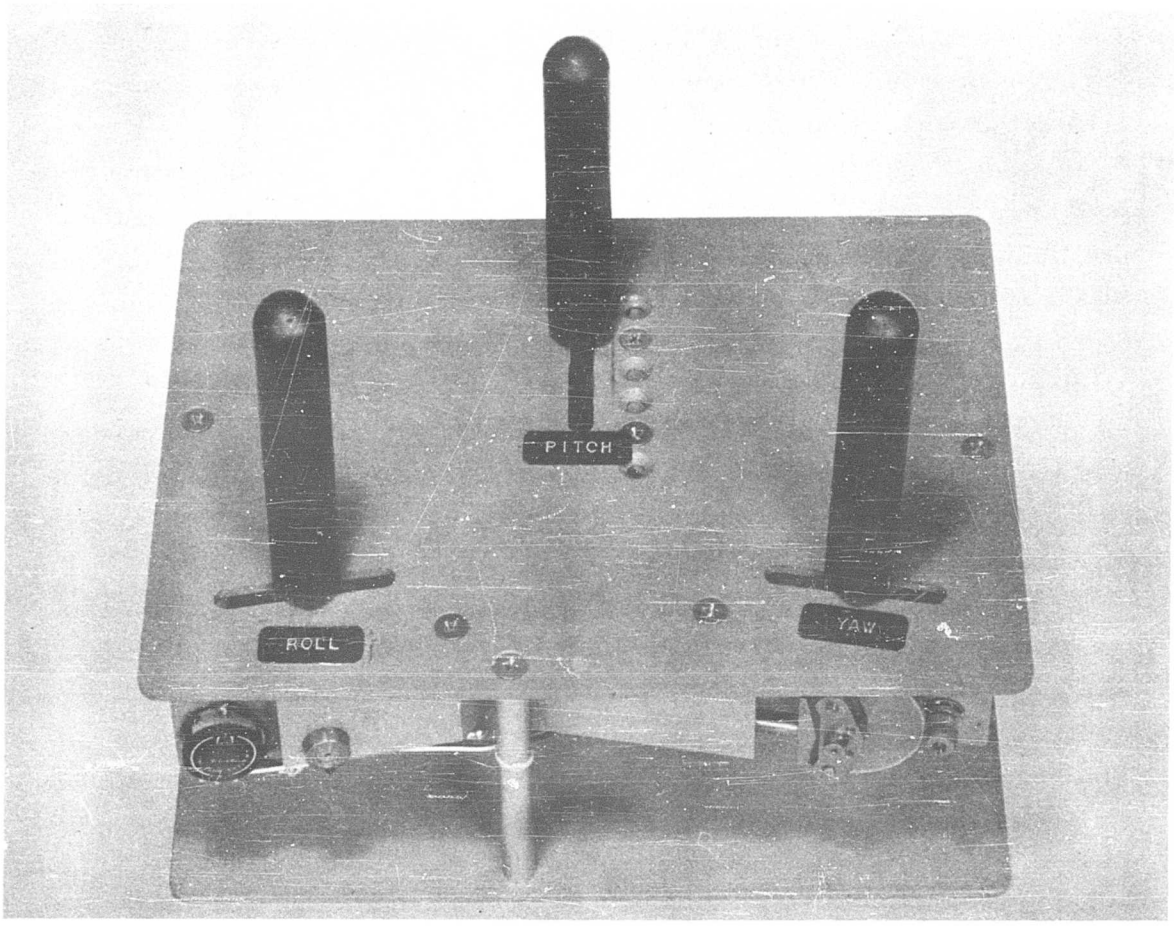

Figure 8. Single-Axis Sticks

From these studies it was concluded that the region of optimum torque-to-inertia ratio would lie somewhere between 0. 01 and 0. 05.

Effects of Cross-Coupling

The effects of two types of vehicle configuration were studied. The first involved two equal moments of inertia larger than the third. For this class of vehicle shape, there are no cross-coupling torques about the axis with the smallest moment of inertia, and the other two body rates vary sinusoidally with time. In these studies the roll-axis moment of inertia was made smallest.

The second type of vehicle configuration involved three unequal moments of inertia in the order of roll smaller than pitch and pitch smaller than yaw. The cross-coupling effects, in the form of changes in body rates, ranged in the reverse order of the moments of inertia with the roll axis exhibiting the greatest cross-coupling effect.

It was found that fuel consumption increased in the stabilization task with the presence of cross-coupling effects. The primary result of these preliminary studies of cross-coupling effects was the development of control techniques or strategies to minimize fuel consumption.

For the vehicle with two equal and larger moments of inertia the best strategy evolved was to zero the roll rate when the body rate about one of the other axes was at zero. When the roll rate was canceled, the cross-coupling was eliminated and the second body rate would remain zero. The third body rate could then be controlled to zero. Thus, the vehicle could be stabilized by expending energy in only two axes.

The best control strategy for a vehicle with three unequal moments of inertia was to zero the rate about the axis with the smallest cross-coupling effect (largest moment of inertia) at the same instant that the cross-coupling effect is driving the axis with the smallest moment of inertia to zero rate. This maneuver stops the cross-coupling effects, two of the body rates would then remain zero and the third could be controlled to zero. This technique, like the former, allows the vehicle to be stabilized while energy is expended in only two axes.

Actuator Time Delays

The effects of actuator delays of the exponential type were studied briefly. Root locus techniques were used to estimate the effects of these time delays upon system stability with moderate success. It was shown that the addition of small time delays could be adequately compensated by the pilot changing both his gain and the amount of anticipation. However, if time delays are in the vicinity of 0.25 second it is necessary for the pilot to exceed the anticipatory capability which is considered to be maximum, Conklin (1957) and Adams (1961).

Since actuator time delays are expected to be about 0.01 second for inertia-wheels, about 0.10 second for a hydrogen peroxide system, and from 0.003 to 0.05 for a bipropellant system, it was decided that actuator time delays would not be included as a variable in any further experimentation.

Controller/Information Content/Maneuver Comparisons

The preliminary investigations comparing controllers, information content conditions and types of maneuvers were performed primarily to determine control strategies for minimum fuel usage to stabilize a tumbling vehicle to a specified attitude, to change from one static attitude to another static attitude and to maintain an attitude while the vehicle is perturbed by random energy inputs. The latter task, hereafter called the tracking task, simulated rate damping during re-entry maneuvers, minor misalignments of thrust during main engine firings, and noise in the gimbal systems of main engines during firing.

During the initial phases of the study, it became apparent that the maneuver involving a change from a static attitude to another static attitude was quite simple. The performance measure, energy used to change attitudes, varied as a simple inverse function of the time to perform the attitude change. This confirms the analytical conclusions of Kirkman (1962). Energy consumption for this maneuver was very stable across all subjects and display/control conditions. Consequently, it was decided not to use the attitude change maneuver in further investigations.

The five hand controllers used in the preliminary experiments were the (1) on-off toggle switches, (2) pushbuttons, (3) combined three-axis, (4) single axis wheels, and (5) single-axis sticks. The first two controllers allow discrete energy inputs and the last three allow continuous or proportional energy inputs.

In keeping with the objective of studying minimum manual systems, all controllers were mechanized as acceleration controllers. In an acceleration control system, only simple mechanical or electrical links between the hand controller and the reaction jets are necessary.

By displaying the body rates directly to the pilot, an evaluation could be made concerning the value of body-rate information to a minimum manual control system while keeping the order of the control system at the acceleration level. Although the body-rate information could have been used either as a control loop feedback signal to yield a manual rate control system or as a quickening signal to the attitude readouts, it was felt that these alternatives would result in an additional increase in over-all system complexity and additional sources of unreliability.

From performance data, experimenters' observations, and pilots' comments during these preliminary studies, it was quite apparent that the three single-axis sticks provided an inferior means of control. Control movements in more than one axis were nearly impossible to make with one hand operation. The size and arrangement of the sticks on this type of controller is critical. The sticks in this study were four inches only and 3/4-inch in diameter. They were placed at the corners of a five inch equilateral triangle. It is felt that smaller sticks arranged more compactly might be a more adequate design. Scheduling limitations precluded the fabrication of another controller of this type. Consequently, only the other four controllers were used throughout the remainder of the study.

The rate increment to be used for the pushbutton or beep controller was investigated in the preliminary studies. The increments were varied from 0.02 degree per second to 1.5 degrees per second. Minimum error was achieved for the tracking task with a rate increment of 0.25 degree per second. It was observed, however, that no one gain was adequate for performing the stabilization maneuver. The control energy must be high enough to overcome the effects of cross-coupling and low enough to allow fine adjustments. Optimum performance of the stabilization maneuver was achieved with the rate increments set at 0.75 and 0.075 degree per second for the coarse and fine modes, respectively.

It was during the preliminary studies that it became apparent that both coarse and fine scaling would be required on the body-rate displays. In order to keep the displays independent, the fine body-rate meters were added to the

display console. This was also the quickest and most economical way to present the dynamic range of body-rate information required. The alternatives that were discarded were non-linear or logarithmic scaling of body rates and coarse-fine gain changes.

Performance Measure Evaluation

Two system performance measures were utilized. For stabilization and static attitude change maneuvers, a measure of energy expended to perform the maneuver was devised. This was the integral of the commanded accelerations for each axis. For example, if the task were to stabilize the vehicle from a three degree-per-second rotation about each axis, the minimum integral of acceleration required would be three degrees per second about each axis. By overcontrolling, control input reversals and overshooting, the integral of commanded acceleration could be much higher. The integral of commanded acceleration could be converted to exact fuel usage when the vehicle geometry, mass distribution, moment arms, and specific impulse of fuel are fixed. The techniques for making the integral of acceleration to fuel conversion will be covered in the section on the experimental comparison of cross-coupling effects and vehicle shapes. For the tracking task, the rms of the angular deviation from the desired attitude was summed over all three axes and used as the measure of system performance.

Secondary Task

For all three tasks, a secondary performance measure was used to indicate the operator loading while performing the maneuver. The physical description of the secondary task is found in the simulation section of this report. Twelve stimulus lights, arranged in a 3 x 4 array, were programmed to come on in random sequence at five different time intervals of 2.3, 4.2, 5.4, 6.5, and 12.9 seconds. The lights were to be extinguished by depressing the button in the corresponding button array located directly beneath the lights.

The secondary task was included not only as an index of loading but to induce more stress into the laboratory situation to add realism. Garvey and Taylor (1959) give an excellent discussion of the rationale behind the use of secondary tasks in laboratory experimentation.

An a priori decision was made that the index of operator loading should increase as a convex function of increasing reaction time on the secondary task. Thus, the loading index would be more sensitive in the range of minimum and median response times and less sensitive in the upper ranges of response times.

EXPERIMENTAL STUDIES

The purpose in the main experimental program was to determine the effects of major system configuration parameters on performance measures such as fuel expenditure, system stabilization, and operator loading.

The primary experimental technique utilized was the performance of typical attitude control tasks during the simulated flight of a spacecraft. The displays and controls were mechanized through the analog computer to yield accurate dynamic representations of the mechanics of motion and of energy consumption for various attitude control maneuvers.

The four main experimental programs were: (1) torque-to-inertia ratio investigations, (2) controller-information content comparisons, (3) effects of gyroscopic cross-coupling and (4) a comparison of external viewports and attitude instruments or displays.

Torque-to-Inertia Ratio Investigations

It was desired to investigate the effects of varying torque-to-inertia ratios on system performance. From the preliminary studies it was concluded that the optimum ratio fell in the range from 0.01 to 0.05 while performing a stabilization maneuver. A torque-to-inertia value is equivalent to acceleration in radians per second. The torque-to-inertia ratio is analogous to system gain and the ratios used in this study were equal about the three axes.

Method

Two Hughes pilot-engineers served as subjects, using the combined three-axis controller and the on-off toggle switch controller. Both controllers were acceleration controllers and were described earlier in this report. Both subjects had professional pilot experience with approximately 1,200 hours of flying time each. One pilot was current as an FAA certified flight instructor, with ratings for single-engine, multi-engine,

and instrument instruction. The second pilot was a former Air Force jet fighter pilot with operational all-weather interceptor and fighter-bomber experience.

Both subjects used the on-off controller first. The subjects started at opposite ends of the torque-to-inertia ratio range and were given an ascending-descending series, or vice-versa, for both controllers. The ratios of torque-to-inertia used were 0.01, 0.02, 0.03, 0.04, and 0.05. The subjects received sixteen trials at each torque-to-inertia ratio, eight trials on the first run up or down the range and eight on the return series.

The secondary task was mechanized so that the lights appeared at equal time intervals in random sequence. For each torque-to-inertia ratio, controller, subject, and ascending-descending series, two ninety-second trials were performed at each of four frequencies of stimulus lights. The frequencies of stimulus lights were always presented in ascending order from low to high frequency. The frequency values utilized were 15, 20, 30, and 40 lights per minute.

The subjects' task was to maintain the vehicle attitude while random disturbing torques were applied to the pitch and yaw axes, i.e., two-dimensional compensatory tracking. Body-rate information was available from both the combined coarse body-rates display and the separate, fine body-rate displays.

The error signal was composed of the sum of four sine waves, the amplitude and frequency components of which appear in Table I. The sine waves, when summed, yield an rms value of 0.191 deg/sec^2 of acceleration which results in a rate error signal with an rms value of 1.14 deg/sec. A ninety second segment of the random noise signal was recorded on tape. The tape ran continuously between trials. Thus, the error signals for each ninety second trial were identical with respect to energy content but each trial started at a different point on the error signal tape. The performance criterion was the mean square error of angular deviations about the zero attitude points summed about all three axes.

Results

The ms angular error at each torque-to-inertia ratio was averaged over subjects and secondary task frequencies and is plotted in Figure 9.

Table I

Amplitude and Frequency Components of the Sine Waves Summed to Form the Error Signal

Sine Wave	Frequency cps	Amplitude Rad/Sec
1	0.20	0.02
2	0.14	0.04
3	0.13	0.02
4	0.11	0.02
5	0.02	0.02

It can be seen that the best performance occurs in the 0.03 region of torque-to-inertia ratios for both controllers. In Figure 10, it can be seen that the best performance occurs at the 0.03 torque-to-inertia ratio across all levels of frequency on the secondary task.

Discussion

The 0.03 torque-to-inertia ratio is equal to an acceleration capability of $1.72^{o}/sec^{2}$ which is roughly equivalent to one tenth of the average acceleration value fed into the system via the noise signal. Although it seems that there was a very sharp optimum point at 0.03 on the torque-to-inertia ratio range, it must be emphasized that this point was highly dependent on the energy level of the noise signal used in this study. If energy levels expected in the operational system are below the values used in this study, it is anticipated that the optimum torque-to-inertia would be lower. Conversely, for higher energy levels, the optimum torque-to-inertia range should be higher.

Also, time constraints on stabilization and attitude change maneuvers may dictate the use of larger torque-to-inertia ratios. It is expected that the use of higher torque-to-inertia ratios to meet time constraints would

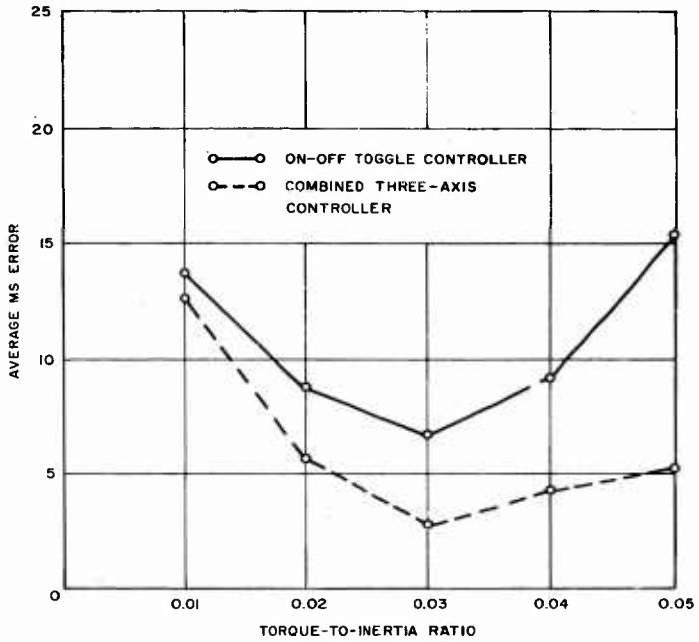

Figure 9. Mean Square Angular Error at Each Torque-to-Inertia Ratio Averaged over Subjects and Secondary Task Frequencies

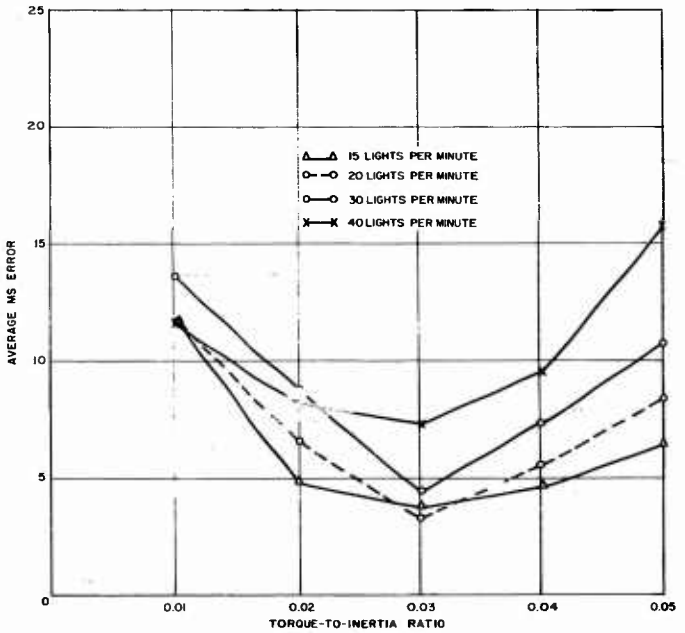

Figure 10. Mean Square Angular Error at Each Torque-to-Inertia Ratio for all Subjects and Controllers

result in more overshoots and overcontrolling particularly with discrete controllers and thus reduce system efficiency in terms of fuel consumption. Utilization of a non-linear response in a proportional controller could also lead to different optimum torque-to-inertia ratios.

Controller-Information Content Comparisons

Of prime interest to manual control system designers and human factors engineers are the configuration and input modes of the manual control devices and the content and form of information displayed. The main control configurations in this study centered around the energy input mode of the controllers and not the physical characteristics and appearance of the input devices. Two general classes of input modes were used, (1) the discrete-step input mode and (2) the continuously variable or proportional mode.

The primary information variable was concerned with the content of information displayed. The form of the displayed information was of secondary concern. In this case, the presence or absence of body-rate information was the primary display variable.

No attempt is intended to discount the importance of anthropometry effects on controller design or the importance of the scaling of displayed information. The hypothesis presented here is that display scaling or redesign of controller feel characteristics will be relatively ineffective unless the essential information is available to a pilot and an efficient control mode is being used. The work of Heinemann (1961) and Fuchs (1962) supports this hypothesis.

Experiments were conducted to investigate variance in pilot performance for two types of attitude control maneuvers in a simulated spacecraft under two display conditions with each of four hand controllers. The two maneuvers performed were the two dimensional tracking task described earlier and a stabilization task. The stabilization task required the pilot to cancel the body rates of a tumbling vehicle in order to bring the vehicle to a static position aligned with the attitude reference system. To minimize fuel consumption the pilot had to interpret the dynamic relationships among the three body rates and three attitude angles in order to choose the most efficient control strategy and to determine the opportune time to initiate corrections. Both the cross-coupling effect and the angular interaction

effect had to be perceived and understood to allow a minimum-fuel solution.

Method

Four Hughes engineers who are licensed pilots served as subjects. Each pilot-engineer received individual indoctrination and training before participating in the experiment. Indoctrination and training sessions were conducted to standardize the subject's knowledge of methods of controlling the attitude of a space vehicle as well as to provide practice on the two specific tasks to be performed during the experiment. Optimum control strategy for vehicles with different ratios of moments of inertia about their axes and their respective cross-coupling effects were demonstrated. Particular emphasis was given to the inertia distributions of the vehicle to be used in the experiment.

When orientation sessions were completed practice sessions were begun. The subjects practiced performing each task until they had reached a stable performance level.

The two maneuvers the pilots performed were: (1) stabilization of a tumbling vehicle to an attitude aligned with the inertial reference system and (2) maintenance of an established attitude aligned with the inertial reference system while the vehicle is perturbed by influences external to the attitude control system in the pitch and yaw axes, i. e., two dimensional tracking. To signify the end of a stabilization maneuver the computer went into automatic hold when the attitudes and body rates about all axes were simultaneously within two degrees of zero and within 0.1° per second of zero, respectively. For the tracking task, each trial lasted for a 90 second period after which the computer went into hold automatically.

Two complete 4 x 4 x 2 factorial designs were used, one for the tracking task and the other for the stabilization task. The three independent variables investigated in both cases were:

1. Pilots (four levels)
2. Controllers (four levels)
   a. Toggle
   b. Pushbutton
   c. Combined three-axis
   d. Wheels

3. Information Content (two levels)
   a. Body-rate and attitude information
   b. Attitude information only

Four trials were conducted per experimental condition. The first trial at each condition was a warm-up trial, and the final three were experimental trials. The components of variance model for these studies was:

$$E(X_{ijk}) = \mu\ldots + \alpha_i + \beta_j + \gamma_k + {}^{\alpha}\beta_{ij} + \alpha\gamma_{ik} + \beta\gamma_{jk} + \alpha\beta\gamma_{ijk} + e_{m(ijk)} \quad (1)$$

where:

α_i = the i^{th} level of variable A, pilots
β_j = the j^{th} level of variable B, controllers
γ_k = the k^{th} level of variable C, information content
$\mu\ldots$ = the general mean of the population
$e_{m(ijk)}$ = experimental error
$E(X_{ijk})$ = the expected value of the observation in the ijk^{th} cell of the experiment.

Pilots and controllers were considered random factors, and information content was considered to be a fixed factor. Expected mean squares for each variance source were derived according to the procedure suggested by Bennett and Franklin (1954).

The four pilots performed the two different maneuvers with each of the four controllers under the two different information conditions. The order of presentation of the controllers was counterbalanced between pilots. The order of performance of the two maneuvers with and without rates was counterbalanced within pilots and across controllers.

The four controllers are described earlier and are pictured in Figures 4, 5, 6 and 7. Two of these controllers, the finger-operated toggle switches and the pushbuttons, belong to the discrete class of controllers. The other two, the combined three-axis hand controller and the finger-operated single-axis wheels, are continuous or proportional controllers.

The display console used in this study was the one described earlier in the Simulation Section and shown in Figure 2. The display

contained attitude angle information for each of the three axes, plus the combined gross body-rate display and fine body-rate readouts showing the rates of spin about each axis. Individual fuel consumption meters for each axis, a meter showing elapsed time and the stimulus lights for the secondary task were also displayed. A green light, in the console at approximately eye level, was activated at the conclusion of each trial. Under the condition of no body-rate information, the coarse and fine body-rate readouts were turned off.

The performance criterion for the stabilization task was the integral of commanded acceleration summed about each axis, with the restriction that the maneuver be completed within five minutes. Failure to complete the maneuver within the time limit resulted in the trial being repeated.

It was necessary to repeat only a very few trials because the time limit was exceeded. It was possible to complete the stabilization maneuver within two minutes. The time limit was exceeded because of conceptual errors in interpreting the dynamic relationships between the rotational motions and vehicular attitude. As a result, opportune sets of conditions from which to initiate the stabilization maneuver were not recognized. For almost every trial in which the time limit was exceeded few, if any, control inputs had been made. Consequently, failed trials were independent of performance on the primary criterion of fuel consumption.

The total fuel consumed was computed by weighting the obtained integral for each axis by the ratio of the moment of inertia in that axis. The weighted integrals were then summed to yield the relative measure of total fuel consumption. Performance on the tracking task was measured in terms of the rms angular error about each axis during a 90-second period. An estimate of operator loading was obtained by measuring response time to the secondary task.

The pilot's station was placed in an enclosed room to minimize distractions to the subjects flying the simulator. Two-way communication between the pilot and the experimenter was accomplished by two Western Electric type 15-A operator's headsets. The subject's microphone was hot and the experimenter's had a press-to-task button.

For the stabilization task the body rates about each of the three axes were always three degrees per second. The eight possible body-rate directional combinations were paired with four non-zero initial attitude angles to make up the eight sets of initial conditions shown in Table II. The order of presentation of the initial conditions for the stabilization task was randomized within controllers and subjects.

The stabilization trials were initiated from an off-axis attitude to preclude the effect obtained by Ritchie et. al. (1960). Their subjects started tumbling from a zero-zero-zero attitude condition. They would cancel rates before any attitude errors had appeared. Thus the task became one of damping out the step input in rates at the start of each trial. It was desired in the studies described here to investigate the ability of subjects to interpret angle and rate relationships with continuous and simultaneous revolution about all three axes.

Table II

Eight Initial Conditions of Body Rates and Attitudes used in the Experimental Program

Rates: Three/Degrees/Second			Attitude Angles		
Roll	Pitch	Yaw	Roll	Pitch	Yaw
Right	Down	Left	L 45°	Up 60°	180°
Right	Up	Left	R 45°	Up 60°	180°
Left	Up	Left	R 45°	Down 60°	180°
Right	Up	Right	L 45°	Down 60°	180°
Left	Up	Right	R 45°	Up 60°	180°
Right	Down	Right	L 45°	Up 60°	180°
Left	Down	Right	R 45°	Down 60°	180°
Left	Down	Left	L 45°	Down 60°	180°

The vehicle configuration simulated for the experiment was a short cylinder with a distribution of moments of inertia in the ratio of 1:4:4. In this case, with two equal moments of inertia larger than the third, there were no cross-coupling torques about the roll axis which had the smallest moment of inertia. The other two body rates varied sinusoidally with time.

The on-off toggle controller, the combined three-axis hand controller and the three single-axis wheels were mechanized to provide a maximum torque-to-inertia ratio of 0.04. The pushbutton controller was mechanized so that each depression or beep resulted in a rate increment of 0.75^{o} per second in the coarse control mode and 0.075^{o} per second in the fine control mode. These values for the pushbutton controller were utilized in the stabilization maneuver only. A fixed value of 0.25^{o} per second was used for the tracking task.

After the completion of the controller-information content experimental studies, a pair comparison study was conducted in order to obtain the subjects' preferences for the four different controllers they had used in the experiments.

Each controller was paired with all others for all task and display conditions. Two decks of cards were prepared. The order of presentation of the controllers in pairs was reversed between decks. Each pilot made judgments between all of the pairs. Two pilots used the first deck and two used the second. A total of ninety-six judgments was made.

Results

The pilots' performances on the stabilization and tracking maneuvers will be treated separately.

Stabilization Task: The analysis of variance of fuel consumed is summarized in Table III. Total fuel measures were transformed to logs in order to meet the homogeneity of various assumption.

Performance differences among pilots and between information content conditions were significant at the 0.01 and the 0.05 levels, respectively. There were no significant interactions and no significant difference among controllers.

The secondary task used in this program proved to be insensitive to changes in operator loading on the primary task. The results of performance on the secondary task and a discussion of the results are presented in Appendix IV.

Table III
Analysis of Variance Summary of Log Transforms of Fuel Consumption Data for the Stabilization Maneuver

Variance Source	SS	df	MS	Appropriate F Ratio	F
πA(Pilots)	0.3906	3	0.1302	MS_a/MS_{ab}	11.84**
πB(Controllers)	0.0372	3	0.0124	MS_b/MS_{ab}	1.13
πC(Information Content)	0.3063	1	0.3063	$\frac{MS_c + MS_{abc}}{MS_{ac} + MS_{bc}}$	6.34*
AB	0.0990	9	0.0110	MS_{ab}/MS_{error}	1.08
AC	0.1210	3	0.0403	MS_{ac}/MS_{abc}	2.12
BC	0.0338	3	0.0113	MS_{bc}/MS_{abc}	0.59
ABC	0.1710	9	0.0190	MS_{abc}/MS_{error}	1.86
Experimental Error	0.7539	64	0.0102		

n = 3

**Significant at the 0.01 level

*Significant at the 0.05 level

πA and B were random treatment effects and C was a fixed treatment effect.

Tracking task: The analysis of log transforms of the rms error scores on the tracking task is summarized in Table IV. The performance difference between the two information conditions was significant at the 0.05 level. The pilot by controller interaction was significant at the 0.01 level and the three way interaction was significant at the 0.05 level.

The pilot preference comparisons are summarized in Table V. The combined three-axis controller was generally preferred for all conditions. The preference was most pronounced for the tracking task where simultaneous, rapid, multi-dimensional inputs were required.

Discussion

The fact that no statistically significant performance differences among controllers appeared was probably due to lack of sensitivity in this experiment. Three of the controllers were of radical design as compared to conventional aircraft controls. The combined three-axis controller was the only controller resembling conventional aircraft controls. It is felt that a more sensitive test among controllers is needed to assess relative performance differences.

Table IV

Analysis of Variance Summary of Log Transforms of RMS Angular Errors on the Tracking Task

Variance Source	SS	df	MS	Appropriate F Ratio	F
πA(Pilots)	0.08591	3	0.02864	MS_a/MS_{ab}	1.09
πB(Controllers)	0.14818	3	0.04939	MS_b/MS_{ab}	1.89
πC(Information Content)	0.36998	1	0.36998	$\frac{MS_c + MS_{abc}}{MS_{ac} + MS_{bc}}$	6.70*
AB	0.23548	9	0.02616	MS_{ab}/MS_e	4.37**
AC	0.06940	3	0.02313	MS_{ac}/MS_{abc}	1.78
BC	0.10203	3	0.03401	MS_{bc}/MS_{abc}	2.62
ABC	0.11689	9	0.01299	MS_{abc}/MS_e	2.17*
Error	0.38246	64	0.00598		

n = 3

**Significant at the 0.01 level

*Significant at the 0.05 level

πA and B were random treatment effects and C was a fixed treatment effect.

Table V

Relative Frequencies of Preferences for the Controllers by Four Subjects

Task	Controller			
	Button	Toggles	Wheels	3-Axis
Stabilization with rates	2/12	5/12	6/12	11/12
Stabilization without rates	2/12	6/12	7/12	9/12
Tracking with rates	1/12	5/12	6/12	12/12
Tracking without rates	0/12	6/12	6/12	12/12
Total	5/48	22/48	25/48	44/48

The 0.04 torque-to-inertia ratio used in these controller comparisons was above the optimum ratio point. This fact should have placed the on-off toggles at a particular disadvantage. However, the pilots were able to adjust to the extent that no differences were found among the controllers used in this study.

It should be emphasized that there are many types of controllers other than the ones studied here. The results of these studies do not suggest that there would be no performance differences among all possible controllers. The four controllers used herein were designed and built after analysis and preliminary simulation studies were conducted to determine desirable controller characteristics. If other types of controllers, i.e. controllers without center-off detents, had been included for comparison purposes, there is little doubt that performance differences among controllers would have been significant.

Figure 11 contains the relative performances of the four controllers under both information content conditions. It can be seen that the combined three-axis controller was considerably better when used with body-rate information. There were no significant effects due to controllers when performance is averaged over both information conditions. There were significant differences when each information condition was considered separately. The combined three-axis controller was significantly better than the other controllers when body-rate information was present.

If the interaction among pilots and controllers shown in Figure 12 is found to be a stable effect for well trained astronauts, this might finally constitute a valid argument for designing individual controllers for individual pilots. The expense of individually tailored controllers would be trivial compared to total space vehicle costs. However, such a contemplation must be tempered by the probable requirement that crew members rotate among stations during extended missions.

It was clearly demonstrated that the presence of body-rate information will result in better system performance. The presence or absence of this information was the most powerful experimental variable for both maneuvers.

Individual performances of all pilots with and without body-rate information on both the stabilization and tracking tasks are shown graphically in Figure 13. All pilots performed better with body-rates presented than

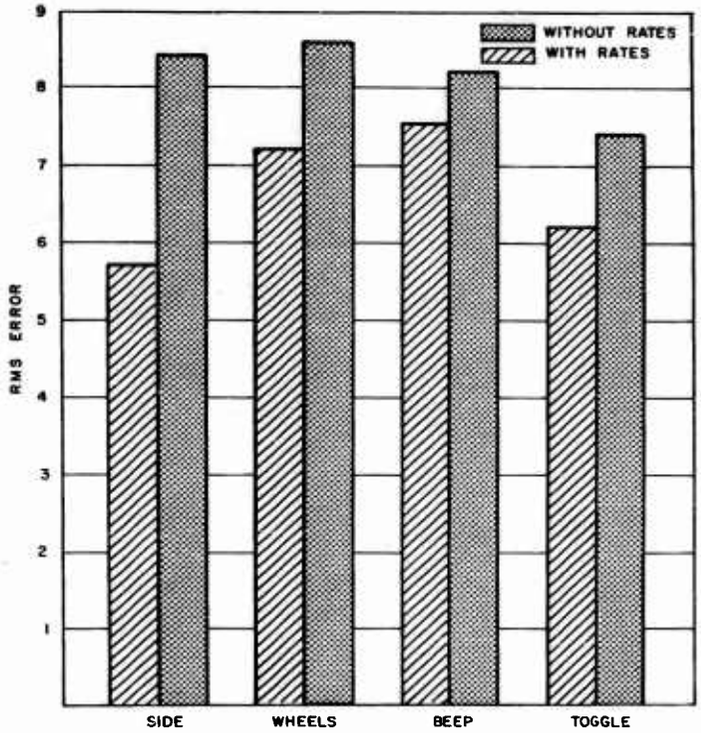

Figure 11. Performance of Four Subjects on the Tracking Task with Each of Four Hand Controllers both with and without Body-Rate Information

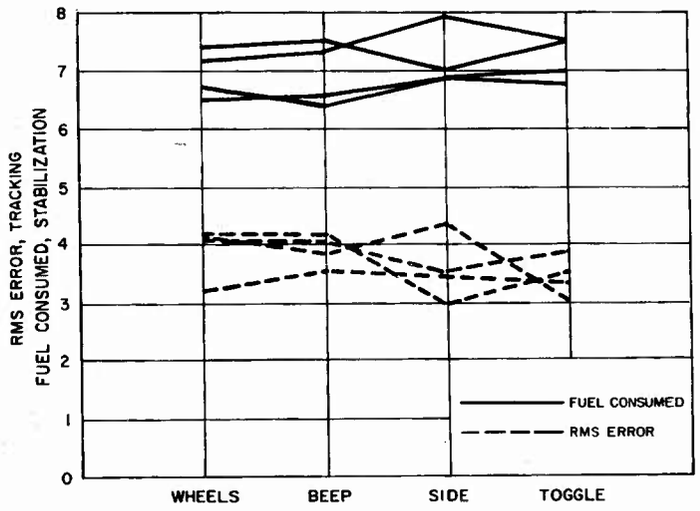

Figure 12. Individual Performances of Four Pilots with Four Hand Controllers on both the Stabilization and Tracking Tasks

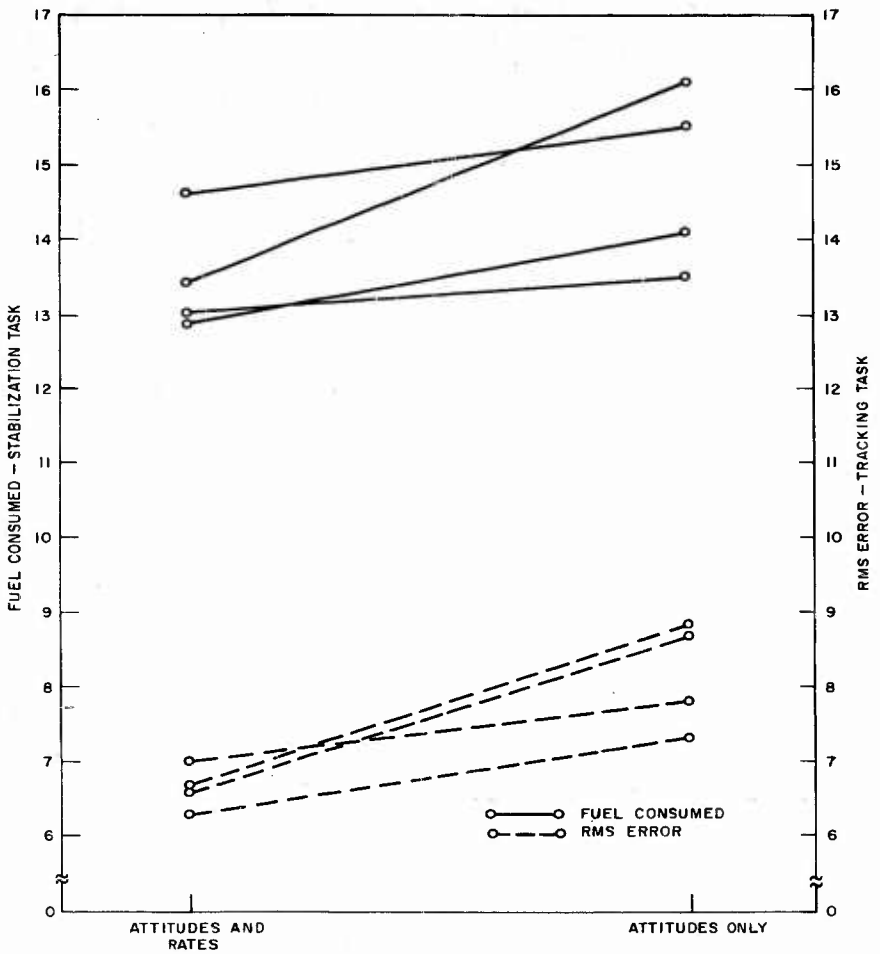

Figure 13. Individual Performances of all Pilots with and without Body-Rate Information on both the Stabilization and Tracking Tasks

without on both tasks. The fact that the performances of some pilots were affected more by the absence of this information than others suggests an interaction among pilots and information content conditions.

Figure 11 indicates that, while all controllers produced poorer performance when body rates were not presented, controllers in the discrete category suffered relatively less from lack of rate information. A more positive interpretation of this interaction effect might be that pilots can take relatively greater advantage of body-rate indications when using a continuous controller. Performance with the combined three-axis controller was best when body-rate information was present. The significant three-way interaction effect has no clearly meaningful interpretation.

An interesting phenomenon was observed on both maneuvers when the proportional controllers were used without the aid of body-rate information. The proportional controllers were actually used as discrete controllers. The pilots made short bursts of controller inputs which contrasted greatly with the long, smooth, continuous controller inputs made when body-rate information was present.

The pilots demonstrated a decided preference for the combined three-axis side controller. This preference was found for all information content and task combinations. In light of these preferences and the advantages of greater input flexibility, it was concluded that the combined three-axis side controller would be recommended over the other types used in this study.

Other design advantages are present for the three-axis side controller. It could also be mechanized as an on-off controller and as a discrete-step-input controller, similar to the operation of the pushbutton controller of this study. The mechanical design of the controller with the intersection of all three axes located within the wrist of the operator allows the forearm to be secured against g forces. The design also allows simple counterbalancing of the mass of the controller about the common pivot point. The single-grip design of the controller also allows activation buttons and triggers to be mounted on the grip. These could be used for communications, mode switching, and gain changes similar to buttons used on aircraft joy sticks, throttles, and radar antenna controllers.

Cross-Coupling Effects

It was anticipated that manual performance would be degraded as the ratios of moments of inertia about the axes increased. This effect was demonstrated in the preliminary studies. Five inertia distributions were studied in the main experimental program, one representing perfect symmetry, one with different moments about the three axes, and three having symmetrical moments about two of the three axes. Characteristics of the five vehicles appear in Table VI. Homogeneous density distribution within each shape was assumed.

Table VI

Inertia Distributions of the Vehicle Shapes Studied

Approximate Shape	Moments of Inertia		
	Roll	Pitch	Yaw
Symmetrical	1	1	1
Short Cylinder	1	4	4
Long Cylinder	1	10	10
Lenticular*	1	1	2
Asymmetrical*	1	2	3

*Limit cases. These values represent the most extreme ratios possible in these categories. The theorem defining limits of moment of inertia ratios was discovered during an investigation of the physical dimensions of vehicles having various ratios. The theoretical development of this theorem is presented in Appendix III.

It should be pointed out that a vehicle can have the external geometric characteristics of the above vehicles and still not have the same moment of inertia ratios as those in Table VI. This is possible when the density is heterogeneously distributed.

The principal cause of performance decrement with a cross-coupled vehicle is the requirement for the pilot to differentiate body rates and program control inputs to coincide with the moments when there is zero deceleration or at least no accelerations about a particular axis in order to minimize fuel consumption.

It was also assumed for purposes of this study that the control axes were perfectly aligned with the principal axes of inertia. Thus only first order cross-coupling effects were present.

Method

The experimental design was a complete 5 x 5 x 2 factorial model with three observations per cell. Five pilots flew each of the five vehicle shapes with and without body-rate information displayed. Pilots and shapes were considered random effects, and information content was considered a fixed effect.

The order of presentation of the vehicle shapes was counterbalanced among pilots, with the restriction that the asymmetrical vehicle always was last in the series. For each vehicle shape the subjects flew four stabilization maneuvers with body rates presented and then four runs without body-rate information. The first trial was a warm-up trial, and the last three were experimental trials.

Initial body rates were always three degrees per second about each axis. The eight possible body-rate directional combinations were paired with four non-zero initial attitudes, and the order of presenting the resulting initial trial conditions was randomized for the various vehicle shapes and subjects.

The simulator cockpit contained the three single-axis attitude indicators, fine and combined body-rate indications, fuel consumed meters, elapsed time meters, the stimulus lights for the secondary task and a light signifying the end of a run. The complete description of the display console is in the Simulator Section of this report.

The combined three-axis controller was used and provided a maximum torque-to-inertia ratio of 0.03 about each axis. The subjects were the four pilot-engineers described previously plus a fifth Hughes pilot-engineer who currently was flying in the Naval Reserve and had approximately 2,700 hours of military flying time and 2,000 hours of civilian flying time.

The subject's task was to stabilize the tumbling vehicle at an attitude aligned with the reference system. The simulator went into automatic hold when all attitude errors were simultaneously within 2 degrees of zero and

the body rates were simultaneously within 0.1 degree per second of zero rate about each axis. The performance criterion was fuel consumed, subject to the restriction that the maneuver had to be completed within five minutes. Response times to the secondary task were collected as a measure of operator loading.

Fuel consumed was determined by taking the integral of the commanded accelerations about each axis and converting these values into fuel consumed by means of the following formula:

$$\text{Fuel consumed} = 2\left[\frac{M}{\text{Sp. I.}}\right]\left[\frac{(\rho^2_x)}{l_x}\Delta_{\omega_x} + \frac{(\rho^2_y)}{l_y}\Delta_{\omega_y} + \frac{(\rho^2_z)}{l_z}\Delta_{\omega_z}\right] \qquad (2)$$

where:

M = Mass of vehicle in slugs

Sp. I. = Specific Impulse of fuel in seconds

ρ = Radius of gyration about an axis in feet

l = Lever arm about an axis in feet

ω = Integral of commanded acceleration in radians per second.

Table VII contains the characteristics of the specific vehicles selected to represent the five classes studied.

Results

The analysis of variance summary for fuel consumed appears in Table VIII. Total fuel measures were transformed to logs to meet the homogeneity of variance assumption.

Performance differences among the five vehicle shapes and between information content conditions were both significant at the 0.01 level. Differences among pilots were not significant, and there were no significant interactions among variables.

The five pilots differed significantly in their reaction times to the secondary task. Performance on this task was insensitive to changes in vehicle shape or information content condition. The average operator

Table VII

Vehicle Geometric Configurations and Inertia Distributions

Typical Shape	Weight lbs	Vol. cu. ft.	Density lbs/ cu. ft.	Mass slugs	Moments of Inertia (slug ft^2)			Radii of Gyration (feet)			Lever Arms (feet)		
					I_{xx}	I_{yy}	I_{zz}	ρ_x	ρ_y	ρ_z	ℓ_x	ℓ_y	ℓ_z
Spherical	15,000	750	20	466	5,924	5,924	5,924	3.56	3.56	3.56	5.63	5.63	5.63
Short Cylinder	15,000	750	20	466	3,260	13,043	13,043	2.64	5.28	5.28	3.74	17.13	17.13
Long Cylinder	15,000	750	20	466	2,331	23,312	23,312	2.23	7.07	7.07	3.16	23.88	23.88
Lenticular	15,000	750	20	466	8,382	8,382	16,729	4.24	4.24	5.99	6.84	6.84	8.55
Asymmetrical	15,000	750	20	466	8,150	16,320	24,480	4.18	5.92	7.25	14.80	19.70	19.70

Table VIII
Analysis of Variance Summary of Log Transforms of Fuel Consumption Measures

Variance Source	SS	df	MS	Appropriate F Ratio	F
πA(pilots)	0.0443	4	0.0111	MS_a/MS_{ab}	1.168
πB(Vehicle Shapes)	1.5974	4	0.3994	MS_b/MS_{ab}	42.04**
πC(Information Content)	0.4008	1	0.4008	$\frac{MS_c + MS_{abc}}{MS_{ac} + MS_{bc}}$	28.86**
AB	0.1519	16	0.0095	MS_{ab}/MS_e	1.03
AC	0.0198	4	0.0050	MS_{ac}/MS_{abc}	0.83
BC	0.0364	4	0.0091	MS_{bc}/MS_{abc}	1.52
ABC	0.0952	16	0.0060	MS_{abc}/MS_e	0.65
error	0.9161	100	0.0092		

n = 3

**Significant at the 0.01 level

πA and B were random treatment effects, and C was a fixed treatment effect.

loading for all conditions in this study was 55 per cent. The subjects varied between 49 and 65 per cent. A more complete discussion of performance on the secondary task is contained in Appendix IV.

In this simulation, the control axes were aligned with the inertial axes. Ritchie et. al. (1961) has demonstrated that misaligned control and inertial axes should cause even larger performance decrements due to cross-coupling effects than were found in this study.

Discussion

It appears that cross-coupling does cause an appreciable decrement in stabilization performance. Figure 14 presents fuel consumption for the various vehicle types. The spherical vehicle, with no cross-coupling, required less fuel than any other shape.

The presentation of body-rate information resulted in reduced fuel consumption for every vehicle shape. This confirms the conclusions drawn

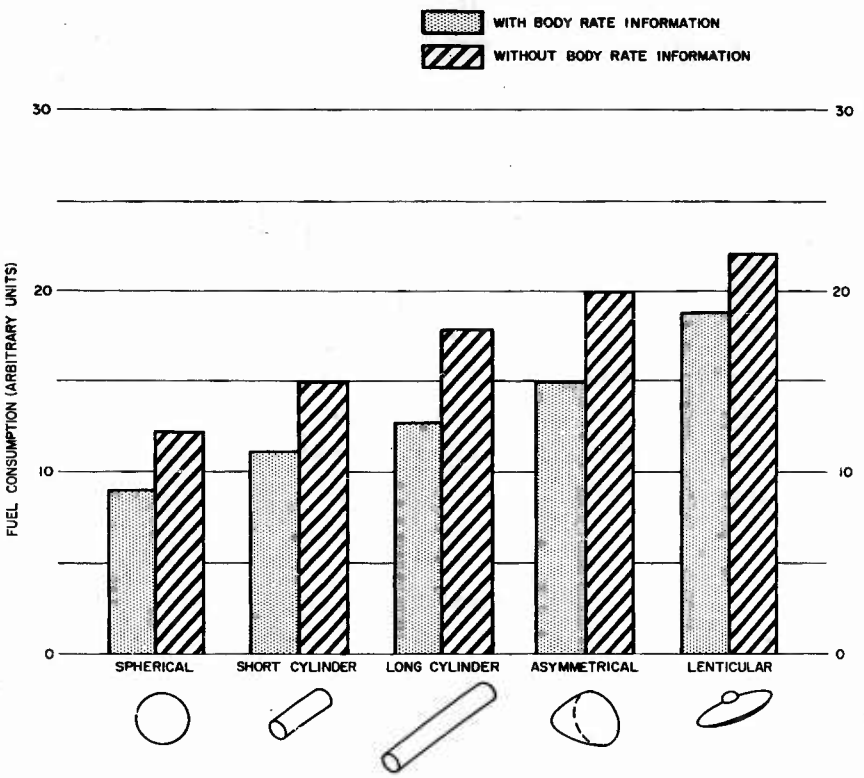

Figure 14. Fuel Consumption for the Various Vehicle Configurations

in the controller-information content comparison experiment that body-rate information is valuable in minimizing fuel consumption and enhancing system performance. Since body-rate information should be relatively easy to obtain from rate gyros, it is recommended that this information be considered a requirement in spacecraft display systems.

It appears that manned spacecraft designers should consider the advantages of distributing mass to approach equal moments of inertia about all three axes.

The experimentally obtained integrals of commanded acceleration about each axis for each vehicle shape and information content condition appear in Table IX.

By inserting the appropriate empirical values from the table and the configuration parameters of a specific vehicle shape into the total fuel consumption formula given previously, an estimate of total fuel required to perform this maneuver with any specific vehicle could be obtained.

Table IX

Integral of Commanded Acceleration in Radians/Sec

Vehicle Shape	Roll*	Pitch*	Yaw*
Spherical with rates	0.0581	0.0622	0.0538
without rates	0.0736	0.0770	0.0683
Short Cylinder with rates	0.0630	0.0766	0.0370
without rates	0.0821	0.0957	0.0548
Long Cylinder with rates	0.0659	0.0699	0.0353
without rates	0.0888	0.0949	0.0608
Lenticular with rates	0.0499	0.0807	0.0574
without rates	0.0547	0.1109	0.0589
Asymmetrical with rates	0.0412	0.0737	0.0501
without rates	0.0491	0.1099	0.0653

*Minimum acceleration per axis to cancel initial rates = 0.05067 radians/second.

As a rule a well trained astronaut operating a manual system will expend about 120 percent of the theoretical minimum energy required to perform stabilization to-specified-attitude-maneuvers under conditions similar to those represented in this experiment. This value would be expected to vary as a function of specific maneuvers and the quality of the

displays and controls provided. With well designed manual systems, performance should compare favorably with that of practically attainable automatic systems. Thus, it appears that the control of vehicle attitude by crew members is a reasonable mode of operation.

External Viewport Study

Space vehicle designers have been seeking the answer to the question of the value of providing astronauts external visibility. Periscopes are costly in terms of system weight, structural integrity, and reliability. Windows provide even more problems of structural integrity plus increasing hazards from radiation, high intensity light, and heat.

Pilots have maintained that a window is necessary for orientation as well as preventing claustrophobia. Certainly it can be argued that one of the reasons that men are going into outer space is, stated simply, to see what is out there.

Information is needed to determine what type of control tasks can be adequately performed while simply looking out the window. In this investigation a comparison was made between a full attitude display presentation and a simplified periscopic viewing port.

Method

External visibility was provided by simulating a periscope with a 180^{o} field of view using a modified Hughes map display with a ten-inch viewing screen. A more complete description of the simulated viewport appears in the simulation section of this report.

The primary task in this study was to null the body rates of a tumbling vehicle. The pilot was to zero all three body rates without constraint as to the vehicle's attitude when stabilized. Stabilized rate limits were defined as less than 0.1^{o} per second about each axis. When this condition was achieved, the computer would go to automatic hold, and performance data were read out. The vehicle shape used had equal moments of inertia about the three axes, and therefore, no cross-coupling effects. The combined three-axis controller was used and provided a maximum torque-to-inertia ratio of 0.03 about each axis. The secondary task was also employed in this study.

Four attitude information conditions were employed. They were: (1) attitude angles and body-rates displayed but no external view, (2) attitude angles displayed but no body rates and no external view, (3) simulated external view with the center of the 180^{o} field aligned with the longitudinal axis of the vehicle, and (4) simulated external view with the center of the 180^{o} field aligned with the vertical axis of the vehicle.

The order of presenting these conditions was: (1) view port straight ahead, (2) view port straight down, (3) attitudes and rates, and (4) attitudes only. Eight trials were made by each of two subjects with each display condition. The order of presenting eight combinations of initial body rates and attitudes was randomized for the eight trials in each cell. The eight initial conditions employed appear in Table II.

Summaries of the pilot experience background of the two subjects can be found in the torque-to-inertia study. Both pilots were familiar with flying the attitude and body-rate displays with no external field of view. The subjects each received approximately two hours practice on each view port condition. Performance data were recorded during practice trials, and stable performance was generally achieved after twenty to thirty trial runs.

The system performance criterion was the integral of commanded acceleration converted to fuel consumption by the procedure described previously. A time limit of five minutes was set to complete the stabilization maneuver.

The experimental design was a 4 x 2 factorial model with eight observations per cell. Pilots and displays were considered as random effects in the components-of-variance model.

Results

The fuel performance data were converted to logs to meet the homogeneity of variance assumption. The summary of the analysis of variance of the log transforms consumed appears in Table X.

Neither of the main effects nor the interaction effect was significant. The obtained median integral of acceleration for each axis appears in Table XI. These values can be converted to fuel consumption by use of the fuel consumption formula and the specific vehicle shape parameters as in Table VII.

Table X

Analysis of Variance Summary of Log Transforms of Fuel Consumed in the View Port Investigations

Variance Source	SS	df	MS	Appropriate F Ratio	F
A (Displays)	0.007899	3	0.002633	MS_a/MS_{ab}	2.66
B (Pilots)	0.002544	1	0.002544	MS_b/MS_{ab}	2.57
AB	0.002975	3	0.000992	MS_{ab}/MS_e	1.83
Error	0.030413	56	0.000543		

n = 8

There were no practically significant differences in the reaction times on the secondary task either among display conditions or between pilots. The operating loading during these tests had a median value of 38 percent.

Table XI

Median Values for the Integral of Commanded Accelerations for Stabilization in Radians per Second

Display Condition	Axis		
	Roll	Pitch	Yaw
Attitudes and Rates	0.05134*	0.05148	0.05068
Attitudes Only	0.05470	0.05162	0.05124
Viewport Ahead	0.05486	0.05276	0.05302
Viewport Down	0.05310	0.05138	0.05102

*Theoretical Minimum is 0.05067

Discussion

Considering that the attitude displays presented very precise angle and body-rate information, and that the two subjects were quite familiar with flying the attitude displays, it is interesting to note that performances

were comparable for the various conditions. The precision with which rates of motion can be sensed and interpreted by observation of movement in the external view must be very high. The noise and relatively low resolution present in this simulation of an external viewport would suggest that an external field of view would allow pilots to sense rates well below the 0.1 degree per second cutoff used in this study. There also appears to have been no appreciable increase in operator loading when concentrating on this type display.

The performance levels found in this study suggest that the external field of view can serve as a fairly precise display of body-rate information. It also appears that the orientation of the external viewport in relation to the vehicle axes does not seem to be critical.

It should be kept in mind that the maneuvers represented in these results were performed in a vehicle with symmetrical mass distribution with the earth always in the field of view. Therefore, further investigation is necessary in order to determine performance levels for maneuvering vehicles with gyroscopic cross-coupling and for situations with only star patterns in the field of view.

MANUAL VEHICLE TRANSLATION CONTROL

by

W. B. Knowles, Jr.

Launch, injection into orbit, orbit or trajectory correction, ejection from orbit, and landing are examples of maneuvers in which control of translation velocities along one or more vehicle axes is required. In most cases where large accelerations or precision vectoring of thrust are required automatic control will be used. Terminal rendezvous and docking, however, are maneuvers in which manual translation control will probably be used. (Liebman, 1961; McDonnell Aircraft, 1961; Houbolt, 1961.) These maneuvers, essentially orbital trajectory correction maneuvers, are part of several missions including assembly of stations and vehicles in earth orbit, in-trajectory refueling and assembly, shuttling between the moon and moon-orbiting vehicle (McDonnell Aircraft, 1961). Manual control is proposed because 1) the sensing and control functions appear to be well within the capabilities of the human operator, 2) use of the pilot, who is already available in the system, eliminates the cost, weight, and space penalties that automatic instrumentation would impose, and 3) some improvement in overall system reliability will also accrue (Houbolt, 1961).

The purpose of this section of the report is to discuss some of the human engineering considerations involved in designing for manual control during rendezvous and docking with primary emphasis on the final docking phase.

SYSTEM DEFINITION

In a rendezvous with an earth orbiting station the approaching vehicle would probably be placed in a parking orbit and then transferred to the orbit of the space station. Use of the parking orbit involves no fuel penalty and does permit easy correction of possible launch errors.

Terminal rendezvous refers to the portion of the maneuver where the transfer between orbits is made (see Figure 15). The docking phase involves the final vernier adjustments in position and velocity needed to bring the vehicles together. Docking is initiated after the terminal rendezvous phase when the vehicles are in practically identical orbits but are separated by relatively small displacements.

Terminal rendezvous or orbit transfer involves translations in the order of tens or hundreds of miles and thrust levels in the order of 0.1 g. Initial conditions for the docking phase are commonly given as 50 to 5000 feet in range with relative velocity errors in the order of two feet per second. Terminal errors in relative position of less than one foot and in relative velocity upon contact of less than one foot per second are assumed to be permissible. Thrust levels during docking will be low, in the order of 0.01 g. (Liebman, 1961; McDonnell Aircraft, 1961.)

DOCKING KINEMATICS

The geometries of typical orbital rendezvous maneuvers are shown in Figure 15. From the point of view of accomplishing a smooth transition from the terminal rendezvous phase to the docking phase the Hohmann transfer shown in Figure 15-C is most desirable. This transfer is also optimum in terms of fuel consumption and other system criteria. The lower diagrams of Figure 15 show the relationships between relative range and altitude as they would appear to an observer on the approaching vehicle.

Examples of other kinds of relative motions possible between two orbiting vehicles are shown in Figure 16. In these examples the station is in a circular orbit while the approaching vehicle is in an eliptical orbit. The diagrams on the right show the relationships between relative range and altitude as they would appear to an observer on the approaching vehicle. The forms of these curves are determined by the discrepancies between the orbits; the distances scale according to the initial relative velocities. Mueller (1962) has systematically explored the relative motions between two orbiting masses for a wide range of orbital deviations assuming relative velocities of an order of magnitude appropriate for the docking problem. It is his conclusion that the term docking should be reserved for that part of the rendezvous where the orbital discrepancies have been eliminated or reduced to very low values and all that remains is to close up any small gap that may exist along the orbital path.

To close in on the space station the approaching vehicle must add velocity along the orbital path which also increases the altitude of the vehicle. This is demonstrated in Figure 17 where vertical miss distances

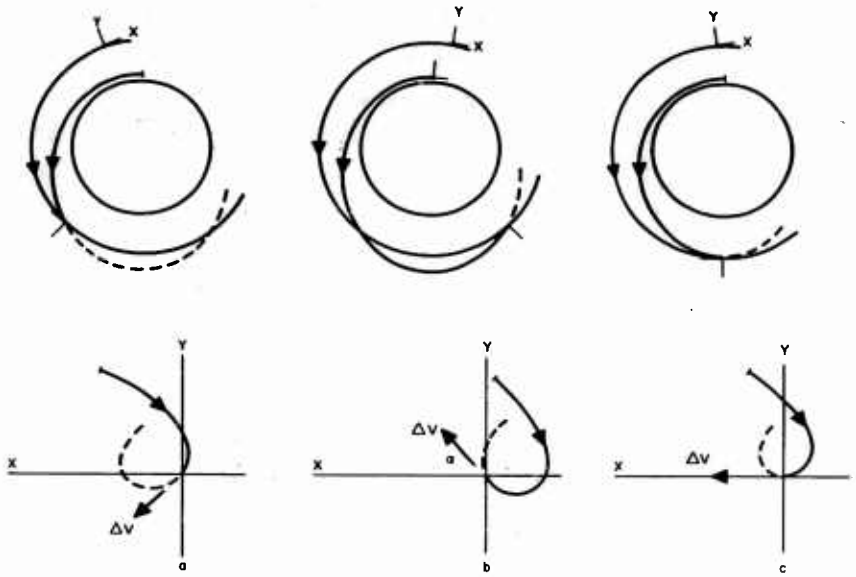

Figure 15. Three Typical Rendezvous Trajectories

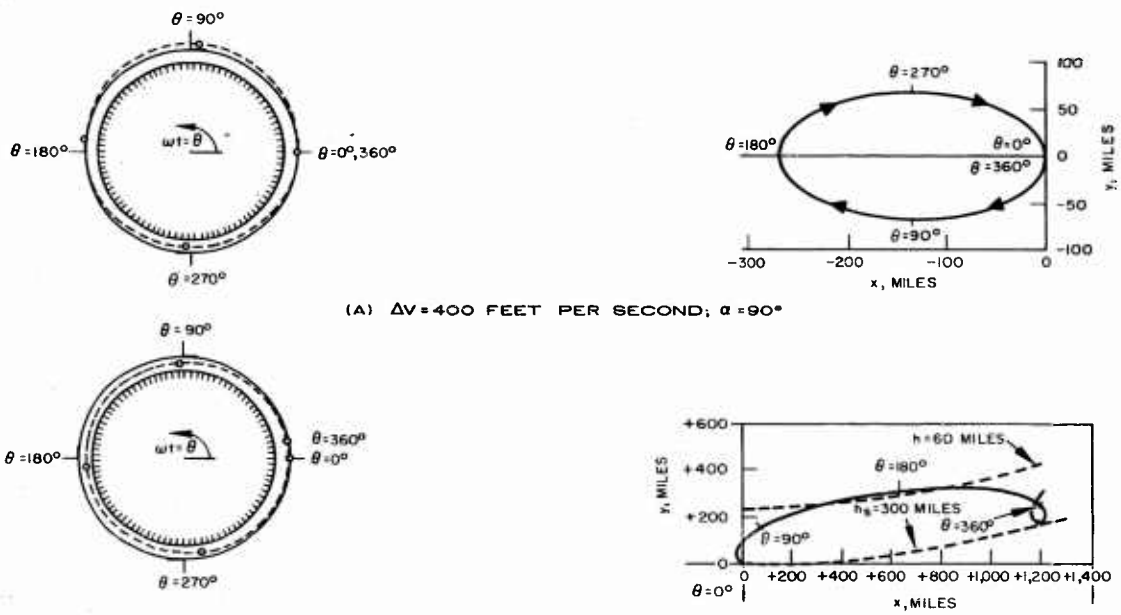

Figure 16. Two Typical Trajectories Showing Motion of Vehicles which at t = 0 (θ = 0) are at the Same Position but in Different Orbits

are shown assuming that the approaching vehicle starts straight in from 2000 feet with an initial velocity and follows a no-thrust trajectory. An orbital altitude of approximately 250 miles is also assumed. The curvature of the paths is due to the combined effects of Coriolis and "tidal" or gravity gradient accelerations. Since the radius of curvature is directly related to the initial closing velocity it can be seen that the vertical miss distance per unit time is greatest for the high velocities. However, the vertical miss distance over the total time taken to close on the target is greater for low velocities simply because it takes much longer to close with low velocities than with high. The net result is that the relative importance of the centrifugal effects are greater at low approach velocities than at high.

In a minimal manual control system where the pilot responds to direct visual information these effects arising from orbital kinematics must be thoroughly understood if changes in apparent position are to be interpreted correctly and if the results of control actions are to be predicted correctly.

The essential geometry defining the orientation of two vehicles relative to one another is shown in Figure 18. The station with the main reference coordinate system is shown on the left; the approaching vehicle with its coordinate system is shown on the right. It is assumed that these coordinate systems rotate so that the Y-axis is oriented toward the earth's center.

The position of the approaching vehicle relative to the station can be described in terms of the rectangular X, Y, Z coordinate system, or in terms of the polar coordinates A, E, and R. The attitude of the approaching vehicle can be described in terms of the Euler angles relating the vehicle axes to the station coordinate system, or it can be described relative to the slant range vector R. To a mathematician these as well as several other alternative ways of looking at the orientation of the vehicles relative to each other are interchangeable, and the choice of one over the other is largely a matter of personal preference and the ease with which the problem at hand can be solved.

Just as the mathematician structures his concept of orientation according to his preferences and purposes, so will the space pilot develop ways of thinking about the orientation of vehicles relative to each other that will suit his needs. The differences between space flight and

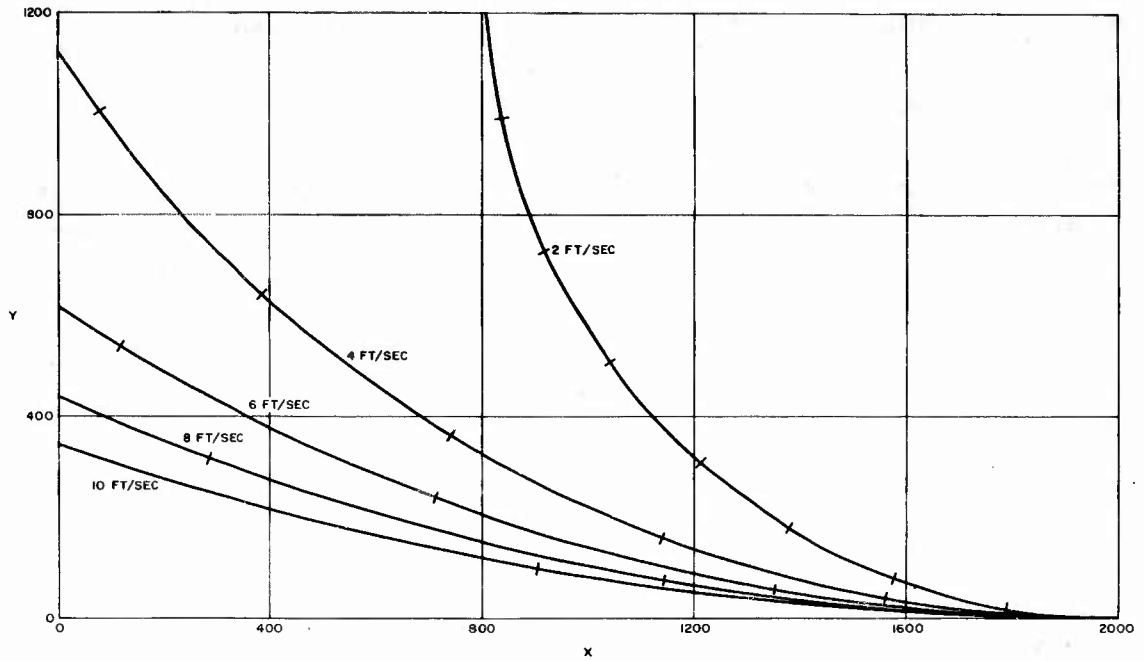

Figure 17. No-Thrust Trajectories Showing Path Taken by Approaching Vehicle Starting from a Range of 2000 ft. with Different Initial Velocities in Direction of the Space Station

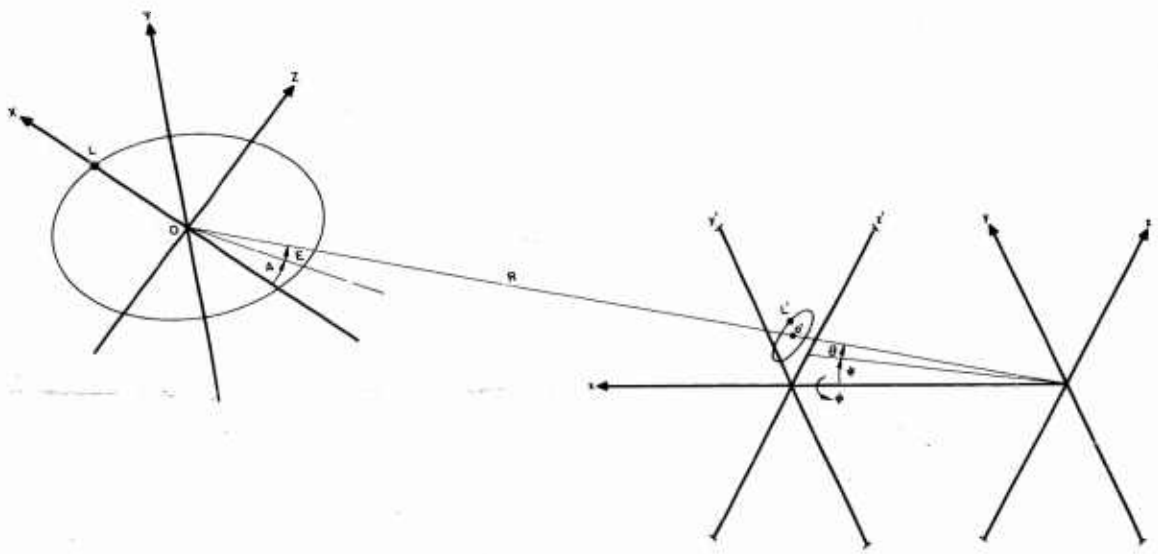

Figure 18. Docking Simulation Geometry

aerodynamic flight are sufficiently great that orientation concepts, or rather concepts about how to effect changes in orientation that have been built up through experience with aerodynamic flight, will no longer be entirely appropriate in controlling space vehicles. In aerodynamic flight, translation is continuously controlled through control of attitude, and most control functions are also reasonably well damped. In space flight, translation is controlled through attitude only to the extent that it may be necessary to change attitude to orient thrust vectors, but in some systems thrust orientation will be independent of attitude. The absence of external damping or restoring forces means that vehicles will be coasting most of the time and that the pilot's control job will be mainly that of monitoring the progress of changes in orientation and executing or checking on the correct application of thrust for the next coasting period.

Carel (General Electric Advanced Electronics Center, 1955) has discussed the factors contributing to the development of orientation concepts in conjunction with the contact analog display work. Wolbers (Douglas Aircraft Company, 1961) summarizes his conclusions to the effect that "if the integration of the pilot and plane is complete the control of the aircraft becomes as automatic and simple as any other over-learned motor act. On the other hand the disruption of the pilot-plane integration (the unified body image) can have serious consequences." Fundamentally the ways in which pilots perceive this dynamic geometry of space flight determine the appropriateness of the display and control instrumentation, and conversely, the display and control instrumentation provided will determine the ways in which the pilot can conceptualize the dynamic geometry. Since most of the simulation studies to date have dealt with only special parts of the overall vehicle control task, these factors have not yet been brought into sharp focus. In a full-scale six-degree-of-freedom simulation they may be expected to become more apparent.

VISUAL FACTORS

In considering a minimum manual system for rendezvous and docking it is necessary to consider the information that is needed to effect rendezvous and to determine the adequacy of the information that may be available through direct viewing.

The essential tasks requiring visual information are 1) identification of station, 2) range determination, 3) range rate determination, 4) cross range determination, 5) cross range rate determination, 6) closing course prediction, 7) approach aspect determination and 8) attitude determination. The visual cues available from a direct view of the station through a window or periscope system are shown in the x' y' display plane of the diagram in Figure 18.

Identification at long ranges will probably be possible on the basis of brightness and apparent movement relative to the celestial background and the approaching vehicle. Baker and Steedman (1961) reviewing the visual environment in space (see also J. L. Brown, 1961; Buddenhagen and Wolpin, 1961; and Shternfeld, 1961) point out that with full illumination by the sun, a highly reflective satellite could have a luminance considerably in excess of 10,000 foot-lamberts. At ranges in the order of thousands of feet the glare effects from such an object would render background stars in the vicinity invisible. If the satellite were in the shadow of the earth but illuminated by light reflected from the moon the luminance would be in the order of 0.01 foot-lambert and the star background would remain visible. (Baker and Steedman, 1961.)

At close range or with telescopic viewing identification will also be possible on the basis of form, markings, and signal lights.

Range and range-rate determination, in the final analysis, depend upon the size and change of the retinal image. Baker and Steedman (1961) have shown that under certain conditions the threshold for directly perceived movement in depth is in the order to two percent change in visual angle. Lineberry, et. al., (1961) and Brissenden (1962) in a simulation of orbital rendezvous have shown that computations of range and range rate obtained by clocking the station image displacement at known thrust could be used to control the vehicle during the terminal rendezvous phase. Knowles and Carel (General Electric Advanced Electronics Center, 1956b) have demonstrated that percent change in relative visual angle was a sufficient cue to predict time-to-go to impact and that this judgment could be made independently of knowledge concerning the absolute size, distances, or rates of closure. The range of velocities and times at which these cues are useful remains to be explored as does the usefulness of the cue in closed-loop control.

Judgments of absolute ranges require knowledge of the absolute size of the station and are best made as in the Wolowicz (1960) study by reference to a calibrated scale of image size. Stadiametric ranging systems have also been proposed as having fairly simple instrumentations based on the inverse square law for illumination (Liebman, 1961). Again these presume a priori knowledge concerning the relevant characteristics of the space station.

Cross-range errors and cross-range rates can be determined by comparison of the position and change of position of the station with respect to the vehicle frame of reference established by the viewing port frame or provided by reticle markings, etc. Thresholds for direct perception of lateral velocities have been determined by R. H. Brown (1954 and 1960). Absolute visual angular velocity threshold values in the order of seven minutes per second and differential threshold in the order of 10 per cent change in rate were reported depending upon the luminance and size of the target. As in the Baker and Steedman study, the target was the only element in an otherwise instructured visual field. Visual rate judgments as a function of field structure have yet to be explored systematically.

Carel (General Electric Advanced Electronics Center, 1956a) has studied the accuracy with which the impact point (the intersection of the flight path with a textured plane) could be determined as a function of the approach velocity, slant, and texture. These studies showed that texture gradient and motion perspective were sufficient cues for maintaining the heading of an aircraft within normally acceptable limits. In space flight, however, these cues would be available only at short ranges when the surface texture and structure of the station can be perceived.

The apparent location and movement of the station with respect to the display or viewing port frame of reference are functions both of the relative positions of the vehicles and of the attitude of the approaching vehicle. Where relatively slow line-of-sight maneuvers are performed this confounding of angular information sources poses no problem. In other circumstances it may be necessary to provide auxiliary attitude and attitude-rate information.

The aspect from which the station is approached ordinarily would not be too important, and terminal corrections at very small ranges and with very low velocities could be accomplished under direct viewing where

the structure of the station is clearly apparent. However, in the event that the station is powered by a nuclear source, shadow shielding will probably be used and will determine the aspect from which safe approaches may be made. Depending upon the exclusion range, auxiliary instrumentation and communication may be required to assure a safe approach.

CONTROL FACTORS

In a minimum control system it is assumed that the pilot would monitor thrust directly and thus control vehicle attitude and translation through several channels of second order, or acceleration, control. It is well known that human operators tend toward instability in these kinds of systems and that adequate performance is bought at the expense of a great deal of effort (Birmingham and Taylor, 1954; Garvey and Taylor, 1959).

The simulation of space flight problems accomplished to date indicate that portions of the task are well within the pilot's ability to control. The attitude studies reported in this report and by Ritchie (1960) as well as the Project Mercury flights show that within the range of nominal system parameters attitude stabilization can be maintained within acceptable tolerances with a variety of information displays and several different controller configurations.

Likewise several rendezvous simulations (McDonnell Aircraft, 1961; Lineberry, et. al., 1961; Brissenden, 1962; and Wolowicz, et. al., 1960) have demonstrated that the two or three basic channels of control necessary for the co-planar orbital maneuver, pitch, longitudinal, and vertical, also can be handled adequately with simulated visual or meter-type instrument displays and with several different control configurations.

These studies,however, have not yet defined the limits within which direct manual control is truly feasible. They have all been part task simulations in that at most three channels of control have been employed, and only one study has attempted to simulate secondary tasks that the pilot may be required to perform. It is not at all clear how close to being overloaded the pilot has been in these situations. There are some indications that some of the experimental conditions began to press the limits of available pilot bandwidth (Chernikoff, et. al., 1959). Brissenden (1962) found that the computation of range and range rate in the purely manual version of his sighting and timing system could not be accomplished in real time.

Wolowicz (1960) found that "use of pitch control and one-axis thrust control appears to be extremely impractical for pilot-controlled interception." Kasten (1962) reports similar findings. The attitude studies discussed in this report showed that performance was affected by torque-to-inertia ratios and cross-coupling, i.e., the fundamental dynamics of the vehicle. The docking simulation demonstration reported below clearly illustrates that the docking task without rate information and grid reference marks is much more difficult than when these auxiliary sources of information are present.

Garvey and Taylor (1959) have shown that equivalent system performance may be obtained with a number of different display-control configurations, but that the different system configurations will use up different amounts of operator bandwidth. It is not until the limits are reached that appreciable decrements in system performance are obtained. One of the goals of future studies of manual vehicle control should be to define more closely the cost in terms of operator bandwidth of coding information in various ways. This kind of data would be extremely useful in determining where and what kind of instrumentation would have the greatest payoff.

DOCKING DEMONSTRATION

A demonstration of docking under direct visual observation was undertaken using a partial simulation of the situation diagrammed in Figure 18. As in the Wolowicz (1960) study the maneuvers were co-planar. Translational thrust was applied along the x and y axes and rotational thrust was applied about the pitch axis. On-off controls were used and the thrust levels were 0.32 ft/sec^2 for translation and 2.8$^o/sec^2$ for pitch rotation.

The image representing the space station was generated on a dual-beam Tektronix oscilloscope. Figure 19a shows the display as it would appear at the beginning of a run. This figure represents the condition where the approaching vehicle is 2000 feet behind the station, 400 feet below it, and pitched down 20 degrees. Figure 19b shows the image as it would appear when the approaching vehicle is 50 feet behind the station and perfectly aligned with the plane of the station.

The figure then represents the projection of a circle with a dot on the far side as it would appear in a viewing port or on a periscope screen.

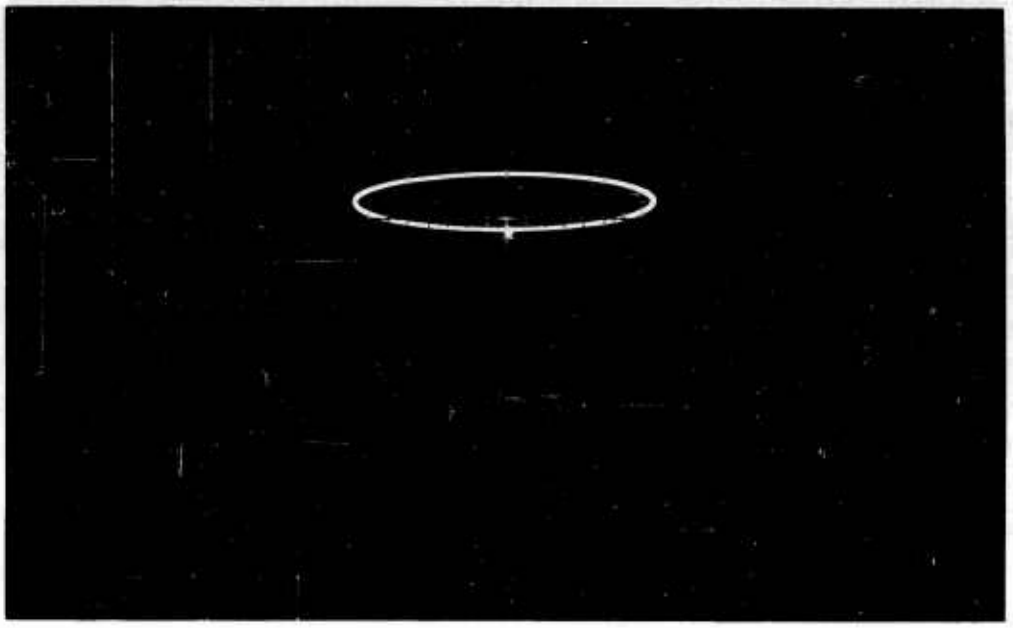

Figure 19a. Image Representing a Space Station as it Would Appear at the Beginning of a Run

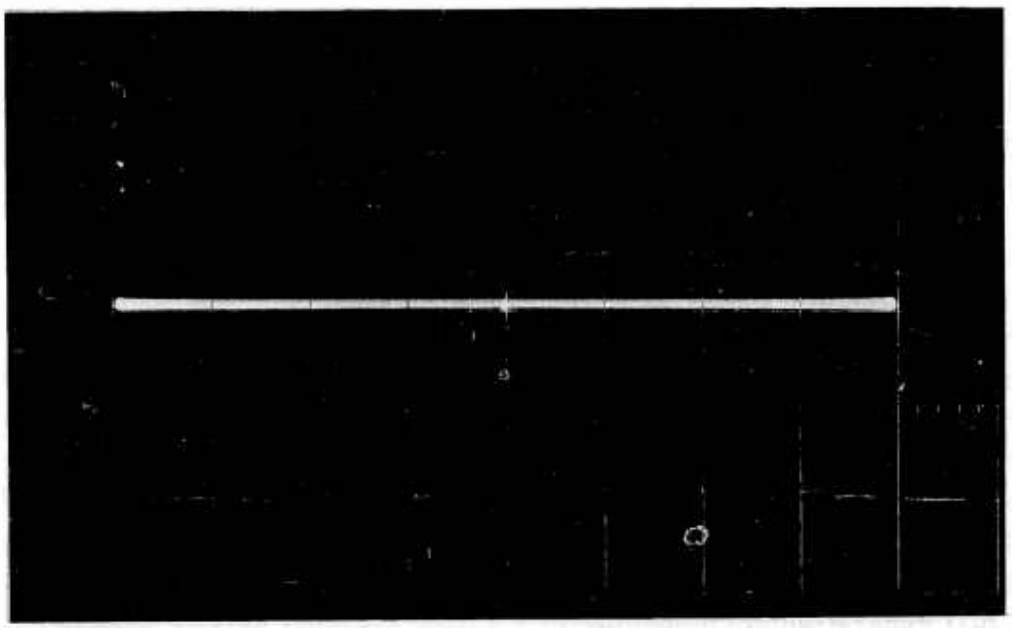

Figure 19b. Image Representing a Space Station as it Would Appear When the Approaching Vehicle is 50 feet Behind the Station and Perfectly Aligned with the Plane of the Station

The image varies from a straight line to an ellipse as a function of elevation angle; it is positioned up or down from the middle of the screen as a function of elevation angle and pitch angle; it increases in length or diameter as an inverse function of range.

The display was scaled so that for distances greater than 250 feet the image diameter changed 1 cm for each 330 feet. A scale change was introduced at 250 feet so that at close ranges 1 cm in diameter equaled 33 feet change in range. The displacements due to elevation and pitch were scaled so that 1 cm deflection equaled 25 degrees.

Auxiliary displays of $\dot{X}$, $\dot{Y}$, and $\dot{\theta}$ were provided on meters which read ± 10 ft/sec full scale for the translation rates and $\pm 10^{\circ}$/sec for pitch rate. The display-control relations were as follows. Throwing the x-thrust switch to the left produced a negative rate which appeared as a meter deflection to the left and an increase in the image diameter. Throwing the y-thrust switch forward produced a positive rate which appeared as an upward deflection of the meter and an opening up of the ellipse with the dot following the upper edge and with the whole image moving down from the center of the scope. Throwing the θ-thrust switch back produced a positive pitch rate which appeared as an upward deflection of the meter and a downward movement of the image but with no change in the shape of the ellipse.

Figures 20 and 21 are records taken from a well practiced subject during two demonstration runs. In both cases the initial conditions were $X = 2000$ feet; $Y = -400$ feet, $\theta = -20^{\circ}$, and pitch rate was continuously disturbed with the same low level random noise used in the attitude study. The instructions were to close to 50 feet as quickly as possible, and upon arrival to be perfectly aligned in Y and θ and with a velocity in X of less than 1 ft/sec. Figure 20 shows the record of a representative run made using the simulated view and the auxiliary rate meters. Figure 21 shows a run made using only the simulated view.

The examples shown were completed successful trials, and the run without the rate meters took only slightly longer to complete. The added difficulty of getting rate information from the image alone is shown primarily in the more cautious application of thrust in x and y and in the actual generation of an opening rate during the final part of the maneuver.

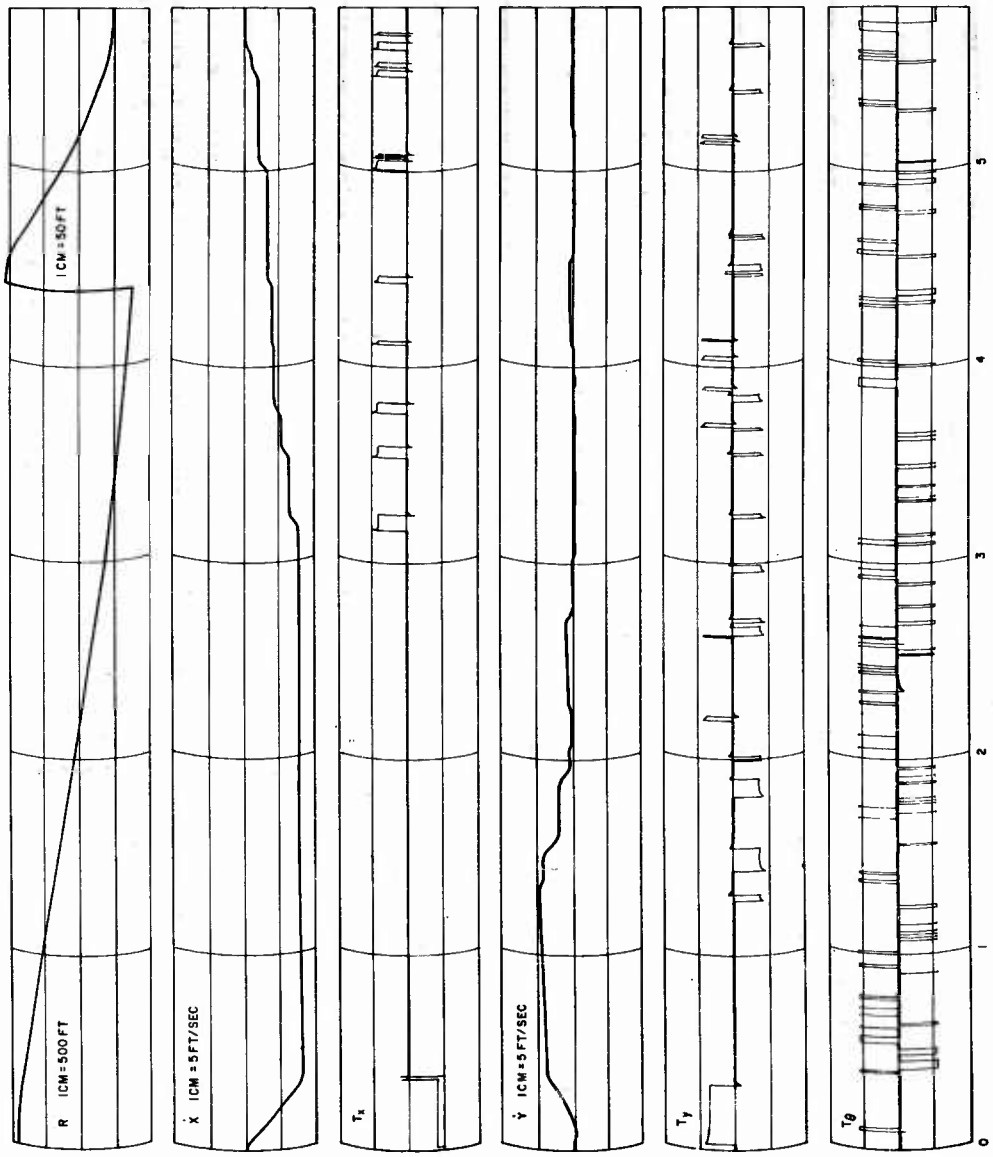

Figure 20. Docking Maneuver with Rates

Figure 21. Docking Maneuver without Rate Meters

It is to be expected that effects such as these would be emphasized in a full six-degree-of-freedom system, and the central problem becomes that of finding out where and how best to reduce the perceptual load on the pilot.

MANUAL ORBITAL NAVIGATION

by

D. K. Bauerschmidt, N. A. Boehmer, I. Terris and P. V. Vermont

Orbital navigation as discussed in this report refers to the determination of a vehicle's location and direction of motion in space. This study deals with the methods and equipments necessary to allow maximum useful participation of an astronaut in this task.

There is little argument as to the desirability of the development of a capability of onboard manual orbital navigation. This is desirable not only as a redundant or backup mode but also, if developed to the degree necessary, as a primary navigation mode. As either a secondary or primary mode a manual navigation capability would significantly increase the probablility of mission success.

For the purposes of this study an earth-orbit mission was chosen. The orbits considered were quite eccentric with apogees of approximately 100,000 nautical miles. It was felt that this choice would provide results of a general nature which would be applicable in part to more ambitious manned space programs. This is particularly true for the study and analysis dealing with sensing equipment and techniques. It is somewhat less true, except for generalities, for the portions of the study dealing with trajectory determination, computation techniques, and computation equipment.

The study consisted of several parts. The first was a survey of sensing techniques and equipment presently in use or in development. This included not only those techniques and equipment being considered for manned space systems but also those planned for unmanned systems such as Project Surveyor and the Orbiting Astronomical Observatory (OAO). The second portion of the study was concerned with computational techniques for position and trajectory determination. This phase of study was primarily directed toward the computation requirements resulting from actual trajectories deviating from a precomputed nominal trajectory. During the study and analysis of the sensing and computation requirements for the mission under consideration, the role which the astronaut might play in the performance of these sensing and computation tasks was emphasized. It

was anticipated before the start of this study that even in the so-called minimum manual mode the astronaut would at best require some sensing and computational aids. The final portion of this study dealt briefly with the requirements for and the preliminary designs of these devices.

SENSING TECHNIQUES AND EQUIPMENT

Orbital navigation techniques and equipments presently in use or in development include both ground based and onboard spacecraft facilities. Both types of facilities are surveyed here even though this study is concerned with requirements and performance capabilities for an onboard minimum manual system. A brief description of presently used ground-based facilities will provide a standard for evaluating the accuracy and efficiency of any potentially feasible onboard manned system.

Ground-Based Facilities

The rapid development of ballistic missiles and space systems has placed heavy emphasis upon ground-based tracking and computing facilities. These facilities have been developed and upgraded over a period of years so that they offer at the present time an accurate, available and relatively reliable means of obtaining vehicle position and velocity direction information.

Observations obtained by ground-based facilities depend upon radio, radar and doppler techniques to furnish range, range-rate and angular information. The largest available digital computation facilities and an elaborate network of tracking stations are used for this purpose. In general, optical observations are not used for these observations.

The Deep Space Instrumentation Facilities (DSIF) located in Goldstone, California, Johannesburg, South Africa, and Woomera, Australia have been specifically constructed for the purposes of supporting earth-orbital and lunar space missions. These facilities have an angular accuracy of approximately 0.04° of arc*, a range-rate accuracy of about 0.5 ft/sec., and a range accuracy of a few hundred feet.

*Accuracies are given in terms of one sigma.

The three stations of this facility are placed to permit continuous tracking of near equatorial orbits starting from altitudes of 1000 nautical miles. Observations are taken automatically at intervals which may vary from every 10 minutes to every 10 seconds. The observations are transmitted to ground computers capable of performing lengthy and complicated trajectory determination and smoothing computations, predictions of the uncorrected re-entry condition, and determinations of the required mid-course corrections. The results of these computations, when transmitted to the orbiting vehicle may be used as the basis for executing a corrective maneuver.

Onboard Facilities

Weight, volume and power limitations of all onboard equipment as well as the nature of the observed bodies, such as the earth, moon, stars, etc., limit the onboard optical sensing equipment to instruments using either the infrared or the visual part of the spectrum. This is particularly true when dealing with manually pointed or aligned instruments. Radio frequency communications links serve admirably for voice and data transmission. However, because of limitations on size, weight, and power space-borne radio and radar equipment does not furnish accurate range and angular information except for relatively short ranges.

The operation of sighting celestial bodies from space vehicles can be divided into several categories. Since the fixed stars can be considered as point sources while the sun, moon and planets present a distinct disc, the disc sighting operations and equipment will be different from those required for fixed star sighting. Different types of instruments and sighting operations are discussed below.

Sun Seekers

A variety of automatic instruments for the determination of the direction of the visible sun's disc are available. Generally, their operation is based on differential measurements of the sun's radiation. For example, three radiation sensitive elements can be mounted orthogonally in order to sense the variation in intensity of illumination as a function of the angle of incidence. Differential signals may be generated to rotate the sensor

assembly in the direction of the illumination. Laboratory accuracies of the order of 6 seconds of arc have been reported (Roberson, 1960 and Nidey, 1957).

Planet Trackers

Unlike sun seekers, which do not furnish the visual angle subtended by the disc, horizon scanners and planet trackers sense visible or infrared radiation and scan the periphery of the planet disc or illuminated crescent. Since these devices scan the periphery of the planet's disc they furnish indirectly the direction toward the center of the disc and therefore specify the direction of local vertical. They may also be used to measure the angle subtended by the disc.

The horizon scanner may be considered as a special case of a planet tracker. It is generally used for the establishment of a local vertical reference and as the basis of an altitude determination.

Planet tracker observations are degraded by a number of error sources. In the case of earth observations the following sources of error may be significant: oblateness of the earth*, instrument errors, uncertainty between the true and atmospheric horizon, terrain irregularities, refraction of rays by the atmosphere, atmospheric scattering, radiation and absorption. In addition, considerable difficulty has been encountered in the determination of the geometric center of the full, gibbous and crescent contours of a body.

Some of these errors caused by gibbous and crescent contours are alleviated by the use of infrared sensing equipment (Roberson, 1960). The error produced by the oblateness of the earth depends upon the latitude of the observed horizon points and its effect can be corrected by the use of precomputed correction data. The altitude of the atmospheric horizon depends upon the latitude and time of year. Corrections for this source may also be precomputed, except the uncertainty of whether the true or atmospheric horizon is sighted may remain.

*Earth's polar and equatorial radii are respectively about 3432.3 and 3444.0 nautical miles with the difference amounting to approximately 1/300 of the mean radius.

The stadiametric range determination as obtained by horizon scanners and periscopic sightings is also based upon the observation of the rim of the visible horizon. The geometry shown in Figure 22 exists for this kind of observation.

Two sources of error are discussed below for the sake of exemplification. These are errors due to erroneous angle measurement and errors due to horizon uncertainty.

It can be seen from Figure 22 that

$$r \sin \alpha = R \tag{3}$$

It can be shown, considering errors as infinitesimals of first order, that,

$$\frac{\Delta r_{\Delta\alpha}}{r} = -\frac{\Delta\alpha}{\tan\alpha} \tag{4}$$

$$\frac{\Delta r_{\Delta R}}{r} = -\frac{\Delta R}{R} \tag{5}$$

$$\Delta V_{\Delta\alpha} = \Delta\alpha \tag{6}$$

$$\Delta V_{\Delta R} = \frac{1}{2}\left(\frac{\Delta R}{R}\right) \tan\alpha \tag{7}$$

For long ranges, when $r >> R$,

$$\frac{\Delta r_{\Delta\alpha}}{r} = -\frac{r\Delta\alpha}{R} = -\frac{r\Delta A}{2R} \tag{4a}$$

The following approximate numerical values and maximum obtainable accuracies will be assumed:

$$R = 3440 \text{ n.m.}$$

$$\Delta R = 6 \text{ n.m.}$$

$$\Delta\alpha = 10'' = 4.85 \times 10^{-5} \text{ rad.}$$

$$\Delta A = 20'' = 9.70 \times 10^{-5} \text{ rad.}$$

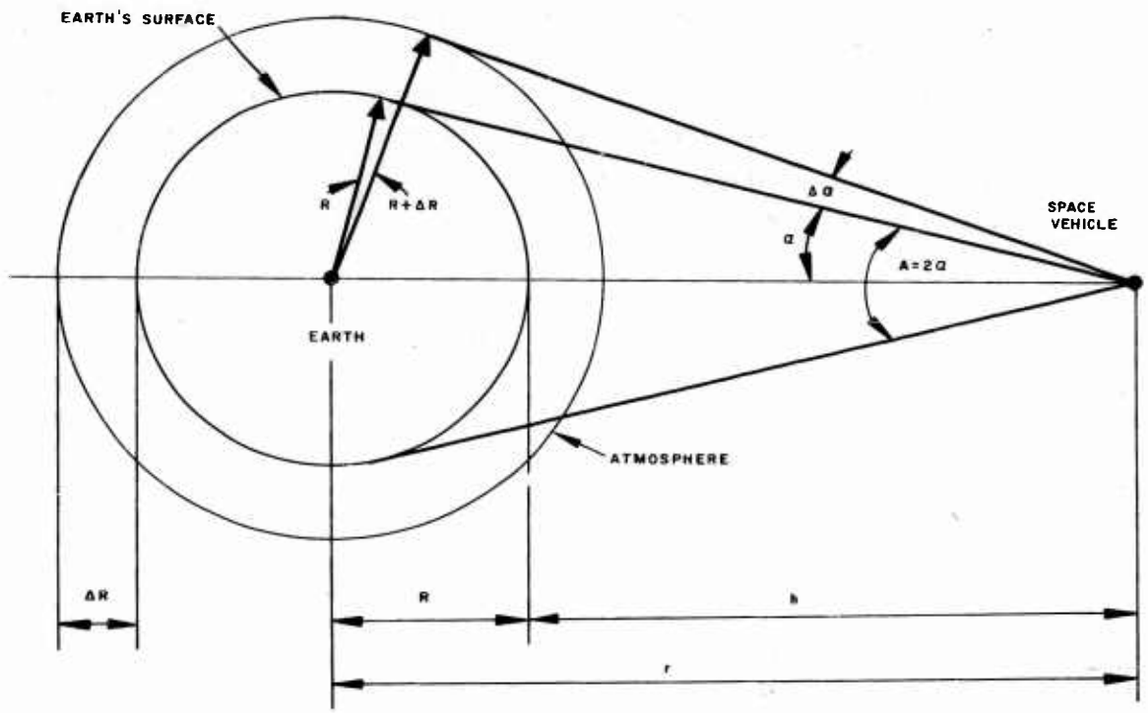

R = EARTH'S RADIUS
h = ALTITUDE
r = RANGE FROM EARTH'S CENTER TO VEHICLE
A = SUBTENDED ANGLE = 2α
ΔR = ALTITUDE OF ATMOSPHERE
α = HALF OF SUBTENDED ANGLE
Δα = ERROR IN MEASUREMENT OF α
$\Delta r_{\Delta\alpha}$ = ERROR IN RANGE DUE TO Δα ERROR
$\Delta r_{\Delta R}$ = ERROR IN RANGE DUE TO ΔR ERROR
$\Delta V_{\Delta\alpha}$ = ERROR IN VERTICAL DIRECTION DUE TO Δα ERROR
$\Delta V_{\Delta R}$ = ERROR IN VERTICAL DIRECTION DUE TO ΔR ERROR

Figure 22. Stadiametric Range Determination Geometry

Using these values a number of quantities were computed and are presented in Table XII. The subtended angle A = 3.18° has been used because with this angle and the parameters assumed the two errors $\Delta r_{\Delta\alpha}$ and $\Delta r_{\Delta R}$ become equal.

Table XII

Ranging Errors

1	2	3	4	5	6	7	8	9	10	11
A deg.	α deg.	r n. m.	h n. m.	$\frac{\Delta r_{\Delta\alpha}}{r}$	$\Delta r_{\Delta\alpha}$ n. m.	$\frac{\Delta r_{\Delta R}}{r}$	$\Delta r_{\Delta R}$ n. m.	$\Delta V_{\Delta\alpha}$	$\Delta V_{\Delta R}$	0.01A
150	75	3,561	121	-1.3×10^{-5}	-0.05	-1.74×10^{-3}	-6.2	10"	11.2'	1.5°
120	60	3,970	530	-2.8×10^{-5}	-0.11	-1.74×10^{-3}	-6.9	10"	5.2'	1.2°
90	45	4,470	1,030	-4.85×10^{-5}	-0.22	-1.74×10^{-3}	-7.8	10"	3'	0.9°
3.18	1.59	124,000	120,560	-1.75×10^{-3}	-216	-1.74×10^{-3}	-216	10"	5"	1.9'

Column 9 gives the error in local vertical for the case where α is measured with an excess at one rim of the earth's disc and a deficit at the opposite rim. Column 10 gives the error in local vertical for the case where one rim is sighted as the true horizon and the other as the atmospheric horizon. Column 11 gives the error in local vertical which is assumed to be roughly equal to 0.01 of the subtended angle (Roberson, 1960), due to the determination of the center of the visible disc by direct visual judgement.

It should be noted that the true error of observation can contain a composite error many times larger than the assumed maximum accuracy of 10 seconds and hence the above table cannot be taken in an absolute sense. The table serves to illustrate several trends. The error in the determination of local vertical decreases as range increases. The relative range error due to horizon uncertainty is independent of range, while the absolute error is proportional to range. The relative range error due to erroneous subtended angle measurement is proportional to the square of range. As a consequence range determination can become critically inaccurate at long ranges.

The overall accuracy of local vertical observations furnished at low altitudes by horizon scanners is at best 0.5°. More sophisticated instrumentation combined with numerical correction for the oblateness

of the earth and the altitude of the atmospheric horizon from precomputed data and based upon averaging (smoothing) methods of a series of observations may furnish local vertical information to an accuracy of about 0.1°.

Periscopes

Periscopes are one form of horizon scanning device. They are used by an astronaut to determine the direction of a body relative to the vehicle axis by centering the view of the body in the viewing screen or porthole. Range may also be determined stadiametrically using periscopic devices. The resulting accuracies of observations using these devices are to a large degree dependent upon the optical design of the periscope itself and on the ability of the astronaut to determine the body's center. Typical total accuracies of this method are roughly of the same order as the accuracy of the horizon scanner discussed above.

Radar Altimeters

Although radar altimeters may determine range very accurately, they are in general restricted to relatively low ranges. The restrictions result from the practical weight and power requirements for operation at long ranges.

Sextants

Sextants are used to measure angles between two bodies and may be automatic or manual. They may be constructed with automatic averaging, stabilization and other refinements. Their accuracy may be as good as 10 seconds of arc.

Sextants can be built in such a way as to permit an accurate determination of subtended visual angle by superimposing (collimating) images of two objects. Readings of angles taken manually with a sextant can be made practically independent from the accuracy with which the vehicle and sextant attitude in space are known. Typical measured angles will be between a fixed star and a discernible landmark on the earth's (or moon's) surface or between a star and the illuminated rim of a planet. Readings of angles could also be taken by visual observation between a fixed star and an estimated center of a planet. It has been found that a human observer can visually estimate the center of a disc with an accuracy of about 1 per cent

of the diameter (Roberson, 1960). The centering of crescent or gibbous shapes is less accurate. When looking at a full disc the accuracy in the vertical direction would be 0.01A (from Table XII). It can be seen that the resulting accuracy is well below the maximum accuracy of observation with a sextant. The error is inversely proportional to range.

Theodolites

Theodolites are similar to automatic star trackers in that they measure the azimuth and elevation angle of the observed object with respect to a particular reference frame such as an inertial platform. The readings will be affected by the accuracy of the instrument itself which can be of the order of 10 seconds and by the accuracy of the reference which may be of the same order of magnitude.

Theodolites may be used by the astronaut in a manner similar to the use of a sextant. These measurements will yield a high degree of accuracy yet are simple enough to be performed manually. Two theodolite telescopes having one common axis of rotation in combination with vehicle roll positioning will permit collimation operations. Angles between a fixed star and a discernible terrestrial landmark or between a fixed star and one of the visible earth's rims will be measured. A theodolite type instrument may also be used to determine the azimuth and elevation angles of the center of a planetary disc with respect to a fixed inertial reference.

ONBOARD TRAJECTORY DETERMINATION

Introduction

The computation of an orbit of a space vehicle requires the use of methods quite different from the well-known methods of classical celestial mechanics which have been successfully applied by astronomers since the time of Newton. The laws governing the motion of celestial bodies are of course the same, but for onboard navigation purposes the time between observations is usually much shorter and a large number of observations different in nature from the classical astronomical observations are made.

The geometry of an orbit can be uniquely defined by six independent parameters, such as the three parameters of position and three of velocity at a given time. Six perfectly accurate independent measurements taken

at a known time would be sufficient to establish uniquely an orbit with absolute accuracy, if the characteristics of the surrounding gravitational fields (attraction by the earth, sun, moon, Jupiter, etc.) also were known with absolute accuracy. Methods of direct numerical solution of this problem are well beyond the possibility of a rapid manual solution. Without engaging in a discussion of the substance and merits of the various known methods of orbit computation, based on the assumption of accurate data, it will be sufficient to state that the choice of a particular method of computation constitutes in itself one of the important facets of a solution.

The assumption of a least sufficient number of perfectly accurate measurements is of course entirely unrealistic. In reality each measurement is assumed to contain error expected to occur according to statistical law and therefore a large number of measurements will be taken. Using one of the available statistical approaches and methods, a most probable solution, i.e., one that best fits the observed data will be found. The choice of a particular statistical method constitutes the second facet in making a decision about the over-all method of solution. The complete computation of the statistically most probable orbit is again well beyond the possibility of manual execution.

Nevertheless, there seem to be several approaches which, at the cost of certain sacrifices, would make possible a manual or nearly manual orbit computation with the help of either a common desk computer or, preferably, a small, simple, and reliable computing unit having a modest memory, control, and entry capability. This computing unit would be used to memorize tables of precomputed and prearranged numerical data and would contain preprogrammed computation schemes so as to reduce the manual operations to the simplest terms, such as entering of observed measured data and specifying the operation to be performed.

At present we are at the beginning of the development of simplified methods of orbit computation. In order to gain some insight into possible solutions, three methods have been studied and are presented in the following sections. Two of these methods are based on the use of precomputed nominal orbits and precomputed elements of operational matrices; the third method is based on the assumption of a simple elliptical orbit, i.e., perturbations caused by celestial bodies other than earth have been

neglected. In this method the elements of correctional statistical matrices are produced in the course of the computation itself. All three methods are based statistically on the method of least squares.

A nominal orbit is one computed from a set of a minimum sufficient number of parameters. It may be the orbit which was initially planned or an orbit which resulted from subsequent revision. The orbit is computed in the best possible rigorous way. A perturbation (small error) is applied singly to each initial parameter and the resulting effect on measurable data at a given instant is computed. It is assumed that for small errors a linear relation (proportionality) exists between the single perturbation of an initial parameter and the resulting error of some measurable observable data at a predetermined later time.

In the two nominal orbit methods described it has been assumed that, after a certain number of observations have been taken, the most probable orbit will be one in which the initial parameters of the nominal orbit have been perturbed in such a way as to reduce to a minimum the sum of the squares of weighted errors, i. e., of the weighted differences between the true measured data and the data that would be observed from the perturbed orbit. The first step of an onboard computation will consist of taking the difference between an observed value and the nominal precomputed and recorded value for this given time. The arithmetic operations consist mostly of taking sums of products. Products are formed through multiplication of initial or intermediate numerical values by precomputed and recorded (tabulated, stored or otherwise memorized) numbers. The end result of computations of an orbit are the numerical values of perturbations of initial orbital parameters, from which the required corrections can be found. Or, by using a modified set of precomputed and recorded data, linearized (proportional) correctional parameters such as the three correctional velocity components can be directly computed and used at predetermined times as the basis for vehicle guidance maneuvers. The guidance maneuvers, according to the particular requirements, can consist of one velocity correction, which will lead the space vehicle toward a point located on the original nominal orbit, or it can consist of two velocity corrections, with the second correction consisting of a thrust impulse that will reestablish the vehicle on the nominal trajectory after the nominal trajectory point is reached. A separate additional computation will be required for

each velocity correction in order to compute the required total velocity increment and the attitude change of the vehicle for properly directing the thrust. This particular computation will be discussed later. A more detailed discussion of the sequences of operation used in one of the methods will also be given later.

A somewhat different principle of computation is used in the method of a simplified elliptical orbit. Trigonometric functions of angles are used in this method. A wide variety of numerical computations including the use of trigonometric tables are required. Generally speaking the computations are more complicated than those discussed for the first two cases.

The two methods of computation based on a nominal orbit differ as follows: the iterative method considers explicitly the uncertainty of assumed injection parameters but the conventional least squares method does not. They differ also in the sequencing and grouping of computational operations. In the first method computations following each observation serve to update certain intermediate computational values which by themselves do not have any geometric or physical meaning. Only after the prescheduled number of observations has been completed and entered in the computations do the updated results yield the final solution of the problem. In the second method a complete up-to-date solution is obtained after each computational step and then used, together with the next set of observations, to obtain the next updated solution. In addition the second method offers the possibility of checking by inspection against gross errors. However, this advantage is gained only at the cost of a larger number of arithmetic operations than are required by the first method.

Neither solution permits the omission of scheduled observations. Non-available missing observation data have to be substituted by interpolated or extrapolated data based on available preceding and succeeding observations. Similar operations of extrapolation and interpolation will be required for data taken at unscheduled times so as to reduce the data values to the predetermined time sequence. In contrast, for the method of the simplified elliptical orbit the observations are taken for their face value as they are made and the sequence of computations, being independent from precomputed data, is free of prearranged timing.

It should be natural to expect future improvements in methods of simplified orbit computation. The desired directions of these improvements can be illustrated by discussing some of the shortcomings of the methods presented in this report.

The most serious defect of methods based on nominal trajectories and linearized perturbations lies in the fact that the results become less accurate with increasing perturbations so as to become worthless for some limit values of initial perturbations, i.e., for cases when the difference between the true and the nominal orbit reaches certain limits. The nominal trajectory methods will give satisfactory results in cases of smaller initial injection errors due to natural accumulations of unavoidable inaccuracies. However, they may be inadequate in cases of larger injection errors due to an outright malfunction creating an emergency condition in which a reliable manual guidance back-up mode may be critically needed. Nominal orbit methods may even be inadequate in cases when a high degree of statistical dispersion of the initial injection conditions is expected. Any attempt of increased accuracy with increased deviations from nominal would require a highly increased memory and numerical operation capacity, so as to make the computations less adaptable to simple and easy manual operation. The method of a simplified elliptical orbit computation is more complicated and perhaps too lengthy for manual computation, but it is independent from any expected nominal orbit. On the other hand, it is not clear at this time under what conditions the elliptical orbit method meets the necessary accuracy requirements. Also these requirements are not exactly known. Further investigation of this matter is desirable. There is some speculation that a simplified and practically acceptable corrections method may be found and applied to the elliptical orbit computation. Such a method is briefly described near the end of this section.

Nominal Orbit Determination Methods

Conventional Least Squares Method

A set of six independent quantities is required to specify the orbit of the spacecraft. These can be the components of position and velocity at injection, the classical elliptic elements, or some other convenient set. In general, let the perturbations in these quantities be denoted by the

6-vector (P). Then, if the orbit were defined by injection position and velocity coordinates, (P) would represent the errors in injection conditions. Now let (O) be an N-vector representing observed deviations of measured quantities from their nominal values at times t_k: k = 0, 1, 2, ...N. It can be shown that the least squares estimate (P*) of (P) is of the form

$$(P^*) = (A'A)^{-1} (A')(O^*) \tag{8}$$

where (A) is an N x 6 matrix of differential coefficients and $O_i^* = \frac{O_i}{\sigma_i}$ where σ_i is the standard deviation of the error on the i^{th} observation. The prime denotes matrix transpose (interchanging rows and columns) and the exponent minus one indicates matrix inversion. The derivation of (8) can be found in Braham (1961) or in Benedict (1961). They both offer the same proof by using a different method of formal representation.

In order to give an example of the nature of manual computations, the arithmetic operations given symbolically by Equation (8) will be made to include corrective maneuver parameters and will be transformed by formal manipulation to the simplest possible form. A step-by-step illustration of the arithmetic operations will also be given.

In Equation (8) the result of matrix operations indicated by the right hand side of the equation will furnish the (P*) matrix. This is a 6 x 1 matrix composed of six perturbation elements as follows:

$$(P^*) = \begin{pmatrix} p_1 \\ p_2 \\ p_3 \\ p_4 \\ p_5 \\ p_6 \end{pmatrix} \tag{9}$$

$$
\begin{aligned}
p_1 &= p_{a1} - p_{c1} \\
p_2 &= p_{a2} - p_{c2} \\
&\text{----------} \\
&\text{----------} \\
p_6 &= p_{a6} - p_{c6}
\end{aligned}
\tag{10}
$$

Here $p_1 \cdots p_6$ are the best estimates of the perturbations of the initial parameters (such as the three coordinates of position and the three components of the velocity vector at the instant of injection). The quantities $p_{a1} \cdots p_{a6}$ are the estimated actual parameters and $p_{c1} \cdots p_{c6}$ the assumed correct parameters that were used in the computation of the nominal orbit. The $p_1 \cdots p_6$ are the unknown quantities to be computed.

For n single observations, (0*) is a n x 1 matrix, as follows:

$$
(0^*) = \begin{pmatrix} o'_1 \\ o'_2 \\ o'_3 \\ -- \\ -- \\ -- \\ o'_n \end{pmatrix}
\tag{11}
$$

$$
\begin{aligned}
o'_1 &= \frac{1}{\sigma_1} (o_{a1} - o_{c1}) = \frac{1}{\sigma_1} o_1 \\
o'_2 &= \frac{1}{\sigma_2} (o_{a2} - o_{c2}) = \frac{1}{\sigma_2} o_2 \\
&\text{----------} \\
&\text{----------} \\
o'_n &= \frac{1}{\sigma_n} (o_{an} - o_{cn}) = \frac{1}{\sigma_n} o_n
\end{aligned}
\tag{12}
$$

Here $o_1, o_2, \ldots o_n$ are the n differences between the actual observed values $o_{a1}, o_{a2}, \ldots o_{an}$ and the expected correct precomputed nominal

values $o_{c1}, o_{c2}, \ldots o_{cn}$; $\sigma_1, \sigma_2, \ldots \sigma_n$ are standard deviations of the errors on the corresponding observations and represent weighting functions.

The (A) matrix is a precomputed n x 6 matrix. Its transpose (A') is a 6 x n matrix, so that the product (A'A) is a square 6 x 6 matrix. A brief review of matrix operations is included in Appendix VII. The inverse $(A'A)^{-1}$ of the product (A'A) is again a 6 x 6 matrix, which, post-multiplied by the 6 x n (A') matrix yields a 6 x n final matrix (B). The matrix (B) is computed from the original precomputed (A) matrix and hence also can be considered as a precomputed matrix. Thus,

$$(P^*) = (B)\,(0^*) \tag{13}$$

Now, the (0*) is a n-rows, one column n x 1 matrix whose elements are functions of observed data multiplied by reciprocals of known constants, representing weighting functions. For example:

$$o'_7 = \frac{1}{\sigma_7}\,(o_{a7} - o_{c7}) = \frac{1}{\sigma_7}\,o_7 \tag{14}$$

where σ_7 is known and $(o_{a7} - o_{c7}) = o_7$ is a function of the observed value o_{a7}. The known reciprocals of σ_i can be considered as row multipliers and may be transferred in form of column multipliers to (B) without altering the product (B) (0*). Thus, another precomputed 6 x n matrix (C) will be obtained instead of (B) and (0*) substituted by a matrix (0), not containing these reciprocals.

$$(P^*) = (C)\,(0) \tag{15}$$

Expanding Equation (15) gives

$$\begin{pmatrix} p_1 \\ p_2 \\ -- \\ -- \\ p_6 \end{pmatrix} = \begin{pmatrix} c_{11} & c_{12} \cdots c_{1n} \\ c_{21} & c_{22} \cdots c_{2n} \\ \cdots & \cdots \quad \cdots \\ \cdots & \cdots \quad \cdots \\ c_{61} & c_{62} \cdots c_{6n} \end{pmatrix} \begin{pmatrix} o_1 \\ o_2 \\ -- \\ -- \\ -- \\ -- \\ o_n \end{pmatrix} \tag{17}$$

The six p elements of Equation (16) are easily computed. For example:

$$p_4 = c_{41} o_1 + c_{42} o_2 + c_{43} o_3 + c_{44} o_4 + .. + c_{4n} o_n \tag{17}$$

Further matrix operations can be applied to the computation of the three components of a corrective velocity vector. Although not explicitly stated, the three position parameters of the initial injection point and the three parameters of the injection velocity must be measured with the help of some reference frame and coordinate system. In order to satisfy the requirements of linearization (proportionality) between small deviations from the nominal of some observable magnitude and small perturbations of the initial parameters it will be advisable to refer the injection perturbations to a system of Cartesian x, y, z co-ordinates and a corresponding unit vector triad, i, j, k, both referred to the same reference, such as an inertial frame. It would not be advisable without using certain precautions, to use spherical co-ordinates which for singular values cease to be well behaved functions. For a similar reason, if a linear relation is assumed between small initial condition perturbations and small corrective velocity components to be applied at a predetermined time, the velocity components also should be referred to a system of Cartesian x, y, z co-ordinates and unit vector triads. It can be assumed that the initial perturbation parameters and the corrective velocity components will be referenced to the same, or to two different initial frames.

The assumption of a linearized (proportional) relation between the perturbation parameters and the corrective velocity components can be expressed as follows. Let the corrective velocity vector $\bar{V}$ be

$$\bar{V} = \bar{i} V_x + \bar{j} V_y + \bar{k} V_z \tag{18}$$

and

$$V_x = k_{x1} p_1 + k_{x2} p_2 + \ldots + k_{x6} p_6 \tag{19}$$

$$V_y = k_{y1} p_1 + k_{y2} p_2 + \ldots + k_{y6} p_6 \tag{20}$$

$$V_z = k_{z1} p_1 + k_{z2} p_2 + \ldots + k_{z6} p_6 \tag{21}$$

In the above the 18 "k" coefficients are precomputed constants. Equations (19) through (21) can be written compactly in matrix form as the matrix product (V) of a 3 x 6 (K) matrix and a 6 x 1 (P*) matrix.

$$(V) = (K)\,(P^*) \tag{22}$$

Expanding (22) will give

$$\begin{pmatrix} V_x \\ V_y \\ V_z \end{pmatrix} = \begin{pmatrix} k_{x1} & k_{x2} \cdots\cdots k_{x6} \\ k_{y1} & k_{y2} \cdots\cdots k_{y6} \\ k_{z1} & k_{z2} \cdots\cdots k_{z6} \end{pmatrix} \begin{pmatrix} p_1 \\ p_2 \\ p_3 \\ p_4 \\ p_5 \\ p_6 \end{pmatrix} \tag{23}$$

By using matrix algebra substitute (22) into Equation (15) or the expanded (17).

$$(V) = (K)\,(P^*) = (K)\,(C)\,(0) \tag{24}$$

Multiplication of the 3 x 6 (K) and the 6 x n (C) matrices furnishes a 3 x n (D) matrix.

$$(V) = (D)\,(0) \tag{25}$$

$$\begin{pmatrix} V_x \\ V_y \\ V_z \end{pmatrix} = \begin{pmatrix} d_{11} & d_{12} \cdots\cdots d_{1n} \\ d_{21} & d_{22} \cdots\cdots d_{2n} \\ d_{31} & d_{32} \cdots\cdots d_{3n} \end{pmatrix} \begin{pmatrix} o_1 \\ o_2 \\ -- \\ -- \\ -- \\ o_n \end{pmatrix} \tag{26}$$

So far we have been concerned with one velocity correction. For two velocity corrections a second set of three corrective velocity components are required. The (V) matrix must be expanded in a 6 x 1 matrix and the (D) matrix must be expanded in a 6 x n matrix.

The three corrective velocity components, V_x, V_y and V_z still cannot be used as such for establishing the control operation of a corrective maneuver. The total velocity change ΔV will have to be computed as follows.

$$\Delta V = \sqrt{V_x^2 + V_y^2 + V_z^2} \tag{27}$$

It is probable that in order to deliver the corrective thrust in the proper direction, two attitude angles will be required, such as of a consecutive roll and pitch maneuver through angles Φ and θ. These computations will most probably be of the form

$$\Phi = \tan^{-1} \frac{V_y}{V_z} \tag{28}$$

$$\theta = \tan^{-1} \frac{V_z}{\Delta V} \tag{29}$$

or of some similar form. The character of the corrective maneuver will depend, of course, on the available control system and no further conjectures will be made in this regard.

The proposed sequence of arithmetic operations will be illustrated in the following discussion.

Independent of the kind of observations, let it be assumed that a total number of n single observation entries will be prescheduled and obtained in succession. Each entry may be the result of just one observation taken at a predetermined time, or the average of several observations clustered about this time. In the later case the averaging would represent the first arithmetic operation and there will be a total of n averaging operations. The simplest arithmetic averaging operation of k observations will consist of k-1 summations and one division, a total of n(k-1) summations and n divisions.

Consider again Equation (26) which may be rewritten in a slightly different manner.

$$\begin{pmatrix} V_x \\ V_y \\ V_z \end{pmatrix} = \begin{pmatrix} d_{11} & d_{12} \cdots\cdots d_{1n} \\ d_{21} & d_{22} \cdots\cdots d_{2n} \\ d_{31} & d_{32} \cdots\cdots d_{3n} \end{pmatrix} \begin{pmatrix} o_{a1} - o_{c1} \\ o_{a2} - o_{c2} \\ \text{---------} \\ \text{---------} \\ \text{---------} \\ \text{---------} \\ o_{an} - o_{cn} \end{pmatrix} \qquad (30)$$

The following values should be tabulated or otherwise memorized: 3n "d" elements, n "o_c" elements (the nominal precomputed correct measurable values), a total of 4n values. After each "o_a" entry (the actually measured value) has been obtained, the algebraic difference $o_{ai} - o_{ci}$ will be computed by subtraction, a total of n subtractions.

The matrix multiplication indicated by Equation (30) could be performed after all observations have been completed. In order to distribute the operational burden more evenly in time it has been proposed, instead, to update the computations while data becomes available.

Thus each time after an entry $o_i = o_{ai} - o_{ci}$ has been obtained three partial, or intermediate sums will be formed as follows.

After the first entry, $o_1 = o_{a1} - o_{c1}$, has been obtained

$$V_x = d_{11} o_1 + \ldots$$

$$V_y = d_{21} o_1 + \ldots$$

$$V_z = d_{31} o_1 + \ldots \qquad (31)$$

After the second entry, $o_2 = o_{a2} - o_{c2}$, has been obtained

$$V_x = \left[d_{11} o_1 \right] + d_{12} o_2 + \ldots$$
$$V_y = \left[d_{21} o_1 \right] + d_{22} o_2 + \ldots \qquad (32)$$
$$V_z = \left[d_{31} o_1 \right] + d_{32} o_2 + \ldots$$

After the i-th entry, $o_i = o_{ai} - o_{ci}$, has been obtained

$$V_x = \left[d_{11} o_1 + d_{12} o_2 + \ldots + d_{1,i-1} o_{i-1} \right] + d_{1,i} o_i + \ldots$$
$$V_y = \left[d_{21} o_1 + d_{22} o_2 + \ldots + d_{2,i-1} o_{i-1} \right] + d_{2,i} o_i + \ldots$$
$$V_z = \left[d_{31} o_1 + d_{32} o_2 + \ldots + d_{3,i-1} o_{i-1} \right] + d_{3,i} o_i + \ldots \qquad (33)$$

In the above formulas the brackets indicate previously computed intermediate sums. Each entry, o_i, will require three multiplications and starting from the second entry onward, three summations, a total of 3 n multiplications and 3 (n-1) summations.

Thus, the following operations will be required per entry.

Averaging of k observations (if applicable)	
Summations k-1	
Divisions 1	
Total, averaging computation, number of operations	k
Deviation from nominal subtraction	1
Matrix elements computation, multiplication	3
Summation (starting from second entry)	3
Total, per entry, operations	7 + k
Computation of corrective velocity components,	
Grand Total, operations	(7+k) n - 3

The above number of operations is computed for the case of one corrective maneuver, requiring three corrective numerical parameters.

In the case of two velocity corrections requiring six corrective numerical parameters the grand total of arithmetic operations will be equal to $n(13 + k) - 6$.

Iterative Method

An iterative procedure for data smoothing is also available which has certain advantages over the conventional least squares method but requires the storage of more precalculated data and more computation. The procedure is given by Equation (34),

$$P^*_n = P^*_{n-1} + \Delta^*_n \left[Y_n - M_n P^*_{n-1} \right] \tag{34}$$

where P^*_n is the optimal estimate, Δ^*_n and M_n are prestored matrices, Y_n is a 3-vector representing observed deviations from the nominal trajectory, the subscript n here refers to the current sighting, and the subscript n-1 refers to the previous sighting. For this process, 39m numbers must be stored for m sightings each composed of three single observations (three entries per sighting) and the following computations are required for each sighting:

1. Subtract the nominal values of the observed angles from the measured values (three subtractions) to obtain Y_n.
2. Premultiply the 6 x 11 P^*_{n-1} by the 3 x 6 M_n matrix (18 multiplications, 15 additions)
3. Subtract $M_n P^*_{n-1}$ from Y_n (three subtractions)
4. Multiply by Δ^*_n (18 multiplications, 12 additions)
5. Add to P^*_{n-1} (six additions)

A total of 75 arithmetic operations per sighting, or 25 operations per single entry is required. Thus both the storage and the computation required are much larger than for the previous method. Note, however, that to obtain a new estimate at each sighting using the conventional least squares technique may require even more storage and computation.

Perhaps the chief advantage of the iterative method is that it allows a step-by-step error check on the measurements and computation. That is, if a currently computed parameter estimate (P^*_n) differed from the

previous estimate by more than a preassigned acceptance level, the astronaut would suspect that an error had been made either in making the measurements, in performing the calculations, or both. The astronaut could then check his calculations and make the necessary corrections. He may substitute interpolated or extrapolated data for data in question and proceed to the next observation.

Non-Nominal Orbit Determination Methods

If no nominal trajectory is known, trajectory and guidance computations are orders of magnitude more difficult. It is well, therefore, to examine the requirements for handling non-nominal trajectories.

It may be argued, on the one hand, that the need for trajectory and guidance computations for other than nominal trajectories would be extremely rare. That is, for any currently planned mission, the need for a minimum onboard capability would result from the failure of injection guidance to place the spacecraft on a nominal trajectory and failure of both the primary onboard computing capability (if any) and ground tracking or communications link. On the other hand, most people feel that, where the man's life is at stake, every possible effort should be made to ensure his safety. It follows that every means of providing backup systems for performing critical functions should be investigated. In surveying possible backup navigation and guidance systems, however, it should be borne in mind that the goal is to devise a system which is as reliable as possible rather than a system which is (a priori) as manual as possible.

The general problem of onboard navigation and guidance can be simplified in some cases through use of the two-body approximation, giving special attention to the estimation and correction of parameters critical to a given mission. Even if the two-body approximation is valid, however, there remains the problem of estimating the trajectory from data containing significant error. A method for determining from noisy measurements the path of a spacecraft moving in an elliptic trajectory has been developed and is presented below.

Elliptical Orbit Determination Methods

Basic Equations. The following general equations for trajectory determination have been discussed in Appendix V. There are four mathematical steps in the orbit determination process.

1. Update the covariance matrix (P*) of the optimal estimation error

$$P^*(t - dt) = \Phi(t; t_o)\, P^*(t_o)\, \Phi'(t; t_o) \tag{35}$$

where t_o is the time of the previous observation, t is the time of the current observation, and (Φ) is the 6 x 6 transition matrix (derived below in "Applications of Basic Equations to Elliptical Orbits") relating perturbations from the estimated trajectory at time t to perturbations from the estimated trajectory at time t_o; that is,

$$\Phi ij = \frac{\partial x_i(t)}{\partial x_j(t_o)} \tag{36}$$

The prime denotes matrix transpose (interchanging rows and columns), and the argument (t - dt) identifies the time immediately preceding the observation.

2. Compute the weighting function Δ^*.

$$\Delta^*(t) = P^*(t - dt)\, M'(t) \left[M(t)\, P^*(t - dt)\, M'(t) + Q(t)\right]^{-1} \tag{37}$$

where (M) is the matrix relating trajectory perturbations to perturbations in observed quantities, and (Q) is the covariance matrix of the measurement errors. The exponent minus one denotes matrix inverse.

3. Update P* after the observation.

$$P^*(t) = P^*(t - dt) - \Delta^*(t)\, M(t)\, P^*(t - dt) \tag{38}$$

4. Compute a new trajectory estimate x*.

$$x^*(t) = x^*(t - dt) + \Delta^*(t)\left[y_m(t) - y_c(t - dt)\right] \tag{39}$$

where y_m are the observed quantities and y_c are computed from $x^*(t - dt)$, which is the best estimate of the trajectory before the time of the observation.

To solve the above equations, x^* and P^* are specified initially, and the matrices (Φ), (M) and (Q) are computed. In addition, calculations are required for updating x^* in the absence of observations and for computing the predicted values y_c of the observables.

Application of Basic Equations to Elliptical Orbits

Coordinates are chosen as follows:

$$x = \begin{bmatrix} r \\ \theta \\ p \\ e \\ \Omega \\ i \end{bmatrix} \quad (40); \qquad y = \begin{bmatrix} r \\ \Phi \\ \epsilon \end{bmatrix} \quad (41)$$

where

r = range from the observed planet

θ = inplane angle measured from the equatorial plane in the direction of orbit

p = semi-latus rectum

e = eccentricity

Ω = longitude of the ascending node

i = inclination angle of the orbital plane with respect to the equatorial plane

Φ = azimuth angle

ϵ = elevation angle

With the coordinates so chosen, both the (Φ) and the (M) matrices have particularly simple forms. The (M) matrix is:

$$M = \begin{pmatrix} 1 & 0 & 0 & 0 & 0 & 0 \\ 0 & \frac{\partial \Phi}{\partial \theta} & 0 & 0 & 1 & \frac{\partial \Phi}{\partial i} \\ 0 & \frac{\partial \epsilon}{\partial \theta} & 0 & 0 & 0 & \frac{\partial \epsilon}{\partial i} \end{pmatrix} \tag{42}$$

where the partial derivatives (43) are found easily from the geometry to be:

$$\frac{\partial \epsilon}{\partial \theta} = \frac{\cos \theta \sin i}{\cos \epsilon_c}$$

$$\frac{\partial \epsilon}{\partial i} = \frac{\sin \theta \cos i}{\cos \epsilon_c}$$

$$\frac{\partial \Phi}{\partial \theta} = \frac{\cos i}{\cos^2 \epsilon_c}$$

$$\frac{\partial \Phi}{\partial i} = - \frac{\sin 2\theta \sin i}{2 \cos^2 \epsilon_c} \tag{43}$$

where

$$\cos \epsilon_c = + \sqrt{1 - \sin^2 \theta \sin^2 i} \tag{44}$$

All but six of the 36 elements of the (Φ) matrix are either zero or unity. Thus,

$$\Phi = \begin{pmatrix} \frac{\partial r}{\partial r_o} & 0 & \frac{\partial r}{\partial p_o} & \frac{\partial r}{\partial e_o} & 0 & 0 \\ \frac{\partial \theta}{\partial r_o} & 1 & \frac{\partial \theta}{\partial p_o} & \frac{\partial \theta}{\partial e_o} & 0 & 0 \\ 0 & 0 & 1 & 0 & 0 & 0 \\ 0 & 0 & 0 & 1 & 0 & 0 \\ 0 & 0 & 0 & 0 & 1 & 0 \\ 0 & 0 & 0 & 0 & 0 & 1 \end{pmatrix} \tag{45}$$

The six non-trivial elements (46) are derived in Appendix VI. They are:

$$\frac{\partial r}{\partial r_o} = \frac{\sin \eta}{\sin \eta_o}$$

$$\frac{\partial \theta}{\partial r_o} = \frac{p}{e \sin \eta_o}\left(\frac{1}{r^2} - \frac{1}{r_o^2}\right)$$

$$\frac{\partial \theta}{\partial p_o} = -\frac{3}{2r^2}\sqrt{\frac{K}{p}}\,(t - t_o) + \frac{1}{r_o e \sin \eta_o}\left(1 - \frac{r_o^2}{r^2}\right)$$

$$\frac{\partial r}{\partial p_o} = \frac{r}{p}\left[1 - \left(\frac{r}{r_o}\right)\frac{\partial r}{\partial r_o} + r e \sin \eta \frac{\partial \theta}{\partial p_o}\right]$$

$$\frac{\partial \theta}{\partial e_o} = \frac{2a}{\mu r^2}\sqrt{\frac{K}{p}}\left[(1 + e^2)(\sin E - \sin E_o) - \frac{3e}{2}(E - E_o)\right.$$

$$\left. - \frac{e}{4}(\sin 2E - \sin 2E_o)\right] - \frac{\cot \eta_o}{e}\left(1 - \frac{r_o^2}{r^2}\right)$$

$$\frac{\partial r}{\partial e_o} = \frac{r^2}{p}\left[\cos \eta_o \frac{\partial r}{\partial r_o} - \cos \eta + e \sin \eta \frac{\partial \theta}{\partial e_o}\right] \qquad (46)$$

where quantities not previously defined are:

η = true anomaly

K = product of the universal gravitational constant and the mass of the attracting body.

a = semimajor axis

μ = mean angular motion

E = eccentric anomaly

Computational Requirements. A computer routine for processing the observation angles would perform the following sequence of calculations for each observation.

1. Update inplane coordinates r, θ to the time t of the observation. r_o, θ_o, p, e, Ω, i are available initially or from the previous calculation at t_o.

a. $$a = \frac{p}{1 - e^2}$$

b. $$\mu = \sqrt{\frac{K}{a^3}}$$

c. $$\cos E_o = \frac{a - r_o}{ae}$$

$$\sin E_o = \pm \sqrt{1 - \cos^2 E_o}$$

d. $$\sin \eta_o = \frac{a\sqrt{1 - e^2}}{r_o} \sin E_o$$

$$\cos \eta_o = \frac{1}{e}\left(\frac{p}{r_o} - 1\right)$$

e. $$\sin \omega = \sin \theta_o \cos \eta_o - \cos \theta_o \sin \eta_o$$

$$\cos \omega = \cos \theta_o \cos \eta_o + \sin \theta_o \sin \eta_o$$

f. $$\sigma = E_o - e \sin E_o - \mu t_o$$

g. Solve for E:

$$\mu t + \sigma = E - e \sin E$$

h. $$r = a(1 - e \cos E)$$

i. $$\sin \eta = \frac{a\sqrt{1 - e^2}}{r} \sin E$$

$$\cos \eta = \frac{1}{e}\left(\frac{p}{r} - 1\right)$$

j. $\sin\theta = \sin\eta \cos\omega + \cos\eta \sin\omega$

$\cos\theta = \cos\eta \cos\omega - \sin\eta \sin\omega$

2. Compute the Φ matrix.

3. Predict the azimuth and elevation angles

a. $\frac{x}{r} = \cos\Omega \cos\theta - \sin\Omega \cos i \sin\theta$

$\frac{y}{r} = \cos\Omega \cos\theta + \cos\Omega \cos i \sin\theta$

$\frac{z}{r} = \sin i \sin\theta$

b. $\sin\epsilon_c = \frac{z}{r}$

$\cos\epsilon_c = + \sqrt{1 - \sin^2\epsilon_c}$

where

$-\frac{\pi}{2} \leq e \leq +\frac{\pi}{2}$

c. $\sin\Phi_c = \frac{y}{r} \frac{1}{\cos\epsilon_c}$

$\cos\Phi_c = \frac{x}{r} \frac{1}{\cos\epsilon_c}$

4. Compute the M matrix.

5. Compute the covariance matrix Q of the measurement errors. The elements of the Q matrix are functions of the basic instrument errors and range.

6. Compute $P^*(t - dt)$, $\Delta^*(t)$, $P^*(t)$

7. Compute a new trajectory estimate.

$$x^*(t) = x^*(t - dt) + \Delta^*(t) \begin{pmatrix} (r_m - r) \\ \sin^{-1}(\sin \Phi_m \cos \Phi_c - \cos \Phi_m \sin \Phi_c) \\ \sin^{-1}(\sin e_m \cos e_c - \cos e_m \sin e_c) \end{pmatrix}$$

The six components of $x^*(t)$ and t are stored for input to step (1) at the next observation.

Simplified Approach

The method described above obviously requires the use of a digital computer. A simplified intuitive approach will be outlined now which, conceivably, could be realized without the use of a computer. The procedure has not been subjected to a detailed analysis and is therefore merely a suggestion of a line of development.

Assume that the azimuth and elevation of the earth from the vehicle are measured with respect to a stellar inertial reference and that range is obtained from subtended angle measurement. Navigation and guidance computations could then be done in the following way. Measurements are made at regularly spaced intervals in time. Rate of change of range and rate of change of in-plane angle are obtained by numerical differentiation; these are used to compute and smooth energy and angular momentum. The four remaining coordinates can be represented as the polar coordinates in the plane of motion and two angles defining the orientation of the plane. It would be hoped that these four quantities could be obtained to sufficient accuracy without smoothing — either from raw data or from a combination of raw data and closed form integration of the equation of motion from injection (assuming zero injection error in position). The computations required for guidance depend more upon the specific mission. For example, a backup guidance system for eccentric earth orbital flights out to an apogee of 10^5 n. m. or so might be called upon to place the vehicle in an orbit having a specified orientation and perigee altitude so that conversion to a nearly circular orbit at perigee and subsequent reentry from that orbit can be effected.

The following computations are required for each observation:

$$\Delta\theta_n = \cos^{-1}\left\{\cos \epsilon_n \cos \epsilon_{n-2} \cos(\Phi_n - \Phi_{n-2}) + \sin \epsilon_n \sin \epsilon_{n-2}\right\}$$

$$\dot{\theta}_{n-1} \approx \frac{\Delta\theta_n}{(2\Delta t)}$$

$$r_n = R \operatorname{ctn} \frac{1}{2} A_n$$

$$\dot{r}_{n-1} \approx \frac{1}{(2\Delta t)} (r_n - r_{n-2})$$

$$h_n = r_{n-1}^2 \dot{\theta}_{n-1}$$

$$h_n^* = (1 - K_1) h_{n-1}^* + K_1 h_n$$

$$W_n = \dot{r}_{n-1}^2 + \frac{h_n^{*2}}{r_{n-1}^2} - \frac{(2\mu)}{r_{n-1}}$$

$$W_n^* = (1 - K_2) W_{n-1}^* + K_2 W_n$$

where

Φ = azimuth angle

ϵ = elevation angle

A = subtended angle

θ = inplane angle

r = range

Δt = constant time interval between observations

R = earth radius

h = angular momentum of the vehicle per unit mass

W = twice the energy of the vehicle per unit mass

μ = constant

K_1, K_2 = tabulated functions of range[1]

The asterisk superscript denotes a smoothed quantity and the subscripts n, n-1, and n-2 refer to the current observation, the previous observation, and the one before that, respectively. Of course, other calculations are required to determine the other four coordinates and to compute a velocity correction, but the equations listed above, since they are computed at each and every observation, would be expected to make up most of the total computation.

A brief comment on the accuracy of the unsmoothed coordinates is in order. These coordinates, let us say, are given by

r = range

θ = inplane angle, measured from the equatorial plane in the direction of motion

Ω = longitude of the ascending mode

i = inclination of the orbital plane with respect to the equatorial plane

The accuracy of the computed angles θ, Ω, i is of the same order as the angular accuracy obtained in sighting the earth. Errors in computed values of θ, Ω, i affect guidance chiefly by causing a misorientation of the vehicle for making a velocity correction. The orientation error due to the attitude control system, however, is probably comparable. If range is obtained directly from subtended angle and the error of the subtended angle is δA, the range error δr is approximately

$$\frac{\delta r}{r} \approx \frac{r}{2R} \quad \delta A \tag{47}$$

which can be quite large. Then, too, some prediction of range is required to allow time for making the guidance computation and orienting the vehicle. Range at the preassigned time for making the velocity correction can be

[1] The K_1 function of range is used here in an attempt to equalize, at least in part, the fact that in the computation of $h = r^2\dot{\theta}$, the poorer accuracy of r with increasing range may corrupt the higher accuracy of $\dot{\theta}$; K_2 is used in a similar manner in the computation of W.

predicted from the range at injection or from an earlier measurement made at the range where $\delta r / \sin\eta$ (η = true anomaly) is a minimum – whichever produces less error in predicted range. The predicted range will be computed as a function of a number of variables (r_o, θ_o, W, h, Ω, i). Error in predicted range is then related to error in initial range by

$$\delta r \approx \frac{\sin\eta}{\sin\eta_o} \delta r_o$$

MANUAL NAVIGATION COMPUTER DESIGN

While the methods of data smoothing described in the preceding section are quite general and can be applied to any well defined mission, they could, depending on the accuracy required, involve a considerable amount of data storage and computation. There are basically two ways of alleviating the storage and computation problem: (1) provide the astronaut with calculating aids (e.g., desk-type calculator, or a small ultra-reliable computer with a manual data entry capability), or; (2) devise computationally simpler techniques appropriate to specific missions.

Since the parameter estimation process involves only table look-up and simple matrix operations, it appears likely that a simple, reliable, rugged, yet lightweight device, can be constructed either to aid or to automate the required calculations. Of course, special purpose computers with GP-type instruction codes can also be considered, but it might be argued that such a system is not sufficiently manual. At any rate, regardless of the size and complexity of such a computer, the man is required to perform about the same tasks – prepare and enter data into the computer and accept and act upon guidance information received from the computer. One further qualification is in order. One would expect that a larger computer would provide more than a minimum amount of information, thus involving perhaps a sophisticated display and providing substantially more to the man than would systems having a minimum computer. By definition, sophisticated approaches are outside the scope of the present study.

The preliminary design of a computer to satisfy the computation requirements of a manual navigation system is described below. For this design exercise it was assumed that the computation requirements performed automatically by this computer would be restricted to the corrective

velocity components, calculations given by Equation (49) which has been previously defined. The 6 x 1 (V) matrix contains a total of six corrective velocity components: V_{x1}, V_{y1}, V_{z1} for the first velocity correction, V_1, and V_{x2}, V_{y2}, V_{z2} for the second corrective velocity, V_2. Matrix (D) is a 6 x 40 matrix where 40 is the number of single entries (observed values). Matrix (O) is a 40 x 1 matrix containing 40 differences between observed and recorded values. The computations performed by the computer will thus be limited to the components of two corrective velocity vectors, as discussed in a preceding section. Attitude change and control operation computations are not included.

$$(V) = (D)(O) \tag{49}$$

The computer must be capable of the repeated multiplication of the two matrices (D) and (O). It must also provide storage for intermediate computational results after each set of observed values are entered. For this study it was assumed that the set of observed values will be entered manually at a rate not exceeding about one every few seconds with the total number of observation sets being less than forty. Since this device will be used primarily in the event of a main computer failure or as the only onboard navigation computer it was assumed that this computer must have a probability of successful operation of 0.999 over a mission length of one week (168 hours). It is in a sense performing manual back up function and has been named the BOOTSTRAP computer.

Design Considerations

Reliability

The most stringent design requirement on this device is the specified reliability. If the failures are assumed to occur at random, the mean time between failures (MTBF) for this machine is computed by Equation (50),

$$p = \exp(-t/\text{MTBF}) \tag{50}$$

where p equals 0.999 and t equals 168 hours. The resulting MTBF is 168,000 hours. This number is astronomical at the present state of the computer art even for a very simple computer. It suggests that the computer system must be either redundant or testable and repairable. Redundancy alone implies at least three identical units with the astronaut

acting as an umpire. Of course, one of these redundant units would generally be available to some extent in the main navigation computer. Onboard repair of equipment requires test routines, diagnostic routines, spare parts and, in general, a larger machine. Using redundancy with a moderate test capability would require two machines and a test procedure for determining which machine has failed but not necessarily a repair capability.

One Machine With Onboard Repair. One approach to the problem of meeting the reliability requirements is to use one computer and provide the capability for repairing any portion of the computer onboard the spacecraft. In the absence of specifications of allowable down time it may be assumed that this configuration would be acceptable under certain conditions. Since any portion of the computer may develop a fault, it is necessary to carry a complete line of spare parts aboard for the computer. Since the computer may develop a fault which is not externally noticeable, test programs must be provided inside the computer to determine internal faults. This results in an increase in size over that of the minimum computer. It is estimated that the test programs and any diagnostic routines required would probably add at least 40 to 50 per cent to the size of the computer. Thus, the total machine components carried aboard the spacecraft in units of minimal machines would be those for the basic machine plus 50 per cent more for test and diagnostic purposes within the machine plus 50 per cent of the total machine in spare parts. This yields a total of 2-1/4 basic computers.

Two Machines With Test Capability. Another approach to the problem of meeting reliability requirements is to use two of the basic machines and provide a capability for testing to determine which machine has made a fault (no diagnosis or repair). The test for fault need not be made when the fault occurs but may be made at any convenient time. The test procedure should be simple but must be able to detect all faults to determine which machine has made the error. A test problem of careful design could perform this test without requiring additional test equipment. A MTBF of 5170 hours for each machine will yield the desired system reliability.

Three Machines. A third approach to achievement of the desired reliability is to use three machines in parallel. No testing within machines would be required since agreement is assumed to indicate correctness. The

majority logic element most likely would be the astronaut. To obtain the system reliability of 0.999 for a one week mission the MTBF of each machine is 8300 hours.

Other techniques which may be employed to improve reliability are (1) multiple computation of results and comparison of answers or (2) redundancy within the machine rather than redundancy of entire machines. The former technique is particularly adaptable to this system as there may be extended periods between scheduled computations, and even the slowest computers would have time to perform repeated calculations and compare answers. Answer comparison may be within the machine or between machines. It is seen that this technique would tend to eliminate the transient failures which may occur within the machine and which are generally not included in the computation of the failure rate of the machine. The latter technique of redundancy within the machine is particularly advisable where high failure rate components such as switches or lights are used. Since it is anticipated that relatively high failure rate components will of necessity be used in the input/output system for the machine, it is advisable that either test features and reparability of the switches and lights or redundancy within the switches and lights be included in the design of the machine. In the case of lights this may be accomplished by supplying two lights in parallel. The switch problem is more complicated as all types of failures cannot be eliminated or substantially reduced by redundancy within one switch unit. However, it is anticipated that the reliability for switches will be much better than the reliability for lights and that simple redundancy will remove the most prevalent types of switch failures.

Computation Requirements

The computation requirements of the machine are determined by the desired accuracy, the amount of computation to be performed, the input rate, and the output rate. The accuracy of the inputs has been specified as 20 bits and the accuracy of the stored constants as approximately 10 bits for some constants and 20 bits for other constants. The word length requirement will be set at 20 bits. The computations to be performed require that the nominal value which is stored within the computer be subtracted from the observed value and the difference multiplied by 6 constants in the (D) matrix. The results of these multiplications are added to the

partial sums which form the (V) matrix. With word length of 20 bits and the amount of computation to be done between each input, namely one subtraction, 6 multiplications and 6 additions, a serial wired program machine could perform this calculation within 3,000 bit times. Since it is perfectly adequate that the answer be generated within 1 second, a clock rate of 3,000 pulses per second is adequate. It will be assumed that the clock rate will be less than 10 kc and most probably less than 5 kc. Exact determination of the clock rate is not necessary at this time and will be deferred until such later time as further requirements can restrict the clock rate.

Another calculation which the machine could perform is the conversion of inputs from a decimal form to a binary form and the conversion of outputs from binary to decimal. However, since these calculations are so much more complicated than those described above, it is recommended that the machine inputs and outputs be in binary form.

Physical Characteristics

The design considerations of the physical characteristics of the machine are determined by the fact that the machine has to fit into a spacecraft environment. Since no specific restrictions have been placed on the machine at this time, it will be said only that the power consumption, size, and weight of the machine should be as small as possible. The time period of the machine is specified by the requirement for use of present day construction techniques. Therefore, it will be assumed that packaging techniques such as welded stick construction and memory techniques such as cores will be used within the machine.

System Design

Input-Output

Since the output will be at most 10 bits, yielding an accuracy of 1 part in 1,000, it is seen that the manual binary to decimal conversion from tables is rather simple. The table would contain only 1,000 entries which could fit easily on 4 sides of 8 x 10 paper. However, the input is 20 bits long since it must have an accuracy of one part in a million. A table for converting the decimal inputs directly to binary inputs would have 1 million entries and require 4,000 sides of paper. One way to reduce the required

size of a conversion table is to break the input decimal number into two parts, the three most significant digits and the three least significant digits, find the conversion for each of these parts, add the two binary number equivalents together, and enter the total on the input switches into the machine. The tables for this procedure would require only 8 sides of paper. The requirement for adding the two halves of the input external to the machine results from the desirability of the astronaut being able to check the number that he put into the machine by examining the switch positions. If he were to enter both halves of the number and have the addition performed within the machine, the first number entered would be unknown to the astronaut when he sets the second number onto the switches unless two banks of switches were provided. The provision of two banks of switches would reduce the reliability of the machine. The input-output problem should be studied in greater depth as the system design is solidified. It should be noted that the sensor outputs may be specified easily in octal numbers. This would reduce the input problem considerably.

The output for the machine is a bank of 10 indicator lights. As a method of increasing reliability, one may provide either two lights in parallel at each indicator or, lights with a test and replacement feature. Standard push-to-test lights may be replaced easily. The use of these lights would result in a system as reliable as the parallel light system. Parallel lights consume twice as much power as the single replaceable lights. Since the output lights require a considerable fraction of the total power required for the computer, a study of the onboard power source is necessary to determine which method of output indication is desirable.

Data input may be made by means of a set of 20 toggle switches (one twenty-bit word). If an octal system were desired, seven 8-position rotary switches might be used. Other input signals which are anticipated at this time may be provided by (1) a start button to indicate when the next group of calculations should be started, (2) a repeat button to indicate that the last set of calculations should be performed again, (3) a clear button to bring the computer back to the starting point, and (4) a single step/automatic switch to permit selection of the desired output.

Memory

Examination of the equation which this computer must solve shows that a total of 280 words of permanent memory are required. This includes the 240 constants that must be stored for the 6 x 40 (D) matrix and the 40 constants that must be stored for the nominal values of the observed quantities in the (O) matrix. The core rope memory developed at MIT is particularly suitable for this purpose. (Alonso and Laning, 1960.) This memory uses 1 core per word with 20 output wires either threading or not threading the cores depending on whether a 1 or a 0 is being stored in the bit position indicated by the output wire. This highly compact memory requires approximately 25 cu. in. It requires an average power of less than 100 mw for operation of the core storage and associated circuits at a 10 kc rate.

Fourteen words of temporary storage are required for this computer. These include a slot in which to store the value of (O) currently being used, 6 locations for storing the partial results and 6 locations for storing the previous results. The latter 6 are necessitated by the requirement for repeating the last set of calculations. It is anticipated that the temporary memory will be a sequential access memory (SAM). This memory has been developed at Hughes Aircraft Company. For sequential read-out only 1 core per word is switched at each bit time. The total number of cores in the memory is 1 per bit per word – or 280 cores. The packing density for this memory is approximately 4 bits/cu. in. This results in a temporary memory of 65 cu. in. Since only 14 cores are switched per bit time, the power requirements are extremely low. It is estimated to be approximately 35 mw, including power in the access circuitry.

The memory addressing register and the associated logic for the two memories will be combined into one register since the memories are not addressed simultaneously. By proper address of the locations the same circuitry can be used for both memories. This will result in a saving in parts and power.

Arithmetic Unit

The arithmetic unit, see Figure 23, is serial in operation and operates on binary numbers represented in a fixed point, true (2's) complement form. The number range is -1 to + $(1 - 2^{-19})$.

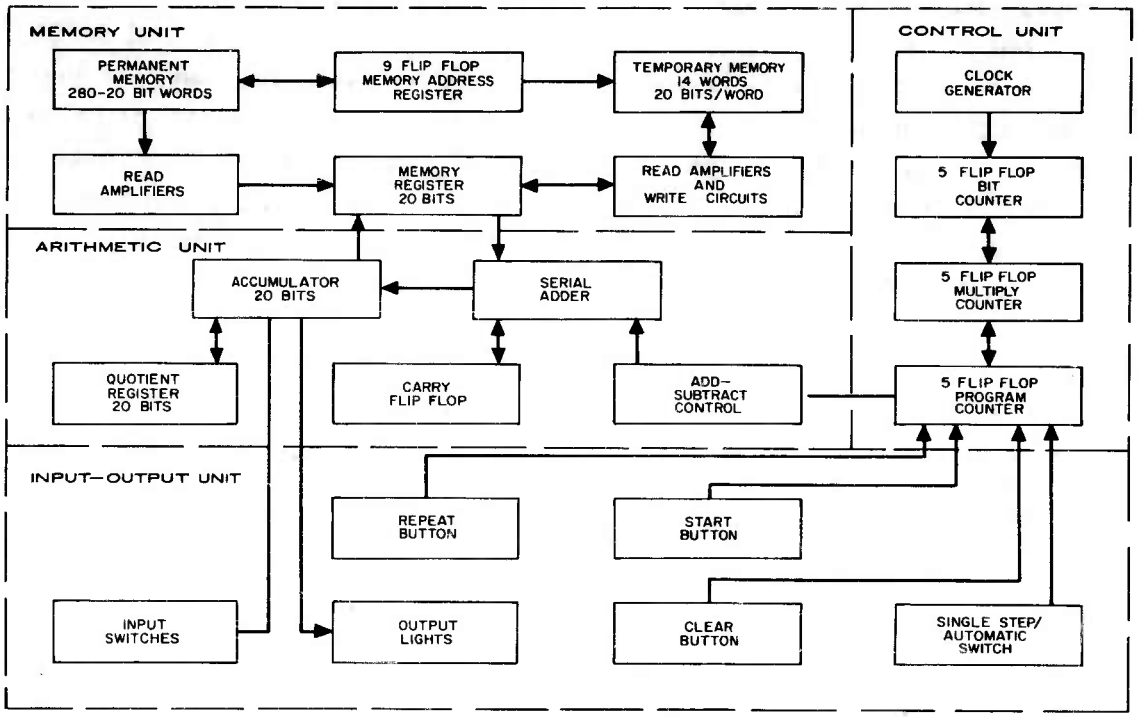

Figure 23. Block Diagram of the BOOTSTRAP Computer

The memory register is a flip-flop register which accepts words in parallel form from the core rope memory and in serial form from the temporary memory. Inputs to the temporary memory are through the memory register and are in serial form. When operating with the adder, the shifting properties of the memory register will be utilized to simplify the design (all inputs to the adder are from the least significant bit).

The accumulator register will be a flip-flop register which will accept inputs from the input toggles and will output information by driving the output lights.

The quotient register is used only for the multiply operation during which only the least significant bit is sensed. This register need be only a simple shifting register. In the interest of power consumption, it will be built into the SAM, although it is shown as a separate register in the block diagram. The selection, drive capability, and write capability for this register will be furnished for the most part by existing SAM circuitry. A power saving of about 350 mw may be realized by not constructing this register entirely of flip-flops.

Control Unit

A block diagram of the control unit is shown in Figure 23. Since the program will be wired, the control unit will consist of a bit counter to count the number of bits in a word, a word counter to be used for the multiply operation, and a program counter to keep track of the place in the program.

Physical Characteristics

The physical characteristics of the machine are as follows:

Total parts	-	5,330
Weight	-	13.0 pounds
Volume	-	280 cubic inches
Power Dissipation	-	4.7 watts without redundant output lights
		5.7 watts with redundant output lights
Clock Rate	-	approximately 5 kc.

The above estimates of weight and volume are based on the welded stick construction used in the Polaris Mark II guidance computer. Power

estimates are based on the following design assumptions: (1) a flip-flop which dissipates 20 mw of power, (2) power dissipation of 35 mw in the temporary memory and its associated circuits, (3) power dissipation of 100 mw in the permanent memory and its associated circuits, and (4) power dissipation of 100 mw per output lamp. It is further assumed that the power to the digital circuits will be regulated to plus or minus 5 per cent and the regulator efficiency will be 75 per cent. The power to the display lamps will not be regulated.

Reliability

For this reliability study it has been assumed that tight quality control will be held on all parts. The failure rates used can be achieved at present with tight quality control.

Table XIII presents parts count and failure rate data for the computer just described. The MTBF for the basic BOOTSTRAP Computer is 10,333 hours.

Table XIII

Reliability Data

No. of Components	Type of Component	Failure Rate Per cent per 1,000 hours (From Houston, 1961)	Failures per 1,000 hours (per cent)
596	Memory core	0.001	0.596
312	Transistors	0.004	1.248
2,494	Diodes	0.0015	3.741
182	Capacitors	0.005	0.910
1,686	Resistors	0.001	1.686
5	Inductors	0.002	0.010
20	Transformers	0.008	0.160
10	Lights (2 in parallel)	0.0025	0.025
24	Switches (partially redundant)	0.01	0.24
10,700	Weld and solder joints	0.00005	0.535
1	Battery[1]	0.5	0.5
5,330[2]	Totals		9.651

[1] A battery is included in the reliability table since a battery possibly may be associated with the computer for power integrity.

[2] Excludes weld and solder joints.

Sequence of Operations

A flow chart of the sequence of computer operations required of the astronaut is presented in Figure 24. Before starting a sequence of computations the astronaut clears the machine. He sets the single step/automatic switch to cause the computer either to stop and display each component of the (V) matrix as it is computed or to display only the last component of the (V) matrix. Then he enters data one word at a time. After each word entry he presses the start button to permit the calculations to be performed on the entered data. If the computer system includes more than one machine these steps are repeated on each of the machines. The outputs of the machines are checked for agreement at the end of a set of computations.

If the machine outputs are not in agreement, the astronaut checks the settings of the input switches to insure that the data has been entered correctly. He may also check for burned out lamps if the system uses press-to-test lamps rather than redundant lamps. The repeat button on one or more of the computers may be depressed in an effort to clear a transient failure.

If these steps do not result in agreement of computer outputs subsequent operations will differ depending upon whether there are two or three computers in the system. In the case of a three-computer system no further checking and/or testing is performed. The two computers in agreement are assumed to be correct. In the case of a two-computer system a test for permanent failure will be made. It should be noted, however, that the test for permanent failure need not be made at the time a permanent failure is detected but may be made at any later time.

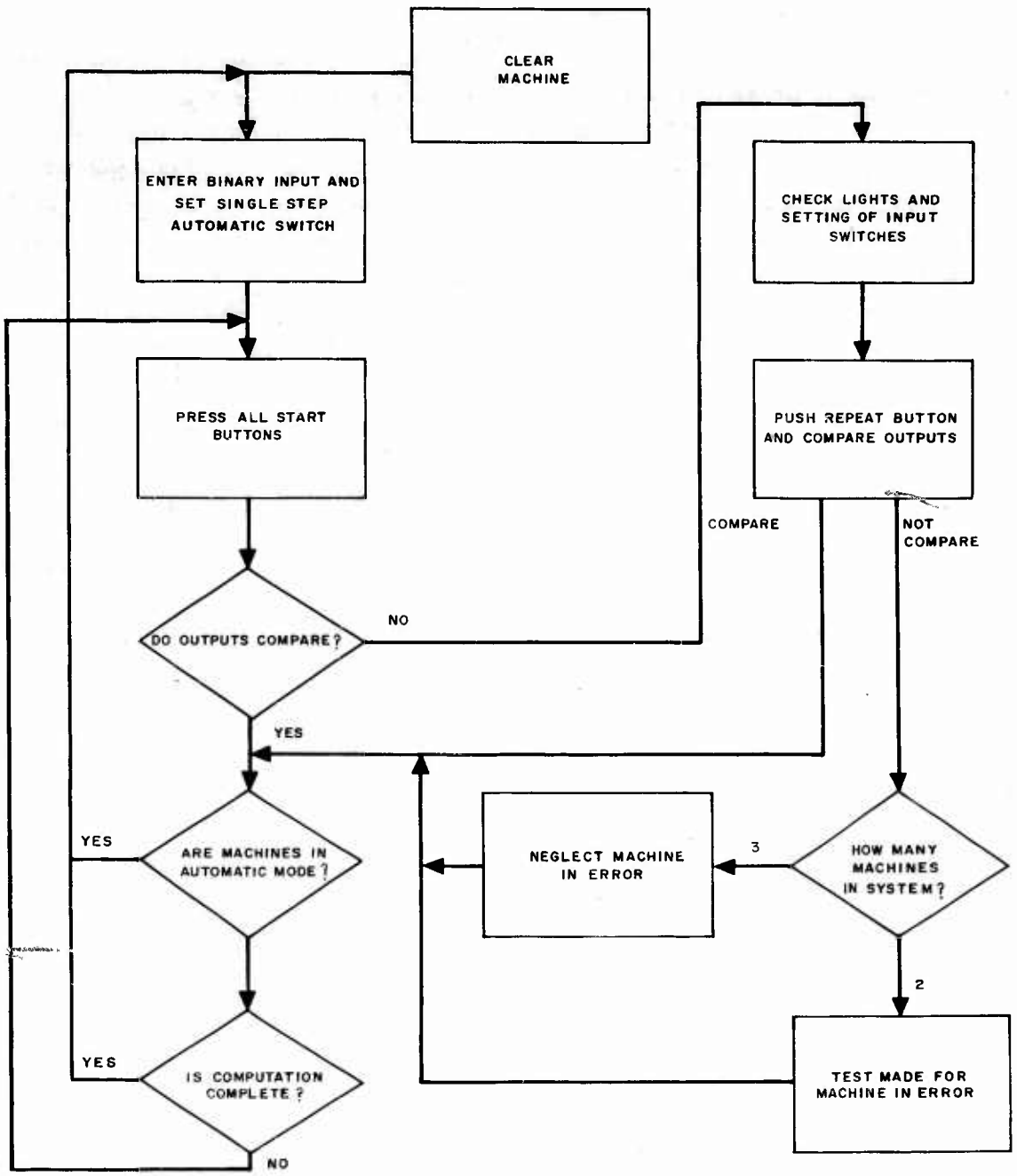

Figure 24. Simplified Computer Operation Diagram

CONCLUSIONS

MANUAL ORIENTATION CONTROL

In general, the attitude control of space vehicles in terms of rate stabilization, angular relationships to a reference system, and recovery from tumbling situations appears to be within the perceptual-motor capabilities of humans. The pilot must have the body-rate and attitude information readable to the desired system performance accuracy and with the dynamic range of expected system capabilities.

Conceptualization of attitudes, body rates, and rate changes in three dimensional space should be fairly easy for well trained astronauts. These studies were conducted with simple and basic display devices. The use of integrated, quickened, and command display devices should make attitude control by crew members more efficient and easier than was found in this study.

Even though these studies were done in the comfortable, safe one g environment of a simulation laboratory, the results should be generalizable to operational situations. Factors which might degrade performance of astronauts such as bulky protective clothing, environmental stresses and zero g were not considered in these studies. However, the astronaut would receive more training, than the subjects in this series of experiments, on both the general problem of attitude control and on operation of his specific system. Certainly a man in a spacecraft would be motivated to perform at his maximum. The positive and negative factors not present in these simulator studies should tend to offset one another and allow prudent generalization of these results to similar operational situations.

General Design Considerations

The data from the cross-coupling experiments point out strongly that vehicles with symmetrical distributions of the moments of inertia are easier to maneuver. It should be possible and profitable for space system designers to distribute the mass within vehicles to approach equal moments of inertia about all axes. One can conceive of almost any external geometric shape having equal moments of inertia by appropriate arrangement

of the mass within the vehicle shell. However, the extreme density required in a spacecraft will surely limit the degree to which this objective can be achieved.

It would appear from the data obtained in these experiments that a manually controlled system will require about 120 per cent of the theoretical minimum energy to accomplish attitude maneuvers similar to those studied. This estimate does not make allowances for fuel reserves necessary in case of malfunctioning subsystems or other emergencies. Efficiency will clearly depend upon the quality of the displays and controls provided.

The results of this study demonstrate that a window can be a useful display device for an astronaut performing attitude control maneuvers. At the same time that the viewing port studies were being conducted, astronaut John H. Glenn demonstrated that a window was indeed valuable in maintenance of attitudes and in attitude rate stabilization. A window or other device providing external visibility should be considered a valuable component of the control-display subsystem as well as a means for scientific observations. In addition to attitude control, an external view should be of prime importance in docking and touchdown maneuvers.

The thrust-sizing of attitude control engines appears to be a function of specific vehicles and missions and not restricted by manual operation. The optimum torque-to-inertia ratios found in these studies fell between 0.01 and 0.05, with a definite optimum point at 0.03. The 0.03 value was optimum for all maneuvers and also resulted in minimum energy expenditures caused by undershoots and overshoots. Varying system design criteria as discussed by Kirkman (1962) may dictate the use of higher torque-to-inertia ratios if rapid attitude change or stabilization is required. Also, if the level of outside disturbing torques is higher than those used in this study, higher torque-to-inertia ratios would be required. However, use of torque-to-inertia ratios larger than 0.05 may require that a continuous or proportional control system be used to enable precise, fine control of energy outputs. This point will be elaborated presently.

Display and Control Considerations

One of the obvious results of the experimental program was the better performance obtained with the aid of body-rate information than without body-rate information. Although a well trained astronaut should be able

to perform all of the attitude maneuvers without the aid of body rates, a pronounced loss of efficiency would result. It is recommended that the sensing and display devices for body-rate information be considered a requirement for manned space vehicles. Body-rate information should be available within the primary or automatic control system. It is suggested that this information also be displayed to the pilot for use in manual control. Although only the minimum manual, i.e., acceleration, control system was investigated in this study, it should be pointed out that the body-rate information could be used with slight additional complexity as a feedback signal to provide a manual rate control system.

Since the crew members could control attitude without body-rate information, it may not be necessary to provide redundant body-rate systems. However, a fuel reserve would be needed to make up for lowered fuel efficiency if the body-rate information were unavailable. The space vehicle design team must trade off the weight of a highly reliable or a redundant body-rate sensing and display system against the added weight and volume of fuel needed if body-rate information is not available.

For the type of maneuvers performed in this study there appears to be a pronounced optimum torque-to-inertia ratio at 0.03. Both fuel consumption and error scores are at a minimum at this value. Even though this same point was found for both discrete and proportional controllers and across all levels of operator loading, this ratio is dependent on the maneuvering requirements of the vehicle. If faster rate corrections than were used in this study are necessary in the vehicle, then a higher ratio of torque-to-inertia would be needed. If the external disturbing torques to be encountered exceed the values used in this study, again, a higher torque-to-inertia ratio would be required. However, if higher ratios are used a gain change in discrete and/or on-off controls would be needed or a proportional control would be required. Fine, precise attitude maneuvers would be impossible with fixed high-gain control systems. The plot of performance over torque-to-inertia ratios in Figure 9 illustrates this point. The on-off controller errors rise sharply above the 0.03 torque-to-inertia ratio whereas the proportional controller curve is much flatter above the 0.03 ratio.

This study demonstrated little in the way of performance differences among controllers. All four of the controllers used in the experimental

program appear to be feasible configurations. The performance obtained with the combined three-axis controller with the presence of body-rate information was significantly better than any other controller under either information condition. One important observation was made concerning the control techniques employed by the subjects when using either of the two proportional controllers. Without the presence of body-rate information, both the combined three-axis side controller and the three single-axis wheels were used as on-off controllers. The subjects would make small, fast, discrete control inputs. This contrasted with the smooth, continuous inputs made when body-rate information was presented. It appeared that subjects could program accelerations continuously to control rates. However, the continuous double integration from accelerations to attitudes could not be accomplished. Consequently, the subjects would make discrete acceleration inputs and wait to observe their effect on attitude angles.

A preliminary design effort was undertaken near the end of this program to design a laboratory model of a display device to allow the simultaneous and continuous presentation of attitudes about all three vehicle axes. An artist's drawing of the display was made from a detailed design layout and is presented in Figure 25. This type of display was conceived by Hopkins, et al (1960).

The utility of such a device was demonstrated in this program during the indoctrination and training of subjects. A model of a vehicle was mounted in a transparent plastic sphere. A block of wood was hollowed out so that a hemisphere of the plastic ball rested in the block. Reference planes were painted on the wooden block at 45° points. The model could be positioned by hand to any desired orientation.

The model was uniquely effective in familiarizing the pilots with simultaneous, large deviations in attitude and in demonstrating simultaneous body rates and their effects on instantaneous attitudes.

Training and Simulation Implications

The training of astronauts should be facilitated by flights in part-task simulators as used in these experiments. The fact that each attitude angle and body rate was presented on a separate indicator provided an exposure to the basics of angular and rate relationships in three dimensional space. Even though a fully operational spacecraft would have more

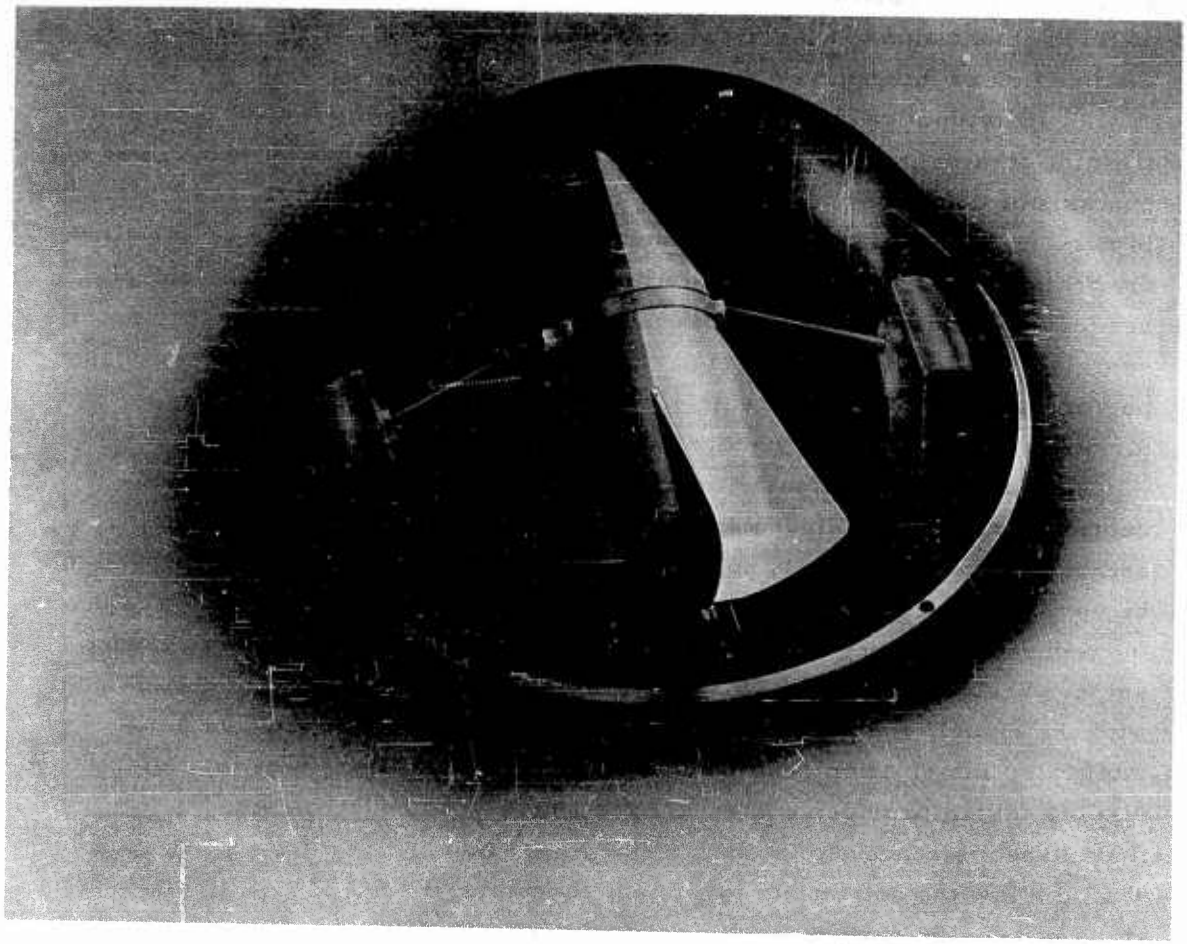

Figure 25. Three-Dimensional Continuous Presentation Attitude Display

sophisticated and/or integrated display devices, exposure to the individual readouts should enable an astronaut to gain a more fundamental understanding of the attitude control problem. Without exposure to the basics of angle body-rate relationships, the astronaut may not be able to perform attitude orientations in the event of failure of specific sensors or partial malfunction of integrated display devices.

Individual readouts for each piece of attitude information also allows training on a degraded system due to loss of body-rate information, loss of one axis of control or loss of one or more of the attitude angle readouts. It is not suggested that training on the individual readout console be substituted for training on specific systems and missions. However, the individual readouts should be valuable tools in a general orientation program to space vehicle attitude control problems and also in transition training from high performance atmospheric vehicles with attitudes damped by aerodynamic forces to space vehicles without external restoring forces.

A three dimensional attitude display similar to the artist's conception presented in Figure 25 should be a useful device for the training of astronauts. The manually positioned model used in this program proved to be very valuable for training the pilots. The pilots had difficulty visualizing and understanding the complex angular and rotational motion relationships. When the angular and rotational relationships were demonstrated with the model, the pilots were subsequently able to interpret the non-integrated information contained on the display console. This type of display device provides continuous presentation of body rates and instantaneous readout of any attitude. A mechanized version of this model should allow the astronauts to quickly conceptualize the complex relationships of angular rates and attitudes.

The simulation of an external field of view by projecting a flat slide onto a viewing surface appears to be of limited application. Although the representation of angular rates and attitudes can be sufficiently accurate, a complete and continuous presentation about all three axes is not possible. Therefore, it is recommended that the flat slide projection technique be used only for general introductory training or exploratory simulation research.

The pacing of a reaction-time secondary task as used in this study is critical. If the pacing is too slow, responses to the secondary task will

be insensitive to changes in the primary task difficulty. Conversely, rapid pacing may cause interference and serious performance decrement on the primary task. Either the optimum stimulus rate of the secondary task should be empirically determined by preliminary studies utilizing both the primary and secondary task, or a different type of secondary task should be employed. For example, a task that is self-pacing might provide a more sensitive measure of operator loading and at the same time not interfere with the performance of the primary task.

The advantages of programming the computing gear of the simulator in a general manner so that signals are available to drive different types of display devices, are self evident. The computer program should also be able to accept continuous and discrete inputs from various control devices.

MANUAL TRANSLATION CONTROL

The following summarizes the conclusions derived from the manual translation control study:

1. Concepts of orientation built up during aerodynamic flight will require modification for orbital flight.
2. Except for direct line-of-sight and very close-range maneuvers, direct visual information is likely to be inadequate for translation control and auxiliary instrumentation will be required.
3. Manual translation control by means of orientation of a single longitudinal thrust axis is difficult. The addition of at least one channel of normal thrust greatly simplifies the task.
4. It remains problematical whether or not absolute judgments of visual rates are sufficiently accurate and precise to effect satisfactory accomplishment of rendezvous and docking missions.
5. The part-task simulation studies accomplished to date have not pressed the limits of the pilot's ability to handle manual control problems. Full-scale six-degree-of-freedom simulations will be required to definitize critical areas of perceptual overload.

MANUAL ORBITAL NAVIGATION

It is clear that a significant manual navigation capability can be developed. It is equally clear that considerable effort needs to be expended toward the design and evaluation of sensing devices and computing equipment for use as part of a manual navigation system.

There are sensing devices available that could be used by an astronaut to obtain position fix data. A meager amount of experimental data is available pertinent to the prediction of manual sighting accuracies. There is at present a need for sensing devices specifically designed to meet the manual handling, visual sighting, and specialized output (octal, binary, etc.) requirements of a manual navigation system.

The trajectory determination computations as presently conceived cannot be easily performed by an astronaut without the aid of a computing device. The most difficult part of the computation for manual navigation consists of the manipulation of matrices and the storage of large amounts of data. Of the trajectory determination methods studied, those relating the present vehicle trajectory to a nominal trajectory are most useful. These methods may be used at the expense of navigation and guidance flexibility, i.e., the data must be sensed at predetermined times, and guidance is relative to a specified orbit. Although no generalizations were made, it should be emphasized that the use of the nominal trajectories as discussed above is not necessarily limited to particular missions assumed for this study.

Using the assumed ground rules for the special purpose BOOTSTRAP computer, it appears that a device can be constructed within the present state of the art to perform the routine, detailed matrix computation and data storage required by the nominal trajectory determination techniques. However, to meet the specified reliability requirements, the BOOTSTRAP computer must be used in conjunction with a second computer. The BOOTSTRAP computer design consists of a core rope permanent memory, a sequential access temporary memory, a wired program, and a serial arithmetic unit. It weighs 13 pounds, consumes 3 watts, and occupies 280 cubic inches. Its mean time between failures is 10,330 hours.

RECOMMENDED FUTURE WORK

MANUAL ORIENTATION CONTROL

The accuracies obtainable by manual systems with only a viewport as a display should be established. This information is needed for designing systems for performing attitude control, docking and touchdown maneuvers. A simulator technique to provide continuous, accurate presentation of the external field of view is needed.

More work is needed on the definition of the effects of misalignment of control axes with inertial axes on attitude control. If serious performance decrements are found to result from misalignments, design techniques such as telescoping and swiveling attitude jets should be studied.

Research and design efforts are needed to establish techniques and devices for the optimum display of attitude and body-rate information. This report was concerned mainly with the information content of displays. New work needs to be done on optimizing the form of displayed information. An example of this type of effort would be design studies of a display device to allow accurate, simultaneous and continuous representation of attitudes about all three axes. Integrated, quickened, and command display techniques should also be investigated.

Controller designs different from those used in this study should be investigated. One that looks particularly promising is a combined three-axis device similar to the one used in this study. However, the controller would be mechanized to have discrete step or on-off outputs, similar to the outputs of the pushbutton control of this study. The controller could be mechanized in either one of two ways. The first method employs activation switches for each direction in each axis. Each time a switch is tripped by movement of the control grip, a metered pulse of energy is released. The second technique involves an activation trigger on the controller grip. The controller would be positioned to select the axes and directions of control inputs, and the trigger would be activated by one finger to release energy in the selected directions to the selected axes.

So many scientists have elaborated on the need for research concerning human responses in the zero g environment that no attempt will be made to summarize or categorize their arguments. In the context of this

report research is needed particularly in the areas of human behavior associated with the responses of vertigo, nystagmus, and nausea.

MANUAL TRANSLATION CONTROL

1. Studies should be aimed at the development of new and efficient ways of thinking about orientation in the space environment. These should also attempt to define the training requirements in terms of the content, methods, and equipment needed. Dynamic simulation in six-degrees-of-freedom will be needed. Provisions should be made in these simulations for considerable flexibility in methods of displaying information and for representing different kinds of vehicle dynamics.
2. Additional detailed analyses are needed to derive the information processing requirements for particular missions or maneuvers. Results of additional studies of human capacities for processing information can then be correlated with these requirements to determine the appropriateness of manual control. The ability to make absolute judgments of range rate and to effect proper orientation of a single thrust vector are examples of human capacities deserving early investigation.
3. At some point in the investigation of attitude and translation control these must be studied together in a full six-degree-of-freedom simulation. The purpose of such a study should be to determine the interactions that occur among methods of displaying information, and the kind, number, and dynamics of the control channels.

MANUAL ORBITAL NAVIGATION

A large amount of work will be required to develop a complete manual orbital navigation capability. A moderate amount of work will be required to develop a capability that will significantly enhance the probability of success of currently planned space missions. Future work should include extensive experimental evaluation of sensing techniques and computational methods.

Mission Oriented Study

The nature of this work is dependent upon the type of mission for which the capability is being developed. For the purpose of this discussion, missions may be divided into the following categories: (1) low-altitude orbital missions, (2) high-altitude orbital missions, (3) lunar missions, and (4) interplanetary missions. Each of these missions will require different navigation and guidance schemes, computational methods and sensing instruments.

Navigation for low-altitude orbital missions may be based on both the observation of celestial bodies and the earth's surface. The navigational techniques required for this mission are particularly well suited for experimental simulation studies. For example, it appears that great advantages can be derived from direct or instrumented observations such as those performed with the aid of a periscope or similar device. It is necessary to determine the nature and accuracy of observations made with these devices. Relatively simple optical and/or closed-circuit television simulations could be used with an earth model for initial studies with more sophisticated simulations being used only after feasible sensing techniques of the required accuracies and appropriate computational methods have been demonstrated. Similar considerations are applicable to circumlunar orbiting and to a lesser degree, because of the unknown or partially known characteristics of the planet surfaces, to circumplanetary missions.

Navigation techniques for elliptical, high altitude orbit missions within the earth's gravitational field have been discussed in this report and several approaches to manual navigation have been discussed. However, additional work which must be performed includes: development of better or alternate methods of computation, determination of manual sensing accuracies, evaluation of manual sensing techniques, establishment of criteria to determine the optimum number and frequency of manual observations, design and evaluation of observational instruments, and specialized computers and manual navigation aids. It is extremely desirable to carry out simulation studies both of single tasks such as those in the sensing and computation areas and of portions of an entire mission. Single computation task simulations may be conveniently established using general purpose computing equipment programmed to represent the manual navigation aid

under study. Simulation of sensing tasks and equipment may require more elaborate facilities, but is well within the bounds of moderate cost and time.

Lunar missions are characterized by the fact that the vehicle will be within the activity spheres of both the earth and moon. This complication will influence the underlying method of computation and most likely the procedures for manual navigation. For example, triangulation sightings taken with the earth-moon distance as the base may be preferable to planet-to-star and subtended-angle observation. In most cases trajectory determination for lunar missions will impose stricter time history requirements, i. e., the vehicle trajectory time history as well as the trajectory shape may have to be considered. Most of the results of the investigations proposed for elliptical orbits will also be applicable to lunar missions.

Interplanetary missions will take the vehicle away from the earth's activity sphere and subject it to predominant effects of the sun or alien planet gravity. Travel time will increase and re-entry conditions will be much more sensitive to intermediate mid-course navigation and guidance accuracy. Ranging operations based on the measurement of angles subtended by planets or the sun may not prove sufficiently accurate. In this case it may be necessary to use triangulation techniques with the known distances between planets, earth and moon taken as base lengths.

General Considerations

Some of the existing and anticipated problems of a more general nature that should be studied are not dependent upon just one type of mission. One of these, the choice between a method of navigation and guidance based on a nominal as opposed to a computed orbit, depends to a marked degree on the distance and duration of travel. With increasing distance and durations of travel, sensitivities to errors become greater. Accuracy requirements of a degree well beyond those obtainable may be imposed, and the use of a nominal orbit precluded. At the same time, the direct orbit computation also will become increasingly more difficult and critically sensitive to errors. A solution may perhaps be found by combining direct orbit computation with repeated mid-course observations. This matter should be thoroughly investigated.

An even more general problem is the determination of the characteristics and the design of instruments for performing manual sighting operations. A large effort could profitably be devoted to the optimization of the astronaut-instrument combination. Much of this question involves the manualness of the sighting procedures and of the sighting instruments. For example, an automatic star tracker could be directly coupled to a computer or may provide readouts to the astronaut. It would be of interest to investigate the relationships between sources of human errors and the factors of mechanical failures so that design criteria leading to the choice of an optimum solution will be evolved.

The above is only a brief list of desirable fields of future investigations. There is no doubt that new problems will arise and present themselves in the course of such investigations.

BIBLIOGRAPHY

Adams, Jack A., "Human Tracking Behavior," Psychological Bulletin, Vol 58, No. 1, pp 55-79, January 1961.

Alonso, R. and Laning, J. H., Jr., Design Principles for a General Control Computer, Report No. R-276, Instrumentation Laboratory, Massachusetts Institute of Technology, Cambridge 39, Massachusetts, April 1960.

Baker, C. A. and Steedman, W. C., "Perceived Movement in Depth as a Function of Luminance and Velocity," Human Factors, Vol 3, pp 166-173, 1961.

Benedict, T. R. and Bordner, G. W., "Minimal Computer – Load Orbit Determination," presented at the Aerospace Support and Operations Meeting of the Institute of Aerospace Sciences, Orlando, Florida, December 1961.

Bennett, C. A. and Franklin, N. L., Statistical Analysis in Chemistry and the Chemical Industry, John Wiley and Sons, New York, 1954.

Birmingham, H. P. and Taylor, F. V., A Human Engineering Approach to the Design of Man-Operated Continuous Control Systems, NRL Report 4333, U. S. Naval Research Laboratory, Washington, D. C., 1954.

Braham, H. S., "The Theory of Midcourse Guidance in Interplanetary Missions," presented in UCLA course on Guidance and Control of Aerospace Vehicles, August 1961. (Available at Aerospace Corporation, El Segundo, California.)

Brissenden, R. F. and Lineberry, E. C., Jr., "Visual Control of Rendezvous", presented at Thirteenth Annual Meeting of the Institute of Aerospace Sciences, New York, N. Y., January 1962.

Brown, J. L. (Editor), Sensory and Perceptual Problems Related to Space Flight, Publication 872, National Academy of Sciences, National Research Council, Washington, D. C., 1961.

Brown, R. H., "Weber Ratio for Visual Discrimination of Velocity," Science, Vol 132, pp 1809-1810, 1960.

Brown, R. H., The Visual Discrimination of Velocity as a Function of the Rate of Movement and Other Factors, NRL Report 4299, U. S. Naval Research Laboratory, Washington, D. C., January 1954.

Buddenhagen, T. F., and Wolpin, M. P., A Study of Visual Simulation Techniques for Astronautical Flight Training, WADD Technical Report 60-756, Wright Air Development Division, Wright-Patterson Air Force Base, Ohio, March 1961.

Chernikoff, R., Duey, J. W. and Taylor, F. V., Two-Dimensional Tracking with Identical and Different Control Dynamics in Each Coordinate, NRL Report 5424, U. S. Naval Research Laboratory, Washington, D. C., November 1959.

Conklin, J. E., "Effect of Control Lag on Performance in a Tracking Task," Journal of Experimental Psychology, Vol 53, pp 261-268, 1957.

Douglas Aircraft Company, Human Factors for the Army-Navy Instrumentation Program, ES 40394, El Segundo, Calif., August 1961.

Easterling, M., A Long Range Precision Ranging System, Technical Report No. 32-80, Jet Propulsion Laboratory, California Institute of Technology, Pasadena, California, July 1961.

Eggleston, J. M. and Beck, H. D., A Study of the Positions and Velocities of a Space Station and a Ferry Vehicle During Rendezvous and Return, NASA Technical Report R-87, Langley Research Center, Langley Field, Va., 1961.

Fuchs, A. H., "The Progression-Regression Hypothesis in Perceptual-Motor Skill Learning," Journal of Experimental Psychology, Vol 63, No. 2, pp 177-182, February 1962.

Garvey, W. D. and Taylor, F. V., "Interaction Among Operator Variables, System Dynamics, and Task-Induced Stress," Journal of Applied Psychology, Vol 43, pp 79-85, 1959.

General Electric Advanced Electronics Center, Instrument Development Program, 5th Quarterly Report, December 1955.

General Electric Advanced Electronics Center, Instrument Development Program, 7th Quarterly Report, Ithaca, New York, June 1956a.

General Electric Advanced Electronics Center, Instrument Development Program, 8th Quarterly Report, Ithaca, New York, September, 1956b.

Heinemann, R. F. D., The Relationship Between the Difficulty Level and Kind of Tracking Problem and the Type of Tracking and Type of Control, Technical Report: NAVTRADEVCEN 342-4, U. S. Naval Training Device Center, Port Washington, Long Island, N. Y., 9 October 1961.

High Reliability Electronic Parts, ERP 61-9, Aerospace Industries Association, Washington, D. C., 12 May 1961.

Hopkins, C. O., Bauerschmidt, D. K., and Anderson, M. J., Display and Control Requirements for Manned Space Flight, WADD Technical Report 60-197, Wright Air Development Division, Wright-Patterson Air Force Base, Ohio, April 1960.

Houbolt, J. C., "Problems and Potentialities of Space Rendezvous," paper presented at the International Symposium on Space Flight and Re-Entry Trajectories, Louvecunnes, France, June 1961.

Kasten, D. F., "Human Performance in Short Orbital Transfer," presented at the 1962 Annual Meeting of the Aerospace Medical Association, Atlantic City, N. J., April 1962.

Kingslake, Rudolf, "The Development of the Zoom Lens," Journal of the SMPTE, Vol 69, pp 539-544, 1959

Kirkman, R. A., "Minimizing Fuel Consumption," Missiles and Space, Vol 40, pp 14-16, March 1962.

Liebman, M. H., Space Rendezvous Study, AED 118R, Hughes Aircraft Company, Culver City, California, December 1961.

Lineberry, E. C., Jr., Brissenden, R. F., and Kurbjun, M. C., Analytical and Preliminary Simulation Study of a Pilot's Ability to Control the Terminal Phase of a Rendezvous with Simple Optical Devices and a Timer, NASA TN D-965, Langley Research Center, Langley Air Force Base, Va., October 1961.

McDonnell Aircraft Corporation, Application of Rendezvous for the Apollo Mission, Report No. 8417, St. Louis, Mo., October 1961.

McLean, J. D., Schmidt, S. F., and McGee, L. A., Optimal Filtering and Linear Prediction Applied to a Space Navigation System for the Circumlunar Mission, NASA TN in preparation.

Mueller, Donald D., Relative Motion in the Docking Phase of Orbital Rendezvous, WADD TR in press.

Nidey, R. A., "Alternating Current Photoelectric Angular Error Sensor," Rev. Sci. Inst., Vol 28, pp 658-659, 1957.

Ritchie, M. C., Hanes, L. F., and Hainsworth, T. E., Manual Attitude Control in Space, Lear Engineering Report No. GR-1366, Lear, Inc., Grand Rapids, Michigan, September 1960.

Roberson, R. E. (Editor), Methods for the Control of Satellites and Space Vehicles, Volume I, Sensing and Actuating Methods, WADD Technical Report 60-643, Wright Air Development Division, Wright-Patterson Air Force Base, 31 July 1960.

Smith, G. L., Schmidt, S. F., and McGee, L. A., An Optimal Filter for Trajectory Determination in an On Board Space Navigation System, NASA TN under preparation.

Shternfeld, A., From Man-Made Earth Satellites to Interplanetary Flights, NCL-130/1 and 2, Technical Documents Liaison Office, Wright-Patterson Air Force Base, Ohio, September 1961.

Wade, T. H., The Algebra of Vectors and Matrices, Addison-Wesley Press, Inc., 1951.

Weltman, G., "Estimation of the Center of Simulated Planetary Bodies," Human Factors, Vol 2, No. 4, pp 211-220, 1960.

Wolowicz, C. H., Drake, H. M. and Videan, E. N., Simulator Investigation of Controls and Displays Required for Terminal Phase of Coplanar Orbital Rendezvous, NASA TN D-511, Flight Research Center, Edwards, California, October 1960.

APPENDIX I. THREE DIMENSIONAL ANGULAR RELATIONSHIPS

by

P. V. Vermont

Human Perception of Three-Dimensional Space: Basic Relationships

Orientation

Perception of three-dimensional space satisfies the common requirements of everyday life by reason of inherited sensory mechanisms and central nervous system structure and acquired experience, but falls short of the basically different requirements of manned space travel. Nevertheless, humans will be confronted very soon with the task of monitoring and directly controlling the events of interplanetary three-dimensional space travel. Hence, it will be appropriate to discuss the different aspects of the geometry and motions involved in space travel and attempt to establish the kind of information that will be useful to the astronaut.

Perception of three-dimensional position and direction seems to be fairly adequate. Humans are able to visualize readily geometrical position reference systems such as the common three-dimensional orthogonal co-ordinate system (see Figure 26) or the slightly more complicated spherical co-ordinates, i.e., the azimuth and elevation angles and range reference system (see Figure 27).

The concept of direction is implicitly contained in both reference systems. The co-ordinates of the point P are taken along, or parallel to, the positive directions of the X, Y, Z axes in the first system; in the second system a direction, from O to P is defined by the two angles, η and e. Regardless of the reference system chosen, a direction in space is defined by two and a position in space by three numerical parameters.

The azimuth-elevation angles are geometrically similar to the longitude (λ) and latitude (L), or right ascension (α) and declination (δ), angles of a sphere marked by Meridian and Parallel lines, the direction being that of a line extending from the center of the sphere 0 to the point P located by the spherical co-ordinates on the spherical surface (see Figure 28).

Perception of orientation is not nearly as easy as perception of position and direction. We will call orientation, or attitude, the angular relation between some axes of a three-dimensional body and an appropriate three-dimensional reference system. It is customary to establish an auxiliary three-dimensional reference system rigidly connected to the body (body axes). The definition of orientation of the body is in this way reduced to the knowledge of angular relations between a reference system (often

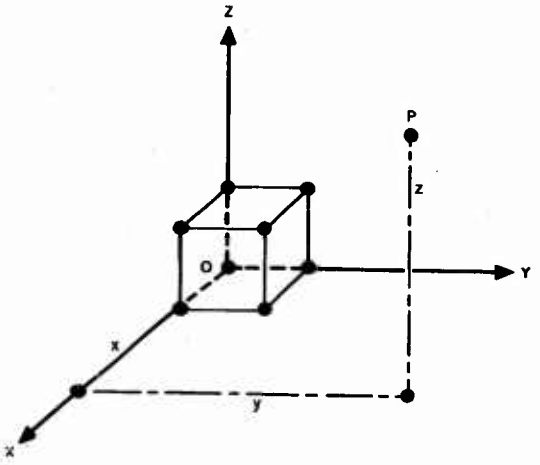

Figure 26. Orthogonal Co-ordinate System

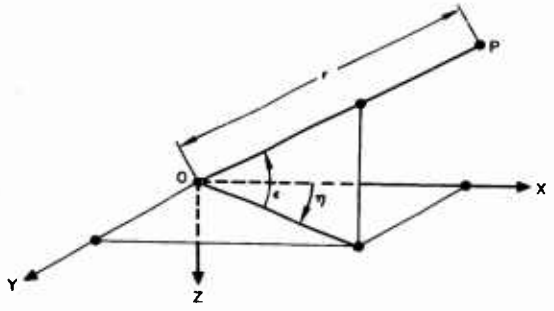

Figure 27. Spherical Co-ordinate System

called fixed system) and body reference system (body axes). The origins of the two systems do not have to coincide, since they can be brought into coincidence for the sake of mathematical manipulation by subjecting one of the systems to a motion of linear translation in which all directions remain parallel to their original directions. A similar translation leaves all angular relationships unaltered (see Figure 29). This translation will not be considered in all successive reasonings relative to body orientation. Only angular relations between systems having a common origin will be investigated.

There are several ways of defining an orientation, or attitude. Among others, one is based on three consecutive rotations about either fixed or consecutively displaced orthogonal body axes, through three definite angles called the Euler angles. The choice of axes and sequences of rotations is arbitrary and there exist a variety of ways of selecting these angles. The sequence customarily used in aerodynamics will be adopted here. The body axes initially are aligned (coincident in direction) with the fixed orthogonal reference axes. The fixed X and Y axes are horizontal, respectively pointing toward local North and East; the fixed Z axis points vertically down. The body X and Z axes are located in the plane of symmetry of the aircraft, the X axis being the longitudinal axis pointing forward, the Z axis pointing in the direction of the pilot's feet; the Y axis points in the direction of the right wing. A similar arbitrary definition of the fixed axis and of the body axes will have to be made for the space vehicle. The body is first rotated through the yaw angle ψ about the fixed Z_0 axis, then through the pitch angle θ about the displaced Y_1 body axis and finally through the roll, or bank angle Φ about the twice displaced X_2 body axis. The positive sense of rotation is determined by the right hand screw rule applied to the axes of rotation and coincides with the positive sense of the conventional components of angular speed p, q and r, (see Figure 30). There are altogether six different axes sequences of this kind. Another kind of sequence used sometimes in theoretical mechanics and gyroscopic theory, consists of using a first axis, then a displaced second axis, then the displaced first axis as consecutive axes of single rotations.

In the sequence of axes customarily used in aerodynamics, the yaw angle is counted through 360° in the direction from North to East, i.e., clockwise looking at a geographic map. The pitch angle θ is counted

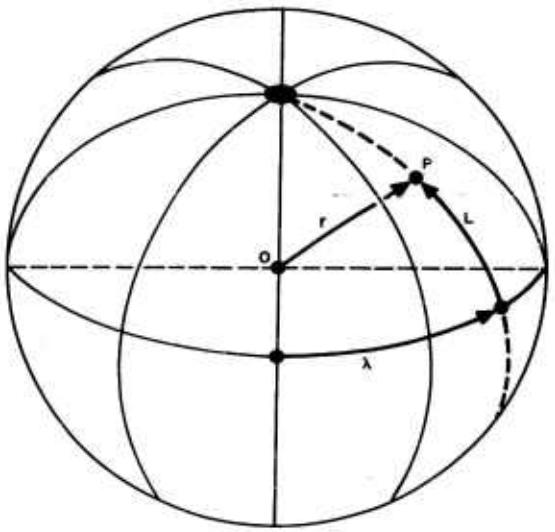

Figure 28. Definition of Spherical Co-ordinates

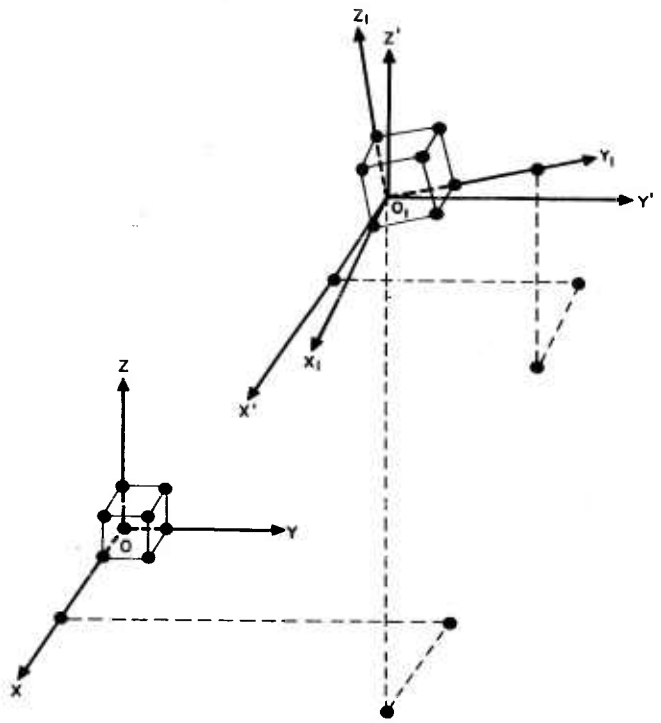

Following axes are parallel to each other:

X and X'
Y and Y'
Z and Z'

X_1, Y_1 and Z_1 are angularly displaced axes.

Figure 29. Example of Translation of Angular Reference System

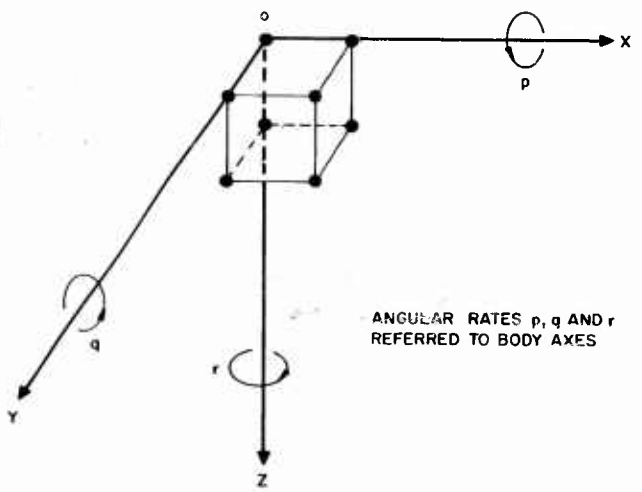

Figure 30. Definition of Positive Rotations

starting from horizontal, $+90^{\circ}$ up and -90° down. The roll angle Φ is measured starting from a horizontal position of the Y axis, through $+180^{\circ}$ of right bank and -180° of left bank. Similar or modified limits may be used in space travel for the sake of computation. These limits do not imply limitations of the actual angular motion of an aircraft or spacecraft. The above definitions of the Euler angles, together with a specified sequence of the single elementary steps, permit a unique solution in terms of Euler angles for a given change of orientation. In the absence of such limitations a similar problem would have many possible solutions.

In order to relate the orientation of an angularly displaced system to a fixed reference system the final orientation of the displaced system can be considered as the result of three consecutive steps already described. Starting from an initial position of coincidence these steps are:

$$\psi = r\,\Delta t_r = \int_{t_o}^{t_1} r\,dt$$

$$\theta = q\,\Delta t_q = \int_{t_1}^{t_2} q\,dt$$

$$\Phi = p\,\Delta t_p = \int_{t_2}^{t_3} p\,dt$$

In case of constant angular rates.

In case of variable angular rates.

Here ψ, θ, Φ, are the Euler angles, p, q, r are the components of angular rates referred to body axes, see Figure 30, and Δt_r, Δt_q, Δt_p, are the durations of each rotation (in case that p, q and r are constant).

Euler angles are not commutative, i.e., the sequence of rotation and the choice of axes cannot be changed without altering the final result. For a given rotation sequence the three numerical values of the Euler angles determine uniquely the orientation of the body. Conversely, for any arbitrary orientation of the body there exists a unique set of the three Euler angles.

Visualization of Euler angles of the kind described above does not offer particular difficulties to a well trained human having some degree of natural disposition for abstract spatial geometry. But, being asymmetrical and non-commutative, the Euler angles are not well suited for geometrical and mathematical manipulation. Instead, direction angles and their cosines, the direction cosines, are widely used because of the formal convenience they offer.

Return to Figure 29 and consider the cosines of the different angles between the body axes and the reference axes. Assign the unit vector triad $\bar{i}$, $\bar{j}$, $\bar{k}$ to the fixed O, X, Y, Z reference system and the triad $\bar{i}_1$, $\bar{j}_1$, $\bar{k}_1$ to the displaced O, X_1, Y_1, Z_1 body reference system.

$$
\begin{array}{c|ccc}
 & \bar{i}_1 & \bar{j}_1 & \bar{k}_1 \\
\hline
\bar{i} & L_1 & M_1 & N_1 \\
\bar{j} & L_2 & M_2 & N_2 \\
\bar{k} & L_3 & M_3 & N_3
\end{array}
\qquad (51)
$$

$$
\begin{array}{c|ccc}
 & X_1 & Y_1 & Z_1 \\
\hline
X & L_1 & M_1 & N_1 \\
Y & L_2 & M_2 & N_2 \\
Z & L_3 & M_3 & N_3
\end{array}
\qquad (52)
$$

Let $L_1 \cos(\bar{i}, \bar{i}_1) = \cos(X, X_1)$ etc. The Matrices (51) and (52) give an orderly arrangement of the 9 direction cosines between the two reference systems. For example, $\cos(\bar{j}, \bar{k}_1) = \cos(Y, Z_1)$ is found at the intersection of the second horizontal row with the third vertical column, as N_2.
The customary way of arranging the direction cosines in a square 3 x 3 matrix is shown below. It is customary to enclose a matrix in round or

square parenthesis in order to distinguish it from a determinant which is enclosed between straight vertical lines.

$$\begin{pmatrix} L_1 & M_1 & N_1 \\ L_2 & M_2 & N_2 \\ L_3 & M_3 & N_3 \end{pmatrix} \tag{53}$$

For the sake of clarity a vertical column to the left and a horizontal row on top showing the relative axes or triads sometimes will be added to a matrix such as represented by (53), see (54).

$$\begin{array}{c|ccc} & \bar{i}_1 & \bar{j}_1 & \bar{k}_1 \\ \hline \bar{i} & L_1 & M_1 & N_1 \\ \bar{j} & L_2 & M_2 & N_2 \\ \bar{k} & L_3 & M_3 & N_3 \end{array} \tag{54}$$

Each direction cosine can be considered as an orthogonal scalar component of one unit vector along the direction of another unit vector (see Figure 31) or as a dot (scalar) product of two unit vectors, compare with Equations (61), (62) and (63). Thus, for example,

$$L_1 = \bar{i} \cdot \bar{i}_1 \tag{55}$$

or

$$\bar{j} = L_2\, \bar{i}_1 + M_2\, \bar{j}_1 + N_2\, \bar{k}_1 \tag{56}$$

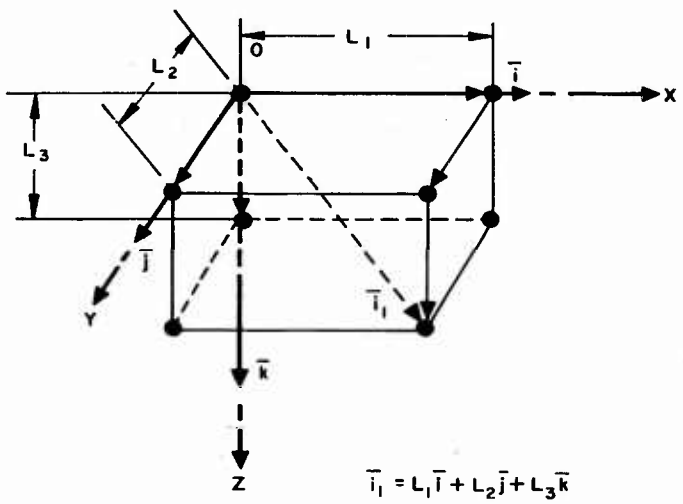

Figure 31. Direction Cosines

or

$$\bar{k}_1 = N_1 \bar{i} + N_2 \bar{j} + N_3 \bar{k} \tag{57}$$

Here L_2, M_2, and N_2 are the scalar components of j along the $\bar{i}_1$, $\bar{j}_1$, $\bar{k}_1$ directions and so on. Being orthogonal scalar components of a unit vector, they yield the following relation:

$$L_2^2 + M_2^2 + N_2^2 = 1 \tag{58}$$

Any three direction cosines contained in a row, or a column, furnish the same relation, i.e.:

$$L_1^2 + M_1^2 + N_1^2 = 1 \tag{59}$$

$$M_1^2 + M_2^2 + M_3^2 = 1 \tag{60}$$

etc., giving a total of six identities.

Consider two vectors:

$$\bar{a} = a_x \bar{i} + a_y \bar{j} + a_z \bar{k} \tag{61}$$

$$\bar{b} = b_x \bar{i} + b_y \bar{j} + b_z \bar{k} \tag{62}$$

Their scalar or dot product is:

$$\bar{a} \cdot \bar{b} = ab \cos (\bar{a}\bar{b}) = a_x b_x + a_y b_y + a_z b_z \tag{63}$$

In the particular case in which two vectors form a right angle,

$$\bar{a} \cdot \bar{b} = ab \cos (\pi/2) = a_x b_x + a_y b_y + a_z b_z = 0 \tag{64}$$

The condition of orthogonality between any two axes belonging to one and the same system yields six more identities of the kind illustrated below:

$$L_2 L_3 + M_2 M_3 + N_2 N_3 = 0 \tag{65}$$

$$L_1 N_1 + L_2 N_2 + L_3 N_3 = 0 \tag{66}$$

etc., all together six formulas.

Vector or cross product multiplication of two vectors $\bar{a}$ and $\bar{b}$ furnishes a third vector, normal to the $\bar{a}\,\bar{b}$ plane and whose modulus is equal to $a\,b \sin(\bar{a}\,\bar{b})$ and can be computed by the following determinant: Thus,

$$\bar{a} \times \bar{b} = \begin{vmatrix} \bar{i} & \bar{j} & \bar{k} \\ a_x & a_y & a_z \\ b_x & b_y & b_z \end{vmatrix}$$

$$= (a_y b_z - a_z b_y)\,\bar{i} + (a_z b_x - a_x b_z)\,\bar{j} + (a_x b_y - a_y b_x)\,\bar{k} \tag{67}$$

In the case of orthogonal unit vectors,

$$\bar{i} \times \bar{j} = \bar{k} \tag{68}$$

Now, from matrix (54),

$$\bar{i} = L_1 \bar{i}_1 + M_1 \bar{j}_1 + N_1 \bar{k}_1$$

$$\bar{j} = L_2 \bar{i}_1 + M_2 \bar{j}_1 + N_2 \bar{k}_1$$

$$\bar{k} = L_3 \bar{i}_1 + M_3 \bar{j}_1 + N_3 \bar{k}_1$$

Then from (67),

$$\bar{i} \times \bar{j} = \begin{vmatrix} \bar{i}_1 & \bar{j}_1 & \bar{k}_1 \\ L_1 & M_1 & N_1 \\ L_2 & M_2 & N_2 \end{vmatrix} = (M_1 N_2 - M_2 N_1)\bar{i}_1 + (N_1 L_2 - N_2 L_1)\bar{j}_1$$

$$+ (L_1 M_2 - L_2 M_1)\bar{k}_1 = \bar{k} = L_3 \bar{i}_1 + M_3 \bar{j}_1 + N_3 \bar{k}_1 \qquad (69)$$

so that

$$L_3 = M_1 N_2 - M_2 N_1 \qquad (70)$$

$$M_3 = N_1 L_2 - N_2 L_1 = -(L_1 N_2 - L_2 N_1) \qquad (71)$$

$$N_3 = L_1 M_2 - L_2 M_1 \qquad (72)$$

It is possible to write six more equations of the same kind. All nine equations can be combined in a single determinant,

$$D = \begin{vmatrix} L_1 & M_1 & N_1 \\ L_2 & M_2 & N_2 \\ L_3 & M_3 & N_3 \end{vmatrix} = 1 \qquad (73)$$

in which each element is equal to its co-factor. In a determinant, the co-factor of an element is equal to the value of the determinant obtained by deleting the row and the column of the element itself and multiplying it by $(-1)^{(r+s)}$ if the element belongs to the r-th row and s-th column. For

example, the element M_3 of the determinant (73) belongs to the 3rd row and 2nd column so that

$$r = 3; \quad s = 2; \quad (-1)^{(r+s)} = (-1)^5 = -1$$

The co-factors m_3 of M_3 is then:

$$m_3 = (-1)^{(3+2)} \begin{vmatrix} L_1 & N_1 \\ L_2 & N_2 \end{vmatrix} = -L_1N_2 + L_2N_1$$

which is identically the same as the right hand part of (71). Thus,

$$M_3 = m_3$$

It should be noted that this last equation is not a common characteristic of determinants in general.

The value of the determinant D can be computed as the sum of products of the elements of one row by their co-factors. Thus:

$$D = L_3(M_1N_2 - M_2N_1) - M_3(L_1N_2 - L_2N_1) + N_3(L_1M_2 - L_2M_1) \tag{74}$$

Substitution of (70), (71), and (72) into (74) yields:

$$D = L_3^2 + M_3^2 + N_3^2 \tag{75}$$

Comparison with (58) eventually gives

$$D = 1 \tag{76}$$

which confirms (73).

Omitting the proof it can be noted that D = -1 is another possible general case. It is not applicable to our kind of problems, where right handed systems only will be considered. The D = -1 case refers to a matrix of direction cosines between a right handed and a left handed reference system. Equations (58) through (76) show that the elements of a matrix of direction cosines such as shown in Matrices (51) through (54), i.e.:

$$\begin{pmatrix} L_1 & M_1 & N_1 \\ L_2 & M_2 & N_2 \\ L_3 & M_3 & N_3 \end{pmatrix} \tag{77}$$

are mutually interdependent in a way that can be expressed by 21 algebraic formulas, which in their turn are interdependent in a certain well defined way. It can be stated that values of any three independent elements determine the whole matrix. This confirms the intuitive fact, already suggested by the number of Euler angles, that the orientation of a body has three degrees of freedom and is fully determined by three numerical parameters.

The usefulness of the direction cosines method will be illustrated further on. But it can already be seen from preceding explanations that the direction cosines method leaves little chance for human imagination and visualization. It is a dry method, requiring formal mathematical ability and not well adapted for direct imaginative visualization. While the Euler angles seem to be fairly well suited for the purpose of display, the necessity of displaying the direction cosines will be justified only if the astronauts will be asked to participate in one way or another in the different computations pertaining to astronavigation.

So far we have limited our investigation almost entirely to the static aspect of angular relations, although we mentioned the three rotations through the three Euler angles. We should now consider angular displacements and angular rates.

The total motion of a spacecraft will be composed of a translation of its C.G. along some curvilinear trajectory and its angular motion with

respect to the fixed inertial space about its C.G. At any instant the spacecraft will either maintain an unchanging (constant) orientation, or will rotate with a certain angular speed, or rate, about an instantaneous axis of rotation passing through the C.G. In the simplest case this axis will be a fixed axis with respect to both the inertial space and the body axes. In the more complicated general case the axis of rotation will change its direction, in which case the change takes place with respect to both reference systems. Only instantaneous values of angular rates can be dealt with as vectors; it is possible for example, to write vectorially:

$$\bar{\Omega} = p\bar{i} + q\bar{j} + r\bar{k} \tag{78}$$

where:

$\bar{\Omega}$ = instantaneous angular rate vector of the spacecraft, a vector coincident with the direction of the axis of rotation whose magnitude (scalar modulus) represents to a chosen scale the angular speed of the body. The vector points in the direction in which a right hand screw, subject to the above rotation, would advance.

p,q, r = angular rate (scalars) components of $\bar{\Omega}$ along the body axes.

$\bar{i}, \bar{j}, \bar{k}$ = unit vectors of the body axes triad.

It should be noted right away that the consecutive rotations (angular displacements) through the three Euler angles cannot be handled in any manner whatsoever as vectors. In particular, the result of two consecutive Euler operations, first through the angles ψ_1, θ_1, Φ_1, then through the angles ψ_2, θ_2, Φ_2 is not equal to a single Euler operation through the angles $(\psi_1 + \psi_2)$, $(\theta_1 + \theta_2)$, $(\Phi_1 + \Phi_2)$.

It can be proved in the case of a rigid body with a fixed point (in our case the C.G.) that any arbitrary change of orientation, i.e., an arbitrary complex rotation about a fixed point, can be replaced by a single rotation about a fixed axis passing through this point. Three numerical parameters again define uniquely this rotation: two parameters determine the direction

of the axis of rotation and the third parameter determines the angle through which the body has to rotate. This operation, involving one single step, is the simplest possible. The geometry of the solution cannot be visualized intuitively without a formal solution that will be given subsequently. The formal solution furnishes the direction cosines of the axis of rotation, the angle of the single rotation and the ratios between the three required simultaneous components of angular rates, i.e.:

$$p: \quad q \quad : \quad r. \tag{79}$$

The solution also furnishes the single angles

$$p\Delta t, \quad q\Delta t, \quad \text{and } r\Delta t \tag{80}$$

or

$$\int p\, dt, \qquad \int q\, dt, \qquad \int r\, dt \tag{81}$$

through which the spacecraft will be required to rotate simultaneously. It can be seen that accurate proportional angular rate controls will be required for this mode of angular motion.

Change of orientation by means of Euler angles, to the contrary, does not require proportional angular rate controls; an accurate control of each single angle of rotation only (the consecutive ψ, θ, Φ angles) will be required.

In all probability, both the Euler angle method and the direction cosine method will be used together in computations relative to space travel.

Formal Relation Between Azimuth-Elevation Angles and Direction Cosines

The following relations exist between the azimuth-elevation angles and direction cosines.

Let OP be a unit vector, $|\overline{OP}| = 1$, η and ϵ its azimuth and elevation angles referred to the reference system OXYZ with its unit vector triad $\bar{i}, \bar{j}, \bar{k}$. The directions of the angles and the orientation of the reference system were chosen arbitrarily in the customary way used in aerodynamics. Let $L = OP_x$, $M = OP_y$; $N = OP_z$ be the scalar components of OP along the three axes. OP being a unit vector these components are numerically

equal to the direction cosines of OP. The following relation can be found directly from Figure 32.

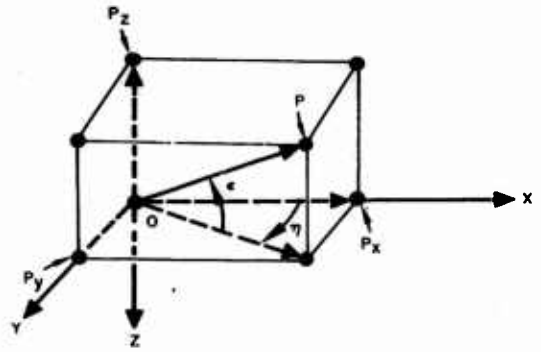

Figure 32. Azimuth-Elevation Angles and Direction Cosines

$$\cos(\widehat{\overline{OP}\,\overline{i}}) = L = \cos e \cos \eta \tag{82}$$

$$\cos(\widehat{\overline{OP}\,\overline{j}}) = M = \cos e \sin \eta \tag{83}$$

$$\cos(\widehat{\overline{OP}\,\overline{k}}) = N = -\sin e \tag{84}$$

$$\eta = \tan^{-1}\left(\frac{M}{L}\right) \tag{85}$$

$$e = -\sin^{-1}(N) \tag{86}$$

The Equations (82) through (86) will be used in one of the problems.

Matrix Algebra Applied to Transformation of Coordinates

Consider two reference systems designated either by their system of orthogonal axes $(OX_o\ Y_o\ Z_o)$ and $(OX_1\ Y_1\ Z_1)$ or by their triads of unit vectors, $(\bar{i}_o, \bar{j}_o, \bar{k}_o)$ and $(\bar{i}_1, \bar{j}_1, \bar{k}_1)$. The direction cosines between the two systems are supposed to be known. Let there be a vector $\bar{R}$ whose components X_1, Y_1, Z_1 in the second system are known. Find the components X_o, Y_o, Z_o of this vector in the other (the first) system. Let,

$$\bar{R} = X_1\bar{i}_1 + Y_1\bar{j}_1 + Z_1\bar{k}_1 \tag{87}$$

and let the direction cosines between the two systems be given in the following matrix.

$$
\begin{array}{c|ccc}
 & \bar{i}_1 & \bar{j}_1 & \bar{k}_1 \\
\hline
\bar{i}_o & L_1 & M_1 & N_1 \\
\bar{j}_o & L_2 & M_2 & N_2 \\
\bar{k}_o & L_3 & M_3 & N_3
\end{array}
\tag{88}
$$

Let (88) be the matrix of the known direction cosines. Then:

$$\bar{i}_o = L_1 \bar{i}_1 + M_1 \bar{j}_1 + N_1 \bar{k}_1 \tag{89}$$

$$\bar{j}_o = L_2 \bar{i}_1 + M_2 \bar{j}_1 + N_2 \bar{k}_1 \tag{90}$$

$$\bar{k}_o = L_3 \bar{i}_1 + M_3 \bar{j}_1 + N_3 \bar{k}_1 \tag{91}$$

The dot (scalar) product of (87) by (89) gives:

$$\bar{R} \cdot \bar{i}_o = (R)(1) \cos (\bar{R}\bar{i}) = X_o = X_1 L_1 + Y_1 M_1 + Z_1 N_1 \tag{92}$$

Similarly,

$$X_o = X_1 L_1 + Y_1 M_1 + Z_1 N_1 \tag{92}$$

$$Y_o = X_1 L_2 + Y_1 M_2 + Z_1 N_2 \tag{93}$$

$$Z_o = X_1 L_3 + Y_1 M_3 + Z_1 N_3 \tag{94}$$

The Equations (92) through (94) can be obtained formally by forming the sums of products of the successive elements of horizontal rows by the successive elements of a vertical column. Symbolically:

$$\begin{pmatrix} X_o \\ Y_o \\ Z_o \end{pmatrix} = \begin{pmatrix} L_1 & M_1 & N_1 \\ L_2 & M_2 & N_2 \\ L_3 & M_3 & N_3 \end{pmatrix} \begin{pmatrix} X_1 \\ Y_1 \\ Z_1 \end{pmatrix} = \begin{pmatrix} L_1 X_1 + M_1 Y_1 + N_1 Z_1 \\ L_2 X_1 + M_2 Y_1 + N_2 Z_1 \\ L_3 X_1 + M_3 Y_1 + N_3 Z_1 \end{pmatrix} \tag{95}$$

which means that the vertical column of X_1, Y_1, Z_1 multiplied (operate on) by the matrix L_1 ... etc., furnishes the vertical column to the extreme right whose elements (sums of three products) are equal, one by one, to the elements of the vertical column at the extreme left. This is a characteristic step of matrix algebra.

It is easy to show, by rewriting some sequences, that in order to obtain X_1, Y_1, Z_1 if X_o, Y_o, Z_o are known a transposed matrix should be used. This is a matrix in which rows and columns are exchanged, as follows.

$$\begin{pmatrix} X_1 \\ Y_1 \\ Z_1 \end{pmatrix} = \begin{pmatrix} L_1 & L_2 & L_3 \\ M_1 & M_2 & M_3 \\ N_1 & N_2 & N_3 \end{pmatrix} \begin{pmatrix} X_o \\ Y_o \\ Z_o \end{pmatrix} \tag{96}$$

Consider again as represented by Matrix (88) the first triad ($\bar{i}_o$, $\bar{j}_o$, $\bar{k}_o$) and second triad ($\bar{i}_1$, $\bar{j}_1$, $\bar{k}_1$) and their 9 direction cosines, but instead of referring to the second triad the vector $\bar{R}$, refer to it, one by one, the three unit vectors of a third triad ($\bar{i}_2$, $\bar{j}_2$, $\bar{k}_2$). Substitute first $\bar{i}_2$ for $\bar{R}$; then X_1, Y_1, Z_1 will assume the values the direction cosines of $\bar{i}_2$ with respect to ($\bar{i}_1$, $\bar{j}_1$, $\bar{k}_1$).

Call them L_1^1, L_2^1, L_3^1. The direction cosines L_1^0, L_2^0, L_3^0 of $\bar{i}_2$ with respect to the $(\bar{i}_o, \bar{j}_o, \bar{k}_o)$ triad can be formed by using the Equation (95).

$$\begin{pmatrix} L_1^0 \\ L_2^0 \\ L_3^0 \end{pmatrix} = \begin{pmatrix} L_1 & M_1 & N_1 \\ L_2 & M_2 & N_2 \\ L_3 & M_3 & N_3 \end{pmatrix} \begin{pmatrix} L_1^1 \\ L_2^1 \\ L_3^1 \end{pmatrix} \tag{97}$$

The same procedure can be repeated for the two remaining unit vectors, $\bar{j}_2$ and $\bar{k}_2$ and all three operations put together as follows.

$$= \begin{pmatrix} L_1^0 & M_1^0 & N_1^0 \\ L_2^0 & M_2^0 & N_2^0 \\ L_3^0 & M_3^0 & N_3^0 \end{pmatrix} = \begin{pmatrix} L_1 & M_1 & N_1 \\ L_2 & M_2 & N_2 \\ L_3 & M_3 & N_3 \end{pmatrix} \begin{pmatrix} L_1^1 & M_1^1 & N_1^1 \\ L_2^1 & M_2^1 & N_2^1 \\ L_3^1 & M_3^1 & N_3^1 \end{pmatrix} \tag{98}$$

$$= \left(\begin{array}{c|c|c} L_1 L_1^1 + M_1 L_2^1 + N_1 L_3^1 & L_1 M_1^1 + M_1 M_2^1 + N_1 M_3^1 & L_1 N_1^1 + M_1 N_2^1 + N_1 N_3^1 \\ L_2 L_1^1 + M_2 L_2^1 + N_2 L_3^1 & L_2 M_1^1 + M_2 M_2^1 + N_2 M_3^1 & L_2 N_1^1 + M_1 N_2^1 + N_2 N_3^1 \\ L_3 L_1^1 + M_3 L_2^1 + N_3 L_3^1 & L_3 M_1^1 + M_3 M_2^1 + N_3 M_3^1 & L_3 N_1^1 + M_3 N_2^1 + N_3 N_3^1 \end{array}\right)$$

Symbolically, calling each matrix with a capital letter,

$$A = BC \tag{99}$$

This is a matrix multiplication, where the elements of the vertical columns of matrix C are multiplied by the elements of the horizontal rows of matrix B and the sum of the products form the elements of the resulting matrix A. Here the matrices should be interpreted as tables of direction cosines. Multiplication (matrix multiplication) is executed as described above and the equality sign refers to the equality, one by one, between the matrix elements of the A matrix and the matrix elements representing the matrix product BC. The result of multiplication furnishes unknown direction cosines between the triads $(\dot{\bar{i}}_o, \dot{\bar{j}}_o \dot{\bar{k}}_o)$ and $(\bar{i}_2, \bar{j}_2, \bar{k}_2)$.

Matrix multiplication is widely used in operations of angular co-ordinate transformation. Several multiplications can follow each other. Thus, if:

$$A = BC \tag{99}$$

then:

$$AD = BCD \tag{100}$$

or:

$$EA = EBC \tag{101}$$

Matrix multiplication is not commutative,

$$AB \neq BA \tag{102}$$

but it is associative:

$$ABCD = \left[(AB)C\right] \quad D = A \quad \left[B(CD)\right] = (AB)(CD) \tag{103}$$

Consider N + 1 reference systems (or successive orientations of one and the same system), S_0, S_1, S_2 --- S_n and let A_{01} be the direction cosines matrix between S_0 and S_1 in the order shown symbolically by (104).

$$A_{01} = \begin{array}{c} \\ i_o \\ j_o \\ k_o \end{array} \begin{array}{c} \begin{array}{ccc} \bar{i}_1 & \bar{j}_1 & \bar{k}_1 \end{array} \\ \begin{pmatrix} & & \\ & & \\ & & \end{pmatrix} \end{array} \tag{104}$$

In a similar way, let A_{12}, A_{23}-- $A_{(N-1)N}$ be the matrices between S_1 and S_2, S_2 and S_3, S_{N-1} and S_N. Then symbolically:

$$A_{ON} = A_{01}\ A_{12}\ A_{23} \cdots A_{(N-1)N} \tag{105}$$

where A_{ON} is the matrix of direction cosines between S_O and S_N. This stepwise consecutive passage through a sequence of orientations furnishes a method for finding the direction cosines resulting from Euler change of orientation or, vice versa, for finding the three Euler angles corresponding to known direction cosines.

Formal Relation Between Euler Angles and Direction Cosines

Consider three consecutive Euler rotations:

From S_0 to S_1 about Z_0, through ψ.

From S_1 to S_2 about Y_1, through θ.

From S_2 to S_3 about X_2, through Φ.

Each single rotation proceeds in the clockwise sense looking along the direction of the corresponding axis of rotation.

The axes of S_0 are X_0, Y_0 and Z_0.

The axes of S_1 are X_1, Y_1, $Z_1 \equiv Z_0$.

The axes of S_2 are X_2, $Y_2 \equiv Y_1$, Z_2.

The axes of S_3 are $X_3 \equiv X_2$, Y_3, Z_3.

Here $\equiv$ stands for identically the same or coincident.

The following three matrices of direction cosines can be written out for the three consecutive steps.

$$
\begin{array}{c|ccc}
\psi & X_1 & Y_1 & Z_1 \\
\hline
X_o & c\psi & -s\psi & 0 \\
Y_o & s\psi & c\psi & 0 \\
Z_o & 0 & 0 & 1
\end{array}
\qquad (106)
$$

$$
\begin{array}{c|ccc}
\theta & X_2 & Y_2 & Z_2 \\
\hline
X_1 & c\theta & 0 & s\theta \\
Y_1 & 0 & 1 & 0 \\
Z_1 & -s\theta & 0 & c\theta
\end{array}
\qquad (107)
$$

$$
\begin{array}{c|ccc}
\Phi & X_3 & Y_3 & Z_3 \\
\hline
X_2 & 1 & 0 & 0 \\
Y_2 & 0 & c\Phi & -s\Phi \\
Z_2 & 0 & s\Phi & c\Phi
\end{array}
\qquad (108)
$$

In (106) through (108) s is an abbreviation for sin = sine and c for cos = cosine.

The geometry of the consecutive rotations is illustrated in Figure 33. Matrices (106) through (108) give the direction cosines of each single step. The matrices can be rewritten omitting the notation of the axes and angles involved. Let:

$$
A_{01} = \begin{pmatrix} c\psi & -s\psi & 0 \\ s\psi & c\psi & 0 \\ 0 & 0 & 1 \end{pmatrix} \qquad (109)
$$

$$
A_{12} = \begin{pmatrix} c\theta & 0 & s\theta \\ 0 & 1 & 0 \\ -s\theta & 0 & c\theta \end{pmatrix} \qquad (110)
$$

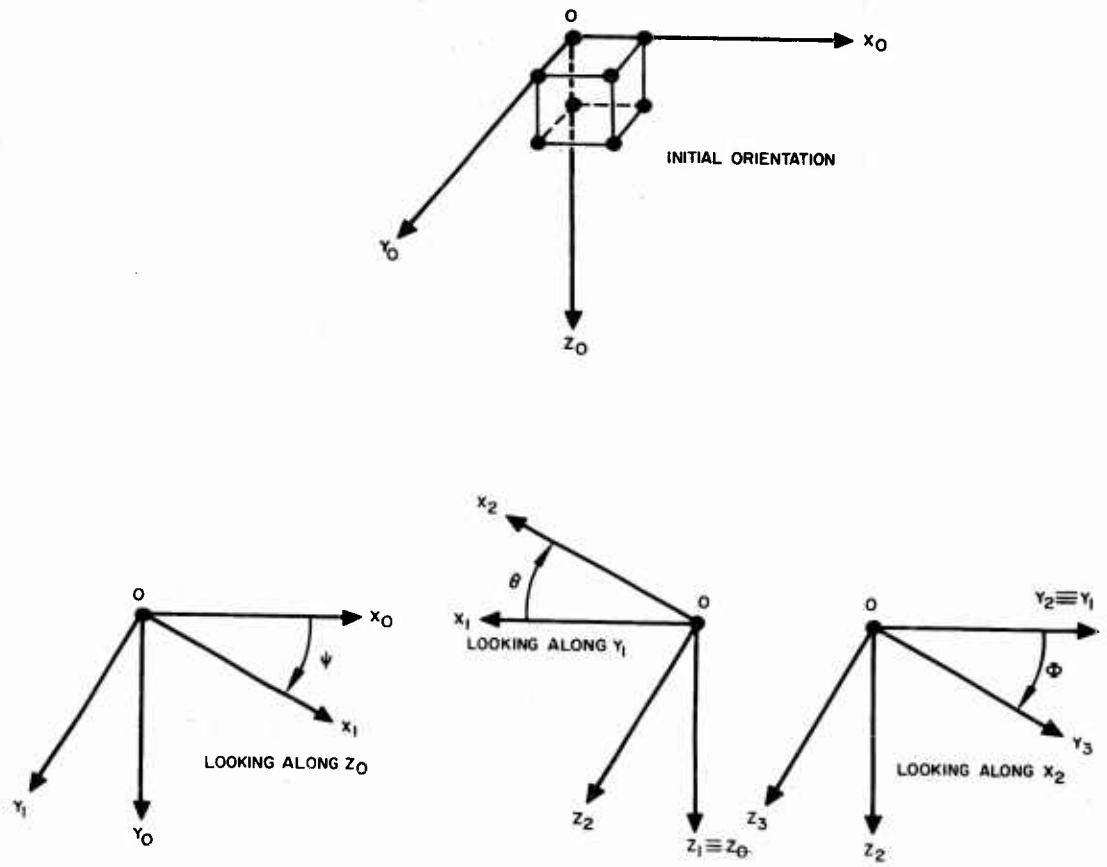

Figure 33. Geometry of Consecutive Rotations

$$A_{23} = \begin{pmatrix} 1 & 0 & 0 \\ 0 & c\phi & -s\phi \\ 0 & s\phi & c\phi \end{pmatrix} \tag{111}$$

Then, according to (105),

$$A_{03} = A_{01}\ A_{12}\ A_{23} \tag{112}$$

The actual matrix multiplication according to (112) furnishes the following relation,

$$A_{03} = \begin{pmatrix} L_1 & M_1 & N_1 \\ L_2 & M_2 & N_2 \\ L_3 & M_3 & N_3 \end{pmatrix} = \begin{pmatrix} c\psi c\theta & -s\psi c\phi + c\psi s\theta s\phi & s\psi s\phi + c\psi s\theta c\phi \\ s\psi c\theta & c\psi c\phi + s\psi s\theta s\phi & -c\psi s\phi + s\psi s\theta c\phi \\ -s\theta & c\theta s\phi & c\theta c\phi \end{pmatrix} \tag{113}$$

where L_1, L_2, etc., are the direction cosines between the different axes, as shown below.

$$\begin{array}{c} \\ X_o \\ Y_o \\ Z_o \end{array} \begin{array}{c} \begin{array}{ccc} X_3 & Y_3 & Z_3 \end{array} \\ \begin{pmatrix} L_1 & M_1 & N_1 \\ L_2 & M_2 & N_2 \\ L_3 & M_3 & N_3 \end{pmatrix} \end{array} \tag{114}$$

The equality between the two matrices means that the corresponding elements of the two matrices are equal, one by one, to each other. For example, $L_3 = -\sin\theta$, or $M_2 = \cos\psi \cos\Phi + \sin\psi \sin\theta \sin\Phi$.

Sometimes it is of interest to have the formal relation for an inverted sequence, i.e., $\Phi \rightarrow \theta \rightarrow \psi$ instead of $\psi \rightarrow \theta \rightarrow \Phi$, or symbolically the A_{30} instead of the A_{03} matrix. Comparing (95) and (96) it can be seen that A_{30} is the transposed A_{03} matrix obtained by exchanging rows and columns, see again (95) and (96).

Let A_{10}, A_{21}, A_{32} and A_{30} be the transposed A_{01}, A_{12}, A_{23}, and A_{03}. Then, in general A_{30} can be obtained either by transposing the A_{03}, or by multiplying in inverted order the transposed matrices of (112). In other words, if

$$A_{03} = A_{01} \; A_{12} \; A_{23} \tag{115}$$

then

$$A_{30} = A_{32} \; A_{21} \; A_{10} \tag{116}$$

Equation (113) furnishes the relation between the Euler angles and direction cosines of the two reference systems, S_o and S_3, angularly displaced with respect to each other. Thus, if the three consecutive Euler angles displacements ψ, θ, Φ are known, the nine direction cosines $L_1 \ldots N_3$ can be computed. If the nine direction cosines are known, it is possible to compute three Euler angles that have to be applied in order to obtain the known direction cosines.

From (113),

$$\psi = \tan^{-1}\left(\frac{L_2}{L_1}\right) \tag{117}$$

$$\theta = \sin^{-1}\left(-L_3\right) \tag{118}$$

$$\Phi = \tan^{-1}\left(\frac{M_3}{N_3}\right) \tag{119}$$

It is appropriate to repeat here the warning that in the application of the Euler method the choice of consecutive axes of rotation (sequence of rotation) and of the positive directions is entirely arbitrary and there is no conformity in this regard between the conventions used by different authors. The resulting formulas differ from (113), but have the same general characteristics and properties. It should be mentioned, in particular, that in some theoretical works only two axes, out of three, are used, for example, as follows:

First rotation about Z_o.

Second rotation about X_1 (the once displaced X_o)

Third rotation about Z_2 (the once displaced $Z_1 \equiv Z_o$)

The instrumentation of such a scheme may seem to be simpler, requiring only two angular motions, yaw ($r\Delta t_{r1}$), roll ($p\Delta t_p$) and another yaw ($r\Delta t_{r2}$). The advantage is only apparent, because the motion of pitch becomes more complicated. In fact, to turn the system through an angle of pitch θ, it would be necessary to perform three steps: positive yaw through $+ \pi/2$, roll through θ, negative yaw through $- \pi/2$.

It is thought that in practical applications, such as spacecraft, it will be more convenient to instrument for all three angular motions, i.e., yaw, pitch and roll (r, q, p).

Another warning refers to the use by different authors of right handed and left handed orthogonal reference systems. The names imply a sequence in order of succession of the three axes, such as $(X \rightarrow Y \rightarrow Z)$ or $(\bar{i} \rightarrow \bar{j} \rightarrow \bar{k})$. In a right handed system the three consecutive axes can be made to coincide respectively with the thumb, index and middle finger of the right hand, in the left handed system the coincidence holds for the same fingers of the left hand. The two systems are symmetrical like an object and its mirror image. They cannot be made to coincide by rotation. The determinant of the matrix of direction cosines existing between the axes of a right handed and a left handed system, arbitrarily oriented, is equal not to +1, as in (73), but to -1. It is expected that in any practical application only systems of one and the same kind will be used, making (73) applicable.

APPENDIX II. ROTATIONAL MOTIONS

by

P. V. Vermont

Angular velocity appears when a body, or some reference system attached to the body, goes through the motion of changing its orientation, i.e., when some lines of the body change their direction. It is possible to show that the most general case of the motion of a body always can be represented as the sum of two motions: a pure translation in which all lines of the body remain parallel to their original direction and a motion of rotation with at least one point of the body remaining fixed. Either simultaneous, or successive application of translation and rotation, in any desired order, lead to the same resulting total displacement of the body. Being unaffected by each other, each one of the two motions can be considered and investigated separately. This section will consider only rotation.

In the case of a space vehicle the total motion can be considered as composed of a translational motion of the C.G. and a rotational motion about the C.G., which if translation is disregarded can be considered as a fixed point (fixed, both in space and with respect to the body). It can be shown in general that the rotational motion of a rigid body about a fixed point consists of each instant of rotational motion about an instantaneous axis of rotation passing through this point. All points of a rigid body located on this axis do not change their position in fixed space while all other points undergo a displacement. The instantaneous axis of rotation can be variable, in which case, still passing through the fixed point, it changes continuously its position with respect to both, the fixed space and the moving body. The locus of the instantaneous positions of the axis forms two cones, one with respect to the fixed space, the other within the moving body, rigidly connected to it. These two cones roll on each other without sliding while the body is subject to the rotational motion. Or, there can be a fixed axis of rotation in which case it is necessarily fixed with respect to both, fixed space and body.

The motion of rotation can be represented vectorially. A vector of angular velocity lies along the instantaneous axis of rotation, with the positive direction coincident with the direction in which a right hand screw subject to this rotation would advance; its modulus (scalar, measure of length) is proportional to the instantaneous angular rate (angular speed). Concurrent (passing through a common point) instantaneous angular velocity vectors can be added vectorially forming a single resultant vector or subdivided in vectorial components. They can be differentiated or integrated according to the rules of vector operations.

An angular velocity (variable or constant) applied to a body for a certain time interval will produce an angular displacement of the body. The term rotation is used somewhat loosely for both, angular displacement (the effect of angular velocity, difference between final and initial orientation) and angular motion (instantaneous condition of change). Any total angular displacement of a rigid body about a fixed point can be replaced by an angular displacement about a fixed axis through a certain angle of rotation.

If $\overline{\Omega}$ is the total vector of angular velocity variable in direction, then its integral with respect to time

$$\int_{t_o}^{t_1} \overline{\Omega} dt \tag{120}$$

has in general no immediate geometric meaning whatsoever. To the contrary, if its direction does not change, or under certain other conditions, the above integral furnishes the numerical value of the angle through which the rotation took place.

Relation Between Body Axis Rates and Euler Angle Rates

It is customary to consider the scalar components along the body axes X, Y, Z of the total vector of angular velocity, $\overline{\Omega}$ and call them respectively p, q and r.

$$\overline{\Omega} = p\overline{i} + q\overline{j} + r\overline{k} \tag{121}$$

$$\Omega = \sqrt{p^2 + q^2 + r^2} \tag{122}$$

Equation (121) determines uniquely the angular velocity represented by the vector $\overline{\Omega}$; p, q and r can be given in radians per second, degrees per second, RPM, etc.

The three Euler angles and their angular rates, $\dot{\Psi}$, $\dot{\theta}$, and $\dot{\Phi}$ can be related to p, q and r as follows.

Consider the three angularly displaced reference systems shown in Figure 34.

$$S_0 = 0(X_0,\ Y_0,\ Z_0)$$

$$S_1 = 0_1(X_1,\ Y_1,\ Z_1)$$

$$S_2 = 0_1(X_2,\ Y_2,\ Z_2) \tag{123}$$

Let S_0 be a fixed reference system, S_2 the instantaneous body axes system.

The origins 0 and 0_1 are separated in the sketch only for clarity; they should be coincident. Rotation through the angle θ about $Y_0 = Y_1$ leads from S_0 to S_1. Rotation through the angle Φ about $X_1 = X_2$ leads from S_1 to S_2. Using matrix notation and direction cosines we have:

$$\begin{array}{cc} & \begin{array}{ccc} & S_1 & \\ \bar{i}_1 & \bar{j}_1 & \bar{k}_1 \end{array} \\ \begin{array}{c} \\ i_o \\ S_0 \quad j_o \\ k_o \end{array} & \begin{pmatrix} c\theta & 0 & s\theta \\ 0 & 1 & 0 \\ -s\theta & 0 & c\theta \end{pmatrix} \end{array} = A_{01} \tag{124}$$

$$\begin{array}{cc} & \begin{array}{ccc} & S_2 & \\ \bar{i}_2 & \bar{j}_2 & \bar{k}_2 \end{array} \\ \begin{array}{c} \\ i_1 \\ S_1 \quad j_1 \\ k_1 \end{array} & \begin{pmatrix} 1 & 0 & 0 \\ 0 & c\Phi & -s\Phi \\ 0 & s\Phi & c\Phi \end{pmatrix} \end{array} = A_{12} \tag{125}$$

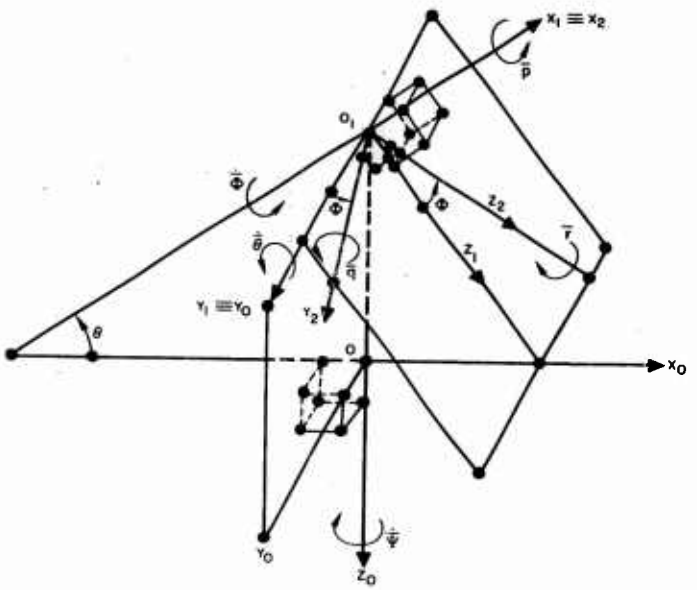

Figure 34. Three Angularly Displaced Reference Systems

$$A_{02} = A_{01} \quad A_{12} \tag{126}$$

or,

$$A_{02} = \begin{pmatrix} c\theta & 0 & s\theta \\ 0 & 1 & 0 \\ -s\theta & 0 & c\theta \end{pmatrix} \begin{pmatrix} 1 & 0 & 0 \\ 0 & c\Phi & -s\Phi \\ 0 & s\Phi & c\Phi \end{pmatrix} \begin{matrix} \bar{i}_o \\ \bar{j}_o \\ \bar{k}_o \end{matrix} \begin{matrix} \overrightarrow{\bar{i}_2 \quad \bar{j}_2 \quad \bar{k}_2} \\ \end{matrix} \begin{pmatrix} c\theta & s\theta s\Phi & s\theta c\Phi \\ 0 & c\Phi & -s\Phi \\ -s\theta & c\theta s\Phi & c\theta c\Phi \end{pmatrix} \tag{127}$$

An increment of Ψ (due to the angular rate $\dot{\Psi}$) will take place if S_2 is rotated about Z_0, giving an angular velocity vector $\dot{\bar{\Psi}} = \dot{\Psi}\bar{k}_o$. The increment of θ (angular rate $\dot{\theta}$) will be due to rotation of S_2 about $Y_0 \equiv Y_1$, giving the angular velocity vector $\dot{\bar{\theta}} \equiv \dot{\theta}\bar{j}_o$. Rotation about $X_1 \equiv X_2$ will produce Φ and the angular velocity vector $\dot{\bar{\Phi}} = \dot{\Phi}\bar{i}_2$. Let's assume that the six unit vectors $\bar{i}_o$, $\bar{j}_o$, $\bar{k}_o$ and $\bar{i}_2$, $\bar{j}_2$, $\bar{k}_2$ are concurrent vectors passing through the C.G. of the vehicle and that the vehicle is subject to an arbitrary angular velocity $\bar{\Omega}$ about an axis also passing through the C.G. The vector $\bar{\Omega}$ can be split in its 3 orthogonal components according to Equation (121).

$$\bar{\Omega} = p\bar{i}_2 + q\bar{j}_2 + r\bar{k}_2 \tag{121}$$

The same vector can also be represented as a vectorial sum of three other concurrent nonorthogonal vectors.

$$\bar{\Omega} = \dot{\Phi}\bar{i}_2 + \dot{\theta}\bar{j}_o + \dot{\Psi}\bar{k}_o \tag{128}$$

It is known that a dot product of an arbitrary vector $\bar{V}$ by a unit vector $\bar{u}$ furnishes the orthogonal component of $\bar{V}$ along $\bar{u}$ (see Figure 35).

$$\bar{V} \cdot \bar{u} = (V)(1)\cos(\bar{V}\,\bar{u}) \tag{129}$$

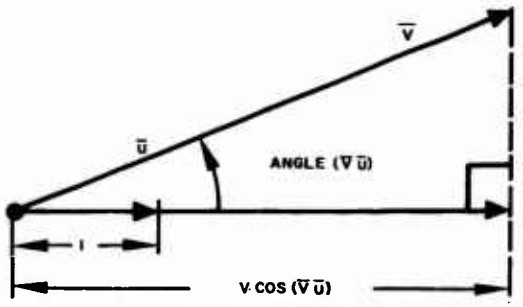

Figure 35. Dot Product of Vectors

Using vector algebra:

$$\bar{\Omega} \cdot \bar{i}_2 = (p)(1)\cos(\bar{i}_2\bar{i}_2) + (q)(1)\cos(\bar{j}_2\bar{i}_2) + (r)(1)\cos(\bar{k}_2\bar{i}_2) \tag{130}$$

but,

$$\cos(\bar{i}_2\bar{i}_2) = \cos 0^o = 1;\ \cos(\bar{j}_2\bar{i}_2) = \cos(\bar{k}_2\bar{i}_2) = \cos\frac{\pi}{2} = 0 \tag{131}$$

$$\bar{\Omega} \cdot \bar{i}_2 = p. \tag{132}$$

Similarly for $\bar{j}_2$ and $\bar{k}_2$ so that:

$$\begin{aligned} p &= \bar{\Omega} \cdot \bar{i}_2 \\ q &= \bar{\Omega} \cdot \bar{j}_2 \\ r &= \bar{\Omega} \cdot \bar{k}_2 \end{aligned} \tag{133}$$

which of course results also directly from Equation (121). Writing $\bar{\Omega}$ as in (128) and substituting from matrix (127) the values of direction cosines between S_0 and S_2 reference systems into Equation (133) yields the following relations:

$$p = (\dot{\Phi}\bar{i}_2 + \dot{\theta}\bar{j}_o + \dot{\Psi}\bar{k}_o) \cdot \bar{i}_2 = \dot{\Phi} - \dot{\Psi}\sin\theta$$

$$q = (\dot{\Phi}\bar{i}_2 + \dot{\theta}\bar{j}_o + \dot{\Psi}\bar{k}_o) \cdot \bar{j}_2 = \dot{\theta}\cos\Phi + \dot{\Psi}\cos\theta\sin\Phi$$

$$r = (\dot{\Phi}\bar{i}_2 + \dot{\theta}\bar{j}_o + \dot{\Psi}\bar{k}_o) \cdot \bar{k}_2 = -\dot{\theta}\sin\Phi + \dot{\Psi}\cos\theta\cos\Phi$$

$$p = \dot{\Phi} - \dot{\Psi}\sin\theta \tag{134}$$

$$q = \dot{\theta}\cos\Phi + \dot{\Psi}\cos\theta\sin\Phi \tag{135}$$

$$r = \dot{\theta}\sin\Phi + \dot{\Psi}\cos\theta\cos\Phi \tag{136}$$

Solving the above for $\dot{\Psi}$, $\dot{\theta}$ and $\dot{\Phi}$ furnishes the well known relation.

$$\dot{\Psi} = (q \sin \Phi + r \cos \Phi) \sec \theta \tag{137}$$

$$\dot{\theta} = q \cos \Phi - r \sin \Phi \tag{138}$$

$$\dot{\Phi} = p + (q \sin \Phi + r \cos \Phi) \tan \theta = p + \dot{\Psi} \sin \theta \tag{139}$$

By integration:

$$\Psi_2 = \Psi_1 + \int_{t_1}^{t_2} \dot{\Psi} dt = \Psi_1 + \int_{t_1}^{t_2} (q \sin \Phi + r \cos \Phi) \sec \theta \, dt \tag{140}$$

$$\theta_2 = \theta_1 + \int_{t_1}^{t_2} \dot{\theta} \, dt = \theta_1 + \int_{t_1}^{t_2} (q \cos \Phi - r \sin \Phi) \, dt \tag{141}$$

$$\Phi_2 = \Phi_1 + \int_{t_1}^{t_2} \dot{\Phi} \, dt = \Phi_1 + \int_{t_1}^{t_2} \left[p + (q \sin \Phi + r \cos \Phi) \tan \theta \right] dt \tag{142}$$

In the above, all three angles Ψ, θ and Φ generally vary with time, while p, q, r can either remain constant or vary with time.

Change of Orientation by Means of Consecutive Changes of Euler Angles

Suppose it is desired in a general case to rotate from some arbitrary orientation S_1 (Ψ_1, θ_1, Φ_1) to another orientation S_2 (Ψ_2, θ_2, Φ_2) in three successive steps by changing successively Ψ, θ, Φ.

First step

$\dot{\Psi} \neq 0$, Ψ is a variable of time

$\dot{\theta} = \dot{\Phi} = 0$; θ_1 and $\dot{\theta}_1$ are constants.

Similar equations can be set up for the two other steps. Each step requires the simultaneous application of all three angular rates p, q and r. The first step will be explained below. From (134) through (136):

$$p = -\dot{\Psi} \sin \theta_1 \tag{143}$$

$$q = \dot{\Psi} \cos \theta_1 \sin \Phi_1 \tag{144}$$

$$r = \dot{\Psi} \cos \theta_1 \cos \Phi_1 \tag{145}$$

From (140)

$$\int_{t_1}^{t_2} \dot{\Psi}\, dt = \Psi_2 - \Psi_1 \tag{146}$$

Integrate (143) and combine with (146)

$$\int_{t_1}^{t_2} p\, dt = \sin\theta_1 \int_{t_1}^{t_2} -\dot{\Psi}\, dt = (\Psi_1 - \Psi_2)\sin\theta_1 \tag{147}$$

The maneuver expressed by (146) can be executed, for example, by taking a constant $\dot{\Psi}$, $\dot{\Psi} = C_{\dot{\Psi}}$. Then from (143) through (147) p also becomes a constant as do q and r and

$$\Delta_t = t_2 - t_1 = \frac{\Psi_2 - \Psi_1}{C_{\dot{\Psi}}} \tag{148}$$

Of course, the same maneuver can be executed with a variable angular rate $\dot{\Psi}$, if either $\dot{\Psi}$ or $\int \dot{\Psi}\, dt$ or $\int p\, dt$ can be continuously measured while time goes on. The two other simultaneous rates, q and r, are dealt with in a similar manner.

Change of Orientation by Means of Consecutive Rotations about Body Axes

There exists another typical way for the change of orientation from S_1 to S_2 by three successive steps of yaw, pitch and roll, each step involving only rotations about one body axis at a time. Call the fixed reference system S_0. From the known two sets of Euler angles of S_1 and S_2, Ψ_1, θ_1, Φ_1, and Ψ_2, θ_2, Φ_2, compute using Equation (113) of Appendix I the two direction cosine matrices, A_{01} and A_{02}. Transpose the A_{01} into A_{10}. Then the A_{12}

$$A_{12} = A_{10}\ A_{02} = \begin{pmatrix} L_1 & M_1 & N_1 \\ L_2 & M_2 & N_2 \\ L_3 & M_3 & N_3 \end{pmatrix} \tag{149}$$

will furnish the direction cosines between S_1 and S_2. Using formulas (117) through (119) of Appendix I, compute from A_{12} the desired Euler angles

$$\Psi_{12} = \tan^{-1}\left(\frac{L_2}{L_1}\right), \tag{150}$$

$$\theta_{12} = \sin^{-1}(-L_3) \text{ and,} \tag{151}$$

$$\Phi_{12} = \tan^{-1}\left(\frac{M_3}{N_3}\right), \tag{152}$$

and execute the maneuver in three successive steps performed one at a time and in the specific sequence in such a way that:

$$\Psi_{12} = \int_{t_0}^{t_1} r\, dt \tag{153}$$

$$\theta_{12} = \int_{t_1}^{t_2} q\, dt \tag{154}$$

$$\Phi_{12} = \int_{t_2}^{t_3} p\, dt \tag{155}$$

Change of Orientation by Means of a Single Rotation about a Fixed Axis

It has already been mentioned that any arbitrary change of orientation (attitude) can take place by way of a single rotation about a fixed axis passing through the C.G., and that if this axis of rotation is fixed with respect to the inertial reference, then it is also necessarily fixed with respect to the rotating body.

Consider for the sake of the present investigation a fixed reference $S_0(X_0, Y_0, Z_0)$, the rotating reference $S(X, Y, Z)$ and its final orientation $S_1(X_1, Y_1, Z_1)$ and assume that initially S_0 and S coincide. The axis of

rotation $\bar{a}$ being a fixed axis, its direction angles, α, β and γ are at the beginning the same in both systems, S_0 and S and will remain so during and at termination of the rotation. Thus, if $\bar{\Omega}$ is the vector of angular velocity of S, then, with reference to the rotating system

$$\bar{\Omega} = \Omega\ (\cos\alpha)\,\bar{i} + \Omega\ (\cos\beta)\,\bar{j} + \Omega\ (\cos\gamma)\ \bar{k} = p\bar{i} + q\bar{j} + r\bar{k}\ . \tag{156}$$

The scalar components of angular velocity referred to the body axes X, Y, Z are then

$$\begin{aligned} p &= \Omega \cos\alpha \\ q &= \Omega \cos\beta \\ r &= \Omega \cos\gamma \end{aligned} \tag{157}$$

and

$$p : q : r = \cos\alpha : \cos\beta : \cos\gamma\ . \tag{158}$$

Equation (158) applied to the instantaneous values of p, q and r holds for either constant or variable angular speed Ω and is a necessary and sufficient condition of the described rotational motion.

Let Γ be the angle through which the body rotates about $\bar{a}$ while changing orientation from S_0 to S_1. Then

$$\Omega = \frac{d\Gamma}{dt} = \dot{\Gamma} \tag{159}$$

and,

$$\Gamma = \int_{t_0}^{t_1} \Gamma\, dt = \int_{t_0}^{t_1} \Omega\, dt. \tag{160}$$

Since α, β and γ remain constant, (157), integrated, furnishes:

$$\int_{t_0}^{t_1} p\,dt = \cos \int_{t_0}^{t_1} \Omega\, dt = \Gamma \cos\alpha \tag{161}$$

Similarly,

$$\int_{t_0}^{t_1} q\,dt = \Gamma \cos \beta \qquad (162)$$

$$\int_{t_0}^{t_1} r\,dt = \Gamma \cos \gamma \qquad (163)$$

It should be kept in mind that according to (158) p, q and r are simultaneous angular rates acting on the body and that their ratio remains constant all through the maneuver. The above formulas could be used for the instrumentation of automatic controls should this maneuver find practical applications.

Let the direction cosines between S_0 and S_1 i. e., between the initial and final orientation of the rotating references, be given by the following matrix.

$$\begin{array}{c|ccc} & i_1 & j_1 & k_1 \\ \hline i_0 & L_1 & M_1 & N_1 \\ j_0 & L_2 & M_2 & N_2 \\ k_0 & L_3 & M_3 & N_3 \end{array} \qquad (164)$$

If the angular displacement from S_0 ($\bar{i}_o$, $\bar{j}_o$, $\bar{k}_o$) to S_1 ($\bar{i}_1$, $\bar{j}_1$, $\bar{k}_1$) is considered as the result of a single rotation of S, initially coincident with S_0, then the direction angles α, β, γ of the axis of rotation $\bar{a}$ and the angle of rotation Γ can be computed as follows:

$$\cos \Gamma = 1/2\,(L_1 + M_2 + N_3 - 1) \qquad (165)$$

$$\cos\alpha = \frac{M_3 - N_2}{2\sin\Gamma} = \pm\sqrt{\frac{1 + (L_1 - M_2 - N_3)}{3 - (L_1 + M_2 + N_3)}} = \pm\sqrt{\frac{L_1 - \cos\Gamma}{1 - \cos\Gamma}} \tag{166}$$

$$\cos\beta = \frac{N_1 - L_3}{2\sin\Gamma} = \pm\sqrt{\frac{1 + (M_2 - L_1 - N_3)}{3 - (L_1 + M_2 + N_3)}} = \pm\sqrt{\frac{M_2 - \cos\Gamma}{1 - \cos\Gamma}} \tag{167}$$

$$\cos\gamma = \frac{L_2 - M_1}{2\sin\Gamma} = \pm\sqrt{\frac{1 + (N_3 - L_1 - M_2)}{3 - (L_1 + M_2 + N_3)}} = \pm\sqrt{\frac{N_3 - \cos\Gamma}{1 - \cos\Gamma}} \tag{168}$$

Here,

$$\alpha = (\hat{\bar{i}_o}\bar{a}) = (\hat{\bar{i}_1}\bar{a}) \tag{169}$$

$$\beta = (\hat{\bar{j}_o}\bar{a}) = (\hat{\bar{j}_1}\bar{a}) \tag{170}$$

$$\gamma = (\hat{\bar{k}_o}\bar{a}) = (\hat{\bar{k}_1}\bar{a}) \tag{171}$$

Besides,

$L_1 = \cos^2\alpha + \sin^2\alpha\cos\Gamma$	$M_1 = -\cos\gamma\sin\Gamma + \cos\alpha\cos\beta(1-\cos\Gamma)$	$N_1 = +\cos\beta\sin\Gamma + \cos\alpha\cos\gamma(1-\cos\Gamma)$
$L_2 = +\cos\gamma\sin\Gamma + \cos\alpha\cos\beta(1-\cos\Gamma)$	$M_2 = \cos^2\beta + \sin^2\beta\cos\Gamma$	$N_2 = -\cos\alpha\sin\Gamma + \cos\beta\cos\gamma(1-\cos\Gamma)$
$L_3 = -\cos\beta\sin\Gamma + \cos\alpha\cos\gamma(1-\cos\Gamma)$	$M_3 = +\cos\alpha\sin\Gamma + \cos\beta\cos\gamma(1-\cos\Gamma)$	$N_3 = \cos^2\gamma + \sin^2\gamma\cos\Gamma$

(172)

Equations (165) through (172) could be used for the solution of the rotational manuever from one orientation to another. The method requires the knowledge of the direction cosines between the two frames, S_0 and S_1 of the initial and final orientation. These always can be found by the use of matrix algebra if the two orientations are known with respect to a third system, as was the case in the previous treatment of a similar problem.

Equations (165) through (172) should be further discussed in order to clarify the sense of rotation of Γ. For the sake of brevity, this discussion, as well as the proof of the formulas, will be omitted. The formulas seem to be sufficiently suited for practical use.

Relation between Body Axes Angular Rates and the Rate of Change of Direction Cosines

Another formal relation should be mentioned for the sake of completeness. Let system S ($\bar{i}$, $\bar{j}$, $\bar{k}$) be the rotating reference frame having common origin with the fixed reference frame S_0 ($\bar{i}_o$, $\bar{j}_o$, $\bar{k}_o$) and let the angular velocity of S be known at any instant by its components p, q, r referred to the rotating system (S) body axes. Then at any instant,

$$\begin{aligned}
\dot{L}_1 &= rM_1 - qN_1 & \dot{M}_1 &= pN_1 - rL_1 & \dot{N}_1 &= qL_1 - pM_1 \\
\dot{L}_2 &= rM_2 - qN_2 & \dot{M}_2 &= pN_2 - rL_2 & \dot{N}_2 &= qL_2 - pM_2 \\
\dot{L}_3 &= rM_3 - qN_3 & \dot{M}_3 &= pN_3 - rL_3 & \dot{N}_3 &= qL_3 - pM_3
\end{aligned} \tag{173}$$

In the above the total angular velocity vector acting on the rotating system S is

$$\bar{\Omega} = p\bar{i} + q\bar{j} + r\bar{k} \tag{174}$$

and at any instant the variable direction cosines between the two systems are

$$\begin{array}{c|ccc}
 & \bar{i} & \bar{j} & \bar{k} \\
\hline
\bar{i}_o & L_1 & M_1 & N_1 \\
\bar{j}_o & L_2 & M_2 & N_2 \\
\bar{k}_o & L_3 & M_3 & N_3
\end{array} \tag{175}$$

No restrictions are imposed on the simultaneous angular rates p, q and r which may or may not vary with time in any arbitrary way.

A formal proof of Equations (173) is given below. Details are omitted for the sake of brevity.

Consider for example the rate of change $\dot{L}_2$ of the direction cosine L_2.

$$L_2 = \bar{j}_o \cdot \bar{i} \tag{176}$$

$$\dot{L}_2 = \dot{\bar{j}}_o \cdot \bar{i} + \bar{j}_o \cdot \dot{\bar{i}} \tag{177}$$

Since $\bar{j}_o$ is a fixed vector

$$\dot{\bar{j}}_o = 0 \tag{178}$$

Any variation of the unit vector $\bar{i}$ will change its direction only, not its magnitude, which is constant. Then $\dot{\bar{i}}$, the time derivative of $\dot{\bar{i}}$ will be equal to the velocity vector of its terminal point which, in turn, is a function of the rotation of $\bar{i}$ only.

$$\dot{\bar{i}} = \bar{\Omega} \cdot \bar{i} = \begin{pmatrix} \bar{i} & \bar{j} & \bar{k} \\ p & q & r \\ 1 & 0 & 0 \end{pmatrix} = r\bar{j} - q\bar{k}$$

$$\dot{\bar{i}} = r\bar{j} - q\bar{k} \tag{179}$$

From the matrix (175) $\bar{j}_o$ can be written as follows:

$$\bar{j}_o = L_2\bar{i} + M_2\bar{j} + N_2\bar{k} \tag{180}$$

Substitution of (178), (179) and (180) into the (177) furnishes:

$$\dot{L}_2 = 0 \cdot \bar{i} + (L_2\bar{i} + M_2\bar{j} + N_2\bar{k}) \cdot (0\bar{i} + r\bar{j} - q\bar{k})$$

$$= \dot{L}_2 = rM_2 - qN_2 \quad . \tag{181}$$

Each single equation of the 9 equations (173) can be separately integrated. For example:

$$L_1 = L_{01} + \int_{t_1}^{t_2} \dot{L}_1 dt \tag{182}$$

Nine integrals will furnish the instantaneous values of the nine direction cosines. These nine values require constant corrections of possible integration errors for the different orthogonality conditions already discussed. It would be sufficient to keep track of the angular motion by integration of only three non-interdependent direction cosines and compute the rest from the different orthogonality conditions.

Direct Use of Inertial Platform Gimbal Angles

Certain simplifications may be obtained by letting the inertial platform gimbal angles appear directly in some of the computations. It should be born in mind that the platform gimbal angle sequence may be entirely different from the sequence used in this report. Nor is it important whether the platform will be suspended by three or four gimbals. The possible differences in platform suspension details will not alter the fact that each platform gimbal angle is basically similar to an Euler angle in representing an orientation difference by one elementary angle at a time. In both, the Euler angles sequence and in a gimbal system each elementary angle can be considered as generated by a rotation about a known axis. The sequence of successive angular displacements, or differences, builds up in both cases the total difference in orientation between the initial and final orientations. In fact, exactly the same formulas can be applied either to a sequence of rotational steps as used in Euler angles or to a gimbal system, as long as the computation scheme and the two systems follow one and the same scheme of angles and sequences. Thus, conclusions of a general nature can be obtained by considering some arbitrary particular case.

As a consequence of the above premises and assuming that the stable platform gimbals have the same angle sequence as our formulas, consider again the maneuver described by (143) through (145) or by (153) through (155). So far, it has been either clearly stated, or tacitly implied that the

Euler angles ψ, θ, and Φ can or will be computed and formulas for their computation have been given. Now, instead of computing these angles it is possible by way of pickoffs to obtain them directly from the instantaneous physical stable platform gimbal angular positions. Formulas of the general type of (134) through (155) can be instrumented for analog computation by the use of resolvers and other customary techniques and in certain cases directly inserted in control loops. Similar techniques may reduce the amount of work to be performed by digital computers.

APPENDIX III. GYROSCOPIC CROSS-COUPLING EFFECTS

by

P. V. Vermont

It is known from theoretical mechanics that each rigid body, no matter how irregular its shape, has three mutually orthogonal principal axes of inertia passing through its center of gravity. Rotation at constant or variable angular rate about one of these axes at a time does not induce in the body unbalanced centrifugal or inertial couples, as is generally the case during rotation about any other axis passing through the C.G.

Let

x, y, z = a set of mutually orthogonal axes not coincident with the principal axes of inertia, with the origin at the C.G. of the body.

$\bar{i}, \bar{j}, \bar{k}$ = the corresponding unit vector triad.

L, M, N = corresponding components of torque acting on the body.

p, q, r = corresponding components of angular velocities about the three axes.

$\dot{p}, \dot{q}, \dot{r}$ = corresponding components of angular accelerations.

I_{xx}, I_{yy}, I_{zz} = moments of inertia about the three axes.

I_{xy}, I_{xz}, I_{yz} = cross products of inertia.

The following relations exist:

$$\left.\begin{aligned} I_{xx} &= \sum (y^2 + z^2)\,\Delta m = \int (y^2 + z^2)\,dm \\ I_{yy} &= \sum (x^2 + z^2)\,\Delta m = \int (x^2 + z^2)\,dm \\ I_{zz} &= \sum (x^2 + y^2)\,\Delta m = \int (x^2 + y^2)\,dm \end{aligned}\right\} \tag{183}$$

$$\left.\begin{aligned} I_{xy} &= \sum xy\,\Delta m = \int xy\,dm \\ I_{xz} &= \sum xz\,\Delta m = \int xz\,dm \\ I_{yz} &= \sum yz\,\Delta m = \int yz\,dm \end{aligned}\right\} \tag{184}$$

Note: Here Δm or dm are elements of mass, and x, y, z are the coordinates of these elements. Summation or integration, as indicated, is performed within the boundaries of the body.

Let the total instantaneous torque be

$$\bar{T} = L\bar{i} + M\bar{j} + N\bar{k} \tag{185}$$

and the total instantaneous angular velocity

$$\bar{\Omega} = p\bar{i} + q\bar{j} + r\bar{k} \tag{186}$$

The moments I_{xx}, I_{yy}, I_{zz} and the cross-products I_{xy}, I_{xz}, I_{yz} of inertia of a body can be found either analytically, for regular geometric shapes, or through computations based on mass distribution, or also experimentally, by swinging or twisting a body of known weight suspended in an appropriate manner and observing the period of oscillatory motion.

The following general relation of the dynamics of angular motion exists.

$$L = I_{xx}\dot{p} + (I_{zz} - I_{yy})qr - I_{xy}(\dot{q} - rp) - I_{xz}(\dot{r} + pq) - I_{yz}(q^2 - r^2) \tag{187}$$

$$M = I_{yy}\dot{q} + (I_{xx} - I_{zz})rp - I_{yz}(\dot{r} - pq) - I_{yx}(\dot{p} + qr) - I_{zx}(r^2 - p^2) \tag{188}$$

$$N = I_{zz}\dot{r} + (I_{yy} - I_{xx})pq - I_{zx}(\dot{p} - qr) - I_{zy}(\dot{q} + rp) - I_{xy}(p^2 - q^2) \tag{189}$$

It can be expected that, as it happens in an aircraft, there will be in the space vehicle a plane of symmetry, containing the x- and the z-axes. In this case $I_{xy} = I_{yz} = 0$ and Equations (187) through (189) become simplified. The y-axis, normal to the plane of symmetry, coincides with one of the principal axes of inertia.

If, furthermore, the x- and the z-axes are so chosen as to coincide with the principal axes of inertia or, in the general case, when the reference axes coincide with the principal axes of inertia, all three cross-products become equal to zero, $I_{xy} = I_{yz} = I_{xz} = 0$, and a much simpler formal set of expressions exists.

$$L = I_{xx}\dot{p} + (I_{zz} - I_{yy})\,qr \tag{190}$$

$$M = I_{yy}\dot{q} + (I_{xx} - I_{zz})\,rp \tag{191}$$

$$N = I_{zz}\dot{r} + (I_{yy} - I_{xx})\,pq \tag{192}$$

It can be seen that in the absence of external torques (L = M = N = 0) but in the presence of all three instantaneous components of angular rates, p, q and r, there will appear three components of angular acceleration (cross-coupling effects).

$$\dot{p} = \frac{I_{yy} - I_{zz}}{I_{xx}}\,qr \tag{193}$$

$$\dot{q} = \frac{I_{zz} - I_{xx}}{I_{yy}}\,rp \tag{194}$$

$$\dot{r} = \frac{I_{xx} - I_{yy}}{I_{zz}}\,pq \tag{195}$$

These components of angular acceleration will be created by unbalanced centrifugal couples. A simple example will illustrate how these couples can appear. If a flat symmetrical body, such as shown in Figure 36, rotates about a principal axis of inertia, such as yy or xx, then all centrifugal forces directed in the opposite sense are balanced and aligned so as to cancel each other out. But when the same body rotates about a diagonal axis dd, then the opposite centrifugal forces, although still equal, are no longer aligned and form a centrifugal couple that will impress on the body an angular acceleration about a rotating axis normal to the plane of the body.

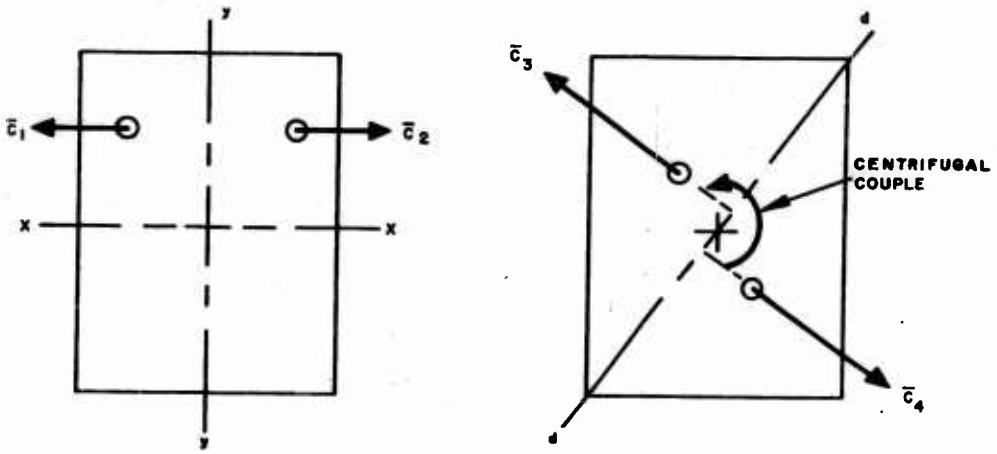

Figure 36. Centrifugal Forces of a Rotating Body

The centrifugal couples will disappear if all three principal moments of inertia are equal, $I_{xx} = I_{yy} = I_{zz}$, as it happens for example in a homogeneous cube or sphere. This follows from (193) through (195) since $\dot{p} = \dot{q} = \dot{r} = 0$. In this case any orthogonal set of three axes with the origin at the C. G. is also a set of principal axes of inertia. Gyroscopic cross-coupling effects do not appear in a similar body.

In the case of a body having three unequal moments of inertia and being subject to the motion of rotation about one of the principal axes of inertia, there will be no gyroscopic couples (cross-coupling effect) acting on the body. This follows again directly from (193) through (195). Let for example $p \neq 0$ but $q = r = 0$; then $\dot{p} = \dot{q} = \dot{r} = 0$.

A torque-free rigid body ($L = M = N = 0$) rotating at a certain instant about an arbitrary axis (such that its angular velocity is $\overline{\Omega} = p\bar{i} + q\bar{j} + r\bar{k}$) and left alone will not try to assume stable conditions of rotational motion. It will instead rotate and wobble along indefinitely with a repetitious, although not necessarily true cyclic motion, in a manner best described by the so called Poinsot's construction.

From the point of view of simplified rotational dynamics it would be desirable to build a space vehicle with equal principal moments of inertia, $I_{xx} = I_{yy} = I_{zz}$. Such a vehicle will not be subject to gyroscopic cross-coupling effects and will exhibit neutral rotational dynamic properties. It is doubtful whether other important design considerations will permit a similar weight distribution. Furthermore, due to expenditure of propulsion fuel and even to displacements of equipment and motions of astronauts, the weight

distribution of a space vehicle may be subject to changes during the course of one trip. It may be assumed that in the worst case all three moments of inertia will be different and that the position of the C. G. and the orientation of the principal axes of inertia will change within the vehicle. The change of the moments of inertia is of less consequence than the change of angular position of the principal axes of inertia. It can be expected that the torquing devices, such as inertial wheels or spheres, vernier rockets, etc., will be designed to act about three mutually orthogonal rotation axes coincident in direction with the mean direction of the principal axes of inertia. This will reduce the cross-coupling effects appearing during rotational motion about any single axis.

It can be seen that generally speaking the automatic controls of rotational motion will have to sense and to counteract at all times the cross-coupling effects. It also can be seen that in general a change of orientation (attitude) executed in three consecutive rotations of yaw, pitch and roll about axes nearly coincident with the principal axes of inertia will develop much less cross-coupling effect than a single rotation about a fixed axis which can assume any possible direction. It also can be seen that in the case of a maneuver of rotation executed manually without the assistance of automatic controls, it will be necessary to present continuously to the astronaut the instantaneous orientation of the vehicle. The astronaut will act in this case as a feedback control device and continuously correct for the cross-coupling effects.

Equations (190) through (192) show that the cross-coupling effects given by (193) through (195) will exist also when external torques L, M, N act on the body. From (190) it follows that:

$$p = \frac{L}{I_{xx}} + \frac{I_{yy} - I_{zz}}{I_{xx}} qr \tag{196}$$

Equation (196) shows also the well known fact that in the absence of the cross-coupling effect the angular acceleration p is proportional to the torque and inversely proportional to the moment of inertia I_{xx}.

It is worthwhile to mention that the three moments of inertia of a rigid body, I_{xx}, I_{yy}, I_{zz}, referred to an arbitrary set of orthogonal axes are bounded in the same way as the lengths of the sides of a triangle: each of the

numerical values is smaller than the sum of the two others and larger than the difference between the two others.

$$I_{xx} < I_{yy} + I_{zz} \tag{197a}$$

$$I_{yy} < I_{xx} + I_{zz} \tag{197b}$$

$$I_{zz} < I_{xx} + I_{yy} \tag{197c}$$

$$I_{xx} > |I_{yy} - I_{zz}| \tag{198a}$$

$$I_{yy} > |I_{xx} - I_{zz}| \tag{198b}$$

$$I_{zz} > |I_{xx} - I_{yy}| \tag{198c}$$

This follows directly from (183).

$$I_{yy} + I_{zz} = \int (x^2 + z^2)\, dm + \int (x^2 + y^2)\, dm = \int x^2 dm + \int z^2 dm + \int x^2 dm + \int y^2 dm$$

$$= \int (y^2 + z^2)\, dm + 2\int x^2\, dm = I_{xx} + 2\int x^2\, dm > I_{xx}$$

Thus, $I_{xx} < I_{yy} + I_{zz}$, etc, which proves the (197a), (197b) and (197c). Transposing one of the terms from right to left in (197b) and (197c) gives:

$$I_{yy} - I_{zz} < I_{xx}$$

$$I_{zz} - I_{yy} < I_{xx}$$

which can be collected in one expression,

$$I_{xx} > |I_{yy} - I_{zz}|$$

This proves Equations (198a), (198b) and (198c).

The following two limit cases are of interest. If one of the dimensions, say x, is equal to zero, then the body is a flat figure and the polar moment I_{xx} is equal to the sum of the two axial moments, I_{yy} and I_{zz},

$$I_{xx} = I_{yy} + I_{zz} \tag{199}$$

If two dimensions, say x and y, are equal to zero, then the body is a straight rod, or bar, and the moment about its axis is zero, while the two other moments are of equal magnitude.

$$I_{zz} = 0 \tag{200}$$

$$I_{xx} = I_{yy} \tag{201}$$

APPENDIX IV. OPERATOR LOADING

by

R. O. Besco and Carolyn S. McElwain

The secondary task utilized to measure operator loading has been described earlier. An a priori decision was made that the index of operator loading should increase as a convex function of increasing reaction time on the secondary task. Thus, the loading index would be more sensitive in the range of minimum and median response times and less sensitive in the upper ranges of response times.

The convex function chosen to define the loading index in this study was as follows:

$$L = 100 \left(1 - \frac{A - R}{KR - B}\right) \tag{202}$$

where:

L = operator loading in percent

R = average response time of a subject obtained while performing the experimental task

B = minimum average response time expected under no load conditions, empirically defined

K = a constant, operationally defined by the experimenter as the multiple of time "B" at which the probability that the subject will respond to the stimulus has approached a practical zero

A = KB; or the upper limit of average response time determined by mechanical pacing of the stimulus frequency, based on the assumptions made for the constant "K".

The minimum response time to this secondary task was defined empirically by collecting 1500 responses from ten Hughes engineers in three trials of five minutes duration for each subject. During these runs the stimulus rate was set at approximately ten lights per minute. The task was performed under no load conditions. The average response latency obtained was 0.724 seconds. This was used as "B" in the loading expression above.

During preliminary studies on the primary task, it was observed that if a subject had not responded to the stimulus light after approximately five seconds, no response would be made. If, however, the light would blink, or a new light would appear, an immediate response would be elicited.

Thus a "K" value of eight for the loading expression was adopted. This provided an upper limit to average response time of 5.792 seconds. With the above "L" expression of operator loading, if the obtained average response time were the same as the minimum average response time, operator loading on the primary task would be zero. Conversely, if the obtained average response time were equal to the maximum, i.e., the subject did not respond to the secondary task, the loading value would be 1.0. The graph of this function appears in Figure 37.

Results

Controller-Information Content Comparisons.

The analysis of the average reaction times to the secondary task while stabilizing attitude is summarized in Table XIV.

Table XIV

Analysis of Variance Summary of Average Reaction Times on the Secondary Task While Stabilizing

Variance Source	SS	df	MS	Appropriate F Ratio	F
πA (Pilots)	0.4725	3	0.1575	MS_a/MS_{ab}	2.5735
πB (Controllers)	0.0443	3	0.0148	MS_b/MS_{ab}	0.2418
πC (Information)	0.0000	1	0.0000	MS_c/MS_{error}	0.00
AB	0.5504	9	0.0612	MS_{ab}/MS_{error}	8.384**
AC	0.0670	3	0.0223	MS_{ac}/MS_{error}	3.055
BC	0.0228	3	0.0076	MS_{bc}/MS_{error}	1.041
Residual Error	0.0653	9	0.0073		

n = 1

**Significant at the 0.01 level

πA and B were random treatment effects and C was a fixed treatment effect.

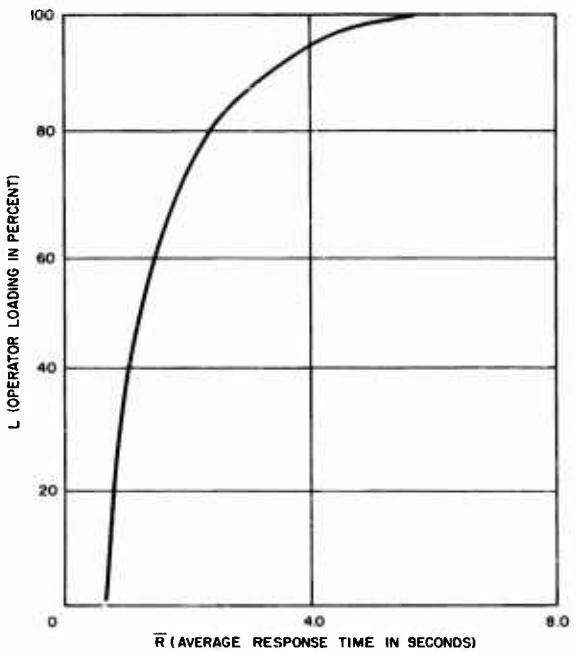

Figure 37. Graph of the Operator Loading Function

The number of stimulus lights was summed over the three trials in each cell. This sum was divided into the total accumulated response time for the three trials to obtain an average reaction time for each pilot at each combination of experimental conditions.

The only significant effect in reaction-time performances on the secondary task while stabilizing attitude was an interaction among pilots and controllers. Mean reaction times for all subject and controller combinations averaged over information conditions appear in Table XV. Operator loading over all pilots and conditions for the stabilization maneuver was 54 per cent.

Table XV

Average Reaction Time in Seconds on the Secondary Task While Stabilizing Attitude

Subject Number	Controller			
	3-axis	Wheels	Buttons	Toggles
1	1.22	1.24	1.20	1.12
2	1.15	1.68	1.34	1.23
3	1.39	1.27	1.60	1.52
4	1.34	1.05	1.13	1.02

The analysis of the average reaction times to the secondary task while tracking is presented in Table XVI. The only significant effect upon reaction times on the secondary task while tracking was the same interaction among pilots and controllers observed while stabilizing attitude. The average reaction times for subjects by controllers are presented in Table XVII. Operator loading averaged over all pilots and conditions for the tracking maneuver was 62 per cent

Cross-Coupling Effects Experiment

The only significant effects on secondary task performance during the cross-coupling experiment were the significant differences among the pilots. Performance on the secondary task was insensitive to changes in vehicle

Table XVI

Analysis of Variance Summary of the Reaction Time on the Secondary Task While Performing the Tracking Task

Variance Source	SS	df	MS	Appropriate F Ratio	F
A (Pilots)	0.4326	3	0.1442	MS_a/MS_{ab}	1.05
B (Controllers)	0.7925	3	0.2692	MS_b/MS_{ab}	1.93
C (Information)	0.0935	1	0.0935	MS_c/MS_e	2.38
AB	1.2337	9	0.1371	MS_{ab}/MS_e	3.49*
AC	0.3146	3	0.1049	MS_{ac}/MS_e	2.67
BC	0.1222	3	0.0407	MS_{bc}/MS_e	0.10
Residual Error	0.3536	9	0.0393		

n = 1

*Significant at the 0.05 level.

Table XVII

Average Reaction Times in Seconds on the Secondary Task While Tracking

Subject Number	Controller			
	3-axis	Wheels	Buttons	Toggles
1	1.28	1.43	1.97	1.28
2	1.00	1.86	1.53	1.59
3	1.40	1.45	2.04	1.72
4	1.45	1.36	1.33	1.15

shape or information content. The average operator loading for all conditions in this study was 55 per cent. The variation in loading scores between subjects ranged from 49 to 65 per cent.

External Viewport Study

There were no practically significant differences in the reaction times on the secondary task for any conditions in this experiment. The average operator loading during these tests was 38 per cent.

Discussion

The secondary task used in this program was quite ineffective in providing a sensitive measure of operator work loading. The task did meet one of the subcriteria for a measure of operator loading in that it did not directly interfere with performance on the primary task.

The stabilization maneuver as a primary task was a difficult conceptual task but was a relatively simple perceptual-motor task. Since the secondary task was of a perceptual-motor character, it not only did not interfere with the primary task but also proved to be insensitive to changes in the conceptual difficulty of the primary task. The results of this program suggest that the conceptual, perceptual and motor aspects of competing tasks can be attended to by the rapid time-sharing of attention at least in the low to medium range of loading.

Further research is needed to define and categorize dimensions of competing tasks in terms of interference and sensitivity to difficulty levels. For example, theory or empirical data is needed to guide the selection of secondary tasks which will not directly interfere with primary task performance yet will be sensitive to changes in primary task difficulty.

APPENDIX V. FILTERING TECHNIQUES FOR ONBOARD TRAJECTORY DETERMINATION

by

N. A. Boehmer

The problem of orbit determination for spacecraft is new and in many ways different from the orbit determination of classical celestial mechanics. With the modern digital computer it is possible to make rapid orbit and trajectory determinations from literally hundreds or thousands of data points. The techniques employed were developed first in connection with the interceptor fire control problem and became known under the title of "The Theory of Redundant Measurements."

Basically, what is done is to reduce the nonlinear equations of motion to linear equations by perturbation techniques and to obtain an optimum estimate of the orbital perturbation parameters by statistical methods. The matrix of perturbation coefficients is obtained with respect to a nominal trajectory. If, as measurements are taken, the estimated trajectory departs sufficiently from the a priori nominal trajectory, a new nominal trajectory must be computed (and perturbed) based on currently estimated trajectory parameters. Then to obtain an improved parameter estimate, the entire estimation procedure is repeated. This requires that all past data must be stored in the computer memory. The Deep Space Instrumentation Facility approach is to compute a new nominal trajectory each time a new measurement becomes available.

Currently employed trajectory determination methods utilizing large ground-based computers involve a horrendous amount of computation in terms of the capability of a practical size onboard computer. This is especially true for early missions requiring self-contained midcourse guidance, where reliability (and hence simplicity) is of prime importance. There are basically two ways in which present methods can be adapted for onboard operation:

1. Precompute and store in the onboard computer memory the matrix of perturbation coefficients corresponding to a predetermined schedule of inflight measurements or develop analytical or empirical formulas for computing the perturbation

coefficients onboard as functions of the currently estimated trajectory.

2. Develop recursion methods for data smoothing which obviate reliance upon an a priori nominal trajectory and the need to store large quantities of past data.

Early ballistic missile systems employed precomputation schemes, e.g., delta guidance, to minimize inflight equipment. Later systems employed an onboard computation scheme (known as explicit guidance) which eliminated certain error sources due to non-nominal missile parameters. However for space flight, uncertainty in launch time is a large obstacle to the precomputation of perturbation coefficients and hence more consideration has been given to explicit methods at the outset than in the case of ballistic missile systems. The problem of linearization is an entire subject in itself. This appendix will be concerned primarily with the remainder of the trajectory determination problem, namely obtaining the optimum trajectory estimate, given the linearized data.

Until recently, attempts to develop data smoothing methods adaptable to onboard computation have not been completely satisfactory. A step-by-step procedure for linear least squares estimation is easily obtained but depends again upon a priori nominal trajectory. The present discussion is based upon a derivation by Kalman (1960). It leads directly to the development of lower order matrix equations which are in a form equivalent to the results obtained by Ames Research Center, NASA. The Ames derivations and applications are contained in two forthcoming publications (Smith, et. al., in preparation and McLean, et. al., in preparation). The trajectory determination method presented in this appendix provides rigorously the optimal trajectory estimate when either

1. The linearized variables are gaussian in which case the optimum is with respect to a rather general class of loss functions; or
2. The optimal estimate is restricted to be a linear function of the linearized variables in which case the optimum is obtained in the least square sense.

APPLICATION OF KALMAN'S FILTERING THEORY TO TRAJECTORY DETERMINATION

The equations of motion are linearized by perturbing the estimated trajectory (note that the estimated or updated trajectory is not the same as a reference or nominal trajectory which is selected before observations begin at $t = t_o$). The perturbation equations may be written as follows:

$$dX(t + 1) = \Phi(t + 1; t)\, dX(t) \tag{203}$$

$$dY_c(t) = M(t)\, dX(t) + u(t) \tag{204}$$

where dX is a 6-vector (say, 3 components of position and 3 components of velocity) representing perturbations from the estimated trajectory; dY_c is a p-vector ($p \leq 6$) representing observed deviations from the estimated trajectory, u(t) is an independent gaussian random process of p-vectors with zero mean, and $\Phi(t + 1; t)$ is a 6 x 6 transition matrix relating perturbations from the estimated trajectory at time t to perturbations from the estimated trajectory at time t + 1. M(t) is a p x 6 matrix relating perturbations dY of the observed quantities to perturbations of the trajectory variables; that is

$$dY_c(t) = dY(t) + u(t) \tag{205}$$

Equations (203) and (204) express the dynamic model of the system.

The following equations are derived in the previously cited references.

$$\Delta^*(t) = \Phi(t + 1; t)\, P^*(t)\, M'(t) \left[M(t)\, P^*(t)\, M'(t) + Q(t) \right]^{-1} \tag{206}$$

$$\Phi^*(t + 1; t) = \Phi(t + 1; t) - \Delta^*(t)\, M(t) \tag{207}$$

$$P^*(t + 1) = \Phi^*(t + 1; t)\, P^*(t)\, \Phi'(t + 1; t) \tag{208}$$

$$dX^*(t/t) = \Phi(t; t + 1)\Phi^*(t + 1; t)\Phi(t; t - 1)\, dX^*(t - 1/t - 1) + \Phi(t; t + 1)\, \Delta^*(t)\, dY(t) \tag{209}$$

COMPUTATIONAL REQUIREMENTS

In Equation (209), the notations dX and dY emphasize that these random variables represent perturbations about the estimated trajectory. To solve the above equations in real time we must specify $P^*(t_o)$ and Q(t)

and compute the matrices Φ and M. $P^*(t_o)$, where t_o is the time of injection into lunar (or interplanetary) orbit, is the covariance matrix of the injection errors and would be specified a priori from boost guidance studies. The p x p covariance matrix Q(t) of the measurement errors is computed as a function of time either explicitly or implicitly.

The iteration of Equations (206) through (209) is started from a linearization about the nominal injection conditions. Suppose the time of the first observations is t_1. The computer integrates simultaneously the nominal (in general estimated) trajectory and six perturbed trajectories from time t_o until time $t_1 - dt$; and computes $\Phi(t_1 - dt; t_o)$ and $M(t_1 - dt)$. The infinitesimal time interval dt is introduced for the purpose of identifying the state of affairs immediately preceding the observation. In the interval $t_o \leq t < t_1$ the optimal estimate (since no new information is yet available) is obviously $dX^* = 0$. The covariance matrix of the optimal estimation error is updated to the time $t_1 - dt$ as follows:

$$\begin{aligned} P^*(t_1 - dt) &= E\,\tilde{X}(t_1 - dt)\,\tilde{X}'(t_1 - dt) \\ &= \Phi(t_1 - dt; t_o)\, E\tilde{X}(t_o)\,\tilde{X}'(t_o)\,\Phi'(t_1 - dt; t_o) \\ &= \Phi(t_1 - dt; t_o)\, P^*(t_o)\,\Phi'(t_1 - dt; t_o) \end{aligned}$$

Now Equations (206)through (209) are applied to the infinitesimal interval $t_1 - dt \leq t \leq t_1$. The results are considerably simplified since, the unperturbed trajectory is the estimated trajectory and hence $dX^*(t_1/t_1)$ contains only the last term, and also since in the limit as $dt \to 0$

$$\Phi(t_1 + dt; t_1) = \Phi(t_1; t_1 + dt) = I = \text{unit matrix.} \tag{211}$$

We compute therefore:

$$\Delta^*(t_1) = P^*(t_1 - dt)\, M'(t_1)\left[M(t_1)\, P^*(t_1 - dt)\, M'(t_1) + Q(t_1)\right]^{-1} \tag{212}$$

$$P^*(t_1) = P^*(t_1 - dt) - \Delta^*(t_1)\, M(t_1)\, P^*(t_1 - dt) \tag{213}$$

$$dX^*(t_1/t_1) = \Delta^*(t_1)\, dY(t_1) \tag{214}$$

where Y_o are the observed quantities and Y_c are computed from $X^*(t_1 - dt)$, the best estimate of the trajectory before the time of the observation, $\Delta^*(t)$ is the weighting function matrix, $P^*(t)$ is the covariance matrix of

the estimation errors and $Q(t)$ is the covariance matrix of the measurement error. The optimal estimate after the observation becomes

$$X^*(t_1) = X^*(t_1 - dt) + dX^*(t_1/t_1) \tag{215}$$

which, together with $P^*(t_1)$, defines the initial conditions for integration of the equations of motion from t_1 until the next observation at t_2. Except for the way in which the initial conditions are determined, the process is identical to that just described.

APPENDIX VI. DERIVATION OF Φ MATRIX ELEMENTS

by

N. A. Boehmer

We have implicitly

$$r = r(r_o, \theta_o, p, e) \tag{216}$$

$$\theta = \theta(r_o, \theta_o, p, e) \tag{217}$$

and we want the eight partial derivatives r, θ with respect to r_o, θ_o, p, e. Perhaps the simplest way of obtaining the partials with respect to r_o, θ_o is to observe that p, e constant implies that energy W and angular momentum h are constant and write

$$r = r(r_o, \theta_o, W, h) \tag{218}$$

$$\theta = \theta(r_o, \theta_o, W, h) \tag{219}$$

Specifically

$$r = r_o + \int_{t_o}^{t} \left(2W + \frac{2K}{r} - \frac{h^2}{r^2}\right)^{1/2} dt \tag{220}$$

from which

$$\frac{\partial r}{\partial r_o} = 1 + \int_{t_o}^{t} \frac{\partial r}{\partial r_o} \frac{\ddot{r}}{\dot{r}} \, dt \tag{221}$$

$$\frac{\partial r}{\partial \theta_o} = \int_{t_o}^{t} \frac{\partial r}{\partial \theta_o} \frac{\ddot{r}}{\dot{r}} \, dt \tag{222}$$

or solving

$$\frac{\partial r}{\partial r_o} = \frac{\dot{r}}{\dot{r}_o} = \frac{\sin \eta}{\sin \eta_o} \tag{221}$$

$$\frac{\partial r}{\partial \theta_o} = 0 \tag{222}$$

From

$$\theta = \theta_o + \int_{t_o}^{t} \frac{h}{r^2}\, dt \tag{223}$$

we have

$$\frac{\partial \theta}{\partial r_o} = - \int_{t_o}^{t} \frac{2h}{r^3} \frac{\partial r}{\partial r_o}\, dt = \frac{\dot{\theta} - \dot{\theta}_o}{\dot{r}_o} = \frac{p}{e \sin \eta_o} \left(\frac{1}{r^2} - \frac{1}{r_o^2} \right) \tag{224}$$

$$\frac{\partial \theta}{\partial \theta_o} = 1 - \int_{t_o}^{t} \frac{2h}{r^3} \frac{\partial r}{\partial \theta_o}\, dt = 1 \tag{225}$$

Partials with respect to p, e are obtained from the polar equation

$$r = \frac{p}{1 + e \cos \eta} \tag{226}$$

whence

$$\frac{\partial r}{\partial p} = \frac{r}{p} \left(1 + r\, e \sin \eta \frac{\partial \eta}{\partial p}\right) \tag{227}$$

$$\frac{\partial r}{\partial e} = - \frac{r^2}{p} \left(\cos \eta - e \sin \eta \frac{\partial \eta}{\partial e}\right) \tag{228}$$

Now using again

$$\theta = \theta_o + \int_{t_o}^{t} \frac{h}{r^2}\, dt \tag{223}$$

and the relation $p = \frac{h^2}{K}$, we get

$$\frac{\partial \theta}{\partial p} = \frac{\partial \eta}{\partial p} + \frac{\partial \omega}{\partial p} = \int_{t_o}^{t} \left(\frac{\dot{\eta}}{2p} - \frac{2\dot{\eta}}{r} \frac{\partial r}{\partial p} \right) dt \tag{229}$$

or, substituting $\frac{\partial r}{\partial p}$ from the previous equations and differentiating with respect to time

$$\frac{d}{dt}\left(\frac{\partial \eta}{\partial p} \right) + \frac{2\dot{\eta} e \sin \eta}{1 + e \cos \eta} \frac{\partial \eta}{\partial p} = - \frac{3\dot{\eta}}{2p} \tag{230}$$

The solution is

$$\frac{\partial \eta}{\partial p} = - \frac{3\dot{\eta}}{2p} (t - t_o) - \frac{r_o}{r^2 e \sin \eta_o} \tag{231}$$

or

$$\frac{\partial \theta}{\partial p} = - \frac{3\eta}{2p} (t - t_o) + \frac{1}{r_o e \sin \eta_o} \left(1 - \frac{r_o^2}{r^2} \right)$$

$$= - \frac{3}{2r^2} \sqrt{\frac{K}{p}} (t - t_o) + \frac{1}{r_o e \sin \eta_o} \left(1 - \frac{r_o^2}{r^2} \right) \tag{232}$$

Differentiating

$$r_o = \frac{p}{1 + e \cos (\theta_o - \omega)} \tag{233}$$

yields

$$\frac{\partial \omega}{\partial p} = \frac{1}{r_o e \sin \eta_o} \tag{234}$$

which, together with $\frac{\partial \theta}{\partial p}$, leads to

$$\frac{\partial r}{\partial p} = \frac{r}{p}\left[1 - \left(\frac{r}{r_o}\right)\frac{\partial r}{\partial r_o} + re \sin\eta \frac{\partial \theta}{\partial p}\right] \tag{235}$$

A similar procedure produces the remaining two derivatives. Thus,

$$\frac{\partial \theta}{\partial e} = \frac{\partial \eta}{\partial e} + \frac{\partial \omega}{\partial e} = -2\int_{t_o}^{t} \frac{\dot{\eta}}{r}\frac{\partial r}{\partial e}\, dt \tag{236}$$

and

$$\frac{d}{dt}\left(\frac{\partial \eta}{\partial e}\right) + \frac{2\dot{\eta} e \sin\eta}{1 + e\cos\eta}\left(\frac{\partial \eta}{\partial e}\right) = \frac{2\dot{\eta}}{e}\left(1 - \frac{r}{p}\right) \tag{237}$$

Solving,

$$\frac{\partial \eta}{\partial e} = \frac{2\dot{\eta}}{e}\int_{t_o}^{t}\left(1 - \frac{r}{p}\right) dt + \left(\frac{r_o}{r}\right)^2 \frac{\cot\eta_o}{e} \tag{238}$$

or

$$\frac{\partial \theta}{\partial e} = \frac{2\dot{\eta}}{e}\int_{t_o}^{t}\left(1 - \frac{r}{p}\right) dt - \frac{\cot\eta_o}{e}\left(1 - \frac{r_o^2}{r^2}\right)$$

$$= \frac{2\dot{\eta}}{p}\int_{t_o}^{t} r\cos\eta\, dt - \frac{\cot\eta_o}{e}\left(1 - \frac{r_o^2}{r^2}\right) \tag{239}$$

The integral is evaluated by means of the substitutions

$$r\cos\eta = a(\cos E - e) \tag{240}$$

$$dt = \frac{dE}{\mu}(1 - e \cos E) \tag{241}$$

The result is

$$\frac{\partial \theta}{\partial e} = \frac{2a}{\mu r^2}\sqrt{\frac{K}{p}}\left[(1 + e^2)(\sin E - \sin E_o) - \frac{3e}{2}(E - E_o) - \frac{e}{4}(\sin 2E - \sin 2E_o)\right] - \frac{\cot \eta_o}{e}\left(1 - \frac{r_o^2}{r^2}\right) \tag{242}$$

We find also

$$\frac{\partial \omega}{\partial e} = -\frac{\cos \eta_o}{e \sin \eta_o} \tag{243}$$

and finally

$$\frac{\partial r}{\partial e} = \frac{r^2}{p}\left[\cos \eta_o \frac{\partial r}{\partial r_o} - \cos \eta + e \sin \eta \frac{\partial \theta}{\partial e}\right] \tag{244}$$

It should be noted that the above formulas cannot be used when t_o is at perigee and apogee. This is a consequence of the choice of coordinates.

APPENDIX VII. BRIEF REVIEW OF MATRIX OPERATIONS

by

P. V. Vermont

Unlike a determinant, whose numerical or algebraic value can be computed, a matrix is merely an orderly arrangement of numerical or algebraic elements in which each element having its own particular value can be given the name of the place it occupies. A matrix is composed of horizontal rows and vertical columns. A rectangular m x n matrix has m rows and n columns and is said to be of the order m by n. A square matrix having m rows and an equal number of columns is said to be of order m.

A matrix can be represented symbolically by a letter.

$$A = \begin{pmatrix} a_{11} & a_{12} & a_{13} \\ a_{21} & a_{22} & a_{23} \\ a_{31} & a_{32} & a_{33} \\ a_{41} & a_{42} & a_{43} \end{pmatrix} \quad ; \quad B = \begin{pmatrix} b_{11} & b_{12} \cdots b_{1n} \\ b_{21} & b_{22} \cdots b_{2n} \\ \text{----------} \\ b_{m1} & b_{m2} \cdots b_{mn} \end{pmatrix}$$

(245, 245-a)

Here (A) is a 4 x 3 matrix composed of 12 elements arranged as shown; (B) is an m x n matrix, composed of m n elements.

Matrix algebra and matrix operations serve to represent in a compact way sequences of algebraic operations and arrangements of results according to a set of arbitrary conventional rules. These rules are arbitrary only to a certain extent since they have been developed in such a way that they can be applied to the solution of various problems in different fields of mathematics.

Addition. Two matrices of equal order can be added by adding corresponding elements. The resulting sums form a matrix of the same order. For example:

$$A = \begin{pmatrix} a_{11} & a_{12} & a_{13} \\ a_{21} & a_{22} & a_{23} \end{pmatrix} \tag{246}$$

$$B = \begin{pmatrix} b_{11} & b_{12} & b_{13} \\ b_{21} & b_{22} & b_{23} \end{pmatrix} \tag{247}$$

$$C = A + B = \begin{pmatrix} c_{11} & c_{12} & c_{13} \\ c_{21} & c_{22} & c_{23} \end{pmatrix}$$

$$= \begin{pmatrix} a_{11} + b_{11} & a_{12} + b_{12} & a_{13} + b_{13} \\ a_{21} + b_{21} & a_{22} + b_{22} & a_{23} + b_{23} \end{pmatrix} \tag{248}$$

The = sign should be interpreted in the sense of equality between single elements, for example

$$c_{22} = a_{22} + b_{22} \tag{249}$$

Matrix addition is commutative and associative:

$$A + B = B + A \tag{250}$$

$$(A + B) + C = A + (B + C) \tag{251}$$

Multiplication. Two matrices (A) and (B) can be multiplied in that order

$$C = A \times B$$

if the number of columns of (A) is equal to the number of rows of (B). Matrix (B) is premultiplied by matrix (A), while (A) is postmultiplied by (B). The resulting matrix will have the same number of rows as the first matrix and the same number of columns as the second matrix. If (A) is m x n and (B) is n x k then (C) is m x k. An element c_{ij} of an i-th row and j-th column of (C) is obtained by taking the i-th row of (A) and j-th column of (B), multiplying the successive elements of these lines by each other and forming the sum of the products. Let:

$$A = \begin{pmatrix} a_{11} & a_{12} & a_{13} \\ a_{21} & a_{22} & a_{23} \\ a_{31} & a_{32} & a_{33} \\ a_{41} & a_{42} & a_{43} \end{pmatrix} \tag{253}$$

$$B = \begin{pmatrix} b_{11} & b_{12} \\ b_{21} & b_{22} \\ b_{31} & b_{32} \end{pmatrix} \tag{254}$$

$$C = AB = \begin{pmatrix} c_{11} & c_{12} \\ c_{21} & c_{22} \\ c_{31} & c_{32} \\ c_{41} & c_{42} \end{pmatrix} \tag{255}$$

Here (A) is a 4 x 3, (B) is a 3 x 2 and (C) is a 4 x 2 matrix. Thus, m = 4, n = 3, k = 2. An element of (C), for example c_{32}, is computed as follows. Take the 3-rd row of (A) and the 2-nd column of (B).

$$a_{31} \quad a_{32} \quad a_{33} \tag{256}$$

$$b_{12}$$

$$b_{22}$$

$$b_{32} \tag{257}$$

Multiply the successive elements, take the sum

$$c_{32} = a_{31}\, b_{12} + a_{32}\, b_{22} + a_{33}\, b_{32} \tag{258}$$

The manual process of multiplying a row by a column becomes quite natural after repeated computations.

Matrix multiplication is not commutative even for square matrices. In general,

$$AB \neq BA \tag{259}$$

Matrix multiplication is associative:

$$ABCD = A(BC)D = AB(CD) = (AB)(CD) \ldots \text{ etc.} \tag{260}$$

The distributive law is applicable to matrix multiplication.

$$A(B + C) = AB + AC \ldots \text{ etc.} \tag{261}$$

Transpose matrix, (A^t) of (A) is one with interchanged row and columns

$$A = \begin{pmatrix} 1 & 5 \\ 2 & 3 \\ 7 & 4 \end{pmatrix} \quad ; \quad A^t = \begin{pmatrix} 1 & 2 & 7 \\ 5 & 3 & 4 \end{pmatrix} \tag{262}$$

Inverse matrix, (A^{-1}) of a square matrix is such a matrix that

$$A^{-1} A = A A^{-1} = I \tag{263}$$

where (I) is a unit matrix, i.e., a square matrix whose elements composing the main diagonal are all unity and all other elements are zeros. For example

$$I = \begin{pmatrix} 1 & 0 & 0 \\ 0 & 1 & 0 \\ 0 & 0 & 1 \end{pmatrix} \tag{264}$$

is a unit matrix of order 3. For a more detailed discussion of inverse matrices as well as of other details consult Wade (1951).

Returning to matrix multiplication and in particular to Equations (255) and (258) consider the case when the (B) matrix would be altered by multiplying each of its rows by some constant.

$$B_1 = \begin{pmatrix} k_1 b_{11} & k_1 b_{12} \\ k_2 b_{21} & k_2 b_{22} \\ k_3 b_{31} & k_3 b_{32} \end{pmatrix} \tag{265}$$

The product $C_1 = AB_1$ also would be altered and its element $(c_{32})_1$ would be:

$$(c_{32})_1 = a_{31} k_1 b_{12} + a_{32} k_2 b_{22} + a_{33} k_3 b_{32} \tag{266}$$

It can be seen that the same result could be obtained if instead of multiplying the rows of (B) by k_1, k_2 and k_3 the columns of (A) were multiplied by these coefficients, as follows.

$$A_1 = \begin{pmatrix} k_1 a_{11} & k_2 a_{12} & k_3 a_{13} \\ k_1 a_{21} & k_2 a_{22} & k_3 a_{23} \\ k_1 a_{31} & k_2 a_{32} & k_3 a_{33} \\ k_1 a_{41} & k_2 a_{42} & k_3 a_{43} \end{pmatrix} \tag{267}$$

Thus, the following is true.

$$C_1 = AB_1 = A_1 B \tag{268}$$

The above property will find its use in the discussion of manual computations.

Aerospace Medical Division, 6570th Aerospace Medical Research Laboratories, Wright-Patterson AFB, Ohio Rpt. No. AMRL-TDR-62-87. HUMAN ENGINEERING CRITERIA FOR MANNED SPACE FLIGHT: MINIMUM MANUAL SYSTEMS. Final report, Aug 62, viii + 227 pp. incl. illus., tables, 42 refs. Unclassified report

Analytical and experimental investigations were made of simple or minimum manual guidance and control systems. A complete three-degree of freedom static simulator was used to study the manual attitude control of space vehicles. Major controller, display and vehicle configuration parameters were compared experimentally. The system kinematics,

(over)

UNCLASSIFIED

1. Control Systems
2. Guidance
3. Control Simulators
4. Space Navigation

I. AFSC Project 7184, Task 718405

II. Behavioral Sciences Laboratory

III. Contract AF 33(616) - 8168

IV. Hughes Aircraft Co., Culver City, Calif.

V. Bauerschmidt, D.K., Besco, R.O.

UNCLASSIFIED

manual control and visual factors of space rendezvous and docking maneuvers were analyzed. Procedures for manual participation in space navigation and guidance were studied and a preliminary design of a simple computational aid was developed. The conclusions of all the studies are presented and recommendations are made for the design of manual guidance and control systems.

UNCLASSIFIED

VI. In ASTIA collection

VII. Aval fr OTS: $3.50

UNCLASSIFIED

Aerospace Medical Division, 6570th Aerospace Medical Research Laboratories, Wright-Patterson AFB, Ohio Rpt. No. AMRL-TDR-62-87. HUMAN ENGINEERING CRITERIA FOR MANNED SPACE FLIGHT: MINIMUM MANUAL SYSTEMS. Final report, Aug 62, viii + 227 pp. incl. illus., tables, 42 refs. Unclassified report

Analytical and experimental investigations were made of simple or minimum manual guidance and control systems. A complete three-degree of freedom static simulator was used to study the manual attitude control of space vehicles. Major controller, display and vehicle configuration parameters were compared experimentally. The system kinematics,

(over)

UNCLASSIFIED

1. Control Systems
2. Guidance
3. Control Simulators
4. Space Navigation

I. AFSC Project 7184, Task 718405

II. Behavioral Sciences Laboratory

III. Contract AF 33(616) - 8168

IV. Hughes Aircraft Co., Culver City, Calif.

V. Bauerschmidt, D.K., Besco, R.O.

UNCLASSIFIED

manual control and visual factors of space rendezvous and docking maneuvers were analyzed. Procedures for manual participation in space navigation and guidance were studied and a preliminary design of a simple computational aid was developed. The conclusions of all the studies are presented and recommendations are made for the design of manual guidance and control systems.

UNCLASSIFIED

VI. In ASTIA collection

VII. Aval fr OTS: $3.50

UNCLASSIFIED

Aerospace Medical Division, 6570th Aerospace Medical Research Laboratories, Wright-Patterson AFB, Ohio Rpt. No. AMRL-TDR-62-87. HUMAN ENGINEERING CRITERIA FOR MANNED SPACE FLIGHT: MINIMUM MANUAL SYSTEMS. Final report, Aug 62, viii + 227 pp. incl. illus., tables, 42 refs. Unclassified report

Analytical and experimental investigations were made of simple or minimum manual guidance and control systems. A complete three-degree of freedom static simulator was used to study the manual attitude control of space vehicles. Major controller, display and vehicle configuration parameters were compared experimentally. The system kinematics,

(over)

UNCLASSIFIED

1. Control Systems
2. Guidance
3. Control Simulators
4. Space Navigation
- I. AFSC Project 7184, Task 718405
- II. Behavioral Sciences Laboratory
- III. Contract AF 33(616) - 8168
- IV. Hughes Aircraft Co., Culver City, Calif.
- V. Bauerschmidt, D.K., Besco, R.O.

UNCLASSIFIED

manual control and visual factors of space rendezvous and docking maneuvers were analyzed. Procedures for manual participation in space navigation and guidance were studied and a preliminary design of a simple computational aid was developed. The conclusions of all the studies are presented and recommendations are made for the design of manual guidance and control systems.

UNCLASSIFIED

- VI. In ASTIA collection
- VII. Aval fr OTS: $3.50

UNCLASSIFIED

Aerospace Medical Division, 6570th Aerospace Medical Research Laboratories, Wright-Patterson AFB, Ohio Rpt. No. AMRL-TDR-62-87. HUMAN ENGINEERING CRITERIA FOR MANNED SPACE FLIGHT: MINIMUM MANUAL SYSTEMS. Final report, Aug 62, viii + 227 pp. incl. illus., tables, 42 refs. Unclassified report

Analytical and experimental investigations were made of simple or minimum manual guidance and control systems. A complete three-degree of freedom static simulator was used to study the manual attitude control of space vehicles. Major controller, display and vehicle configuration parameters were compared experimentally. The system kinematics,

(over)

UNCLASSIFIED

1. Control Systems
2. Guidance
3. Control Simulators
4. Space Navigation
- I. AFSC Project 7184, Task 718405
- II. Behavioral Sciences Laboratory
- III. Contract AF 33(616) - 8168
- IV. Hughes Aircraft Co., Culver City, Calif.
- V. Bauerschmidt, D.K., Besco, R.O.

UNCLASSIFIED

manual control and visual factors of space rendezvous and docking maneuvers were analyzed. Procedures for manual participation in space navigation and guidance were studied and a preliminary design of a simple computational aid was developed. The conclusions of all the studies are presented and recommendations are made for the design of manual guidance and control systems.

UNCLASSIFIED

- VI. In ASTIA collection
- VII. Aval fr OTS: $3.50

UNCLASSIFIED

END